4-27-2015

Innate Immune Induction in Influenza Infection

Thomas Howard Oguin III

INNATE IMMUNE INDUCTION IN INFLUENZA VIRUS

by

Thomas Howard Oguin III

A Dissertation

Submitted in Partial Fulfillment of the

Requirements for the Degree of

Doctor of Philosophy

Major: Biology

The University of Memphis

May 2015

ACKNOWLEDGEMENTS

I would like to thank my major advisors, Drs. Paul Thomas and Omar Skalli. Each one of them have inspired and helped me during this course of study, and without their guidance, I would not have made it this far. Paul has been incredibly supportive throughout every step of this journey, and I'll be forever indebted to him. Omar took a chance and accepted me as his student, and without his guidance and help, I would not have been able to make so much progress. I sincerely hope I can make them both proud. Additionally, I would like to acknowledge to my committee members, Drs. Judith Cole, Andrew Liu, and Thomas Sutter. Each committee member has challenged me to ensure that I was prepared to enter these final stages of training. The members of the Dr. Paul Thomas lab at St. Jude Children's Research Hospital deserve special recognition. Each member, past and present, has contributed to my skills, knowledge and understanding, and I feel especially lucky to have these people as colleagues. None of this work could have been done without the world-class facilities and services available at St. Jude, and I am forever thankful to have the opportunity to work at St. Jude. Last, none of my work would have been possible without the extraordinary support of my family and my friends. Additionally. my Maggie has ensured life remained fun and happy during the years it took to prepare for this manuscript.

PREFACE

The work presented in this dissertation will be described in five chapters. Chapter one will contain a general introduction to my work, discussions of significance of data, and a literature review. Chapter two contains a manuscript published in the Journal of Biological Chemistry (2014) entitled "PHOSPHOLIPASE D FACILITATES EFFICIENT ENTRY OF INFLUENZA VIRUS ALLOWING ESCAPE FROM INNATE IMMUNE INHIBITION," and is presented in the final accepted format of the journal as per the rules set forth by the dissertation preparation guide. Chapter three will detail findings from investigations of the role IRF3 during influenza virus infection. In chapter four, I will present work I've done to uncover the role of MxA during early innate immune signaling after influenza virus infection, and chapter five will be a brief conclusion regarding my dissertation as a whole.

ABSTRACT

Oguin III, Thomas Howard. Ph.D. The University of Memphis. May 2015. Innate Immune Induction in Influenza Infection. Co-Major Professors: Paul Thomas, Ph.D and Omar Skalli, Ph.D.

Influenza virus is a threat to public health on a global scale. Each year, millions of people are infected with influenza virus leading to hundreds of thousands of deaths. Despite progress in developing anti-influenza drugs, every antiviral compound used has caused influenza strains to mutate and become resistant to the drug. In order to improve our defenses against influenza virus, novel research strategies are needed. The innate immune system is the first line of defense against incoming pathogens. Many signaling networks are involved in coordinating an efficacious response to viral insult. We have found that lipid signaling through phospholipase D is critical to influenza pathogenesis. Influenza virus exploits this signaling to quickly infect human lung cells and evade the host antiviral response. By inhibiting this process, we observed a marked protection from infection. One of the critical molecules of the protective innate immune response after phospholipase D inhibition is interferon regulatory factor 3. Surprisingly, we found that mice missing this protein are more likely to survive a lethal influenza infection. This survival advantage depends on an amplified adaptive immune response. We are currently investigating this crosstalk between the innate and adaptive immune systems. One of the most potent direct antiviral effector molecules in the innate arsenal is myxovirus resistance gene 1. While this protein is generally considered to function by binding directly to viral proteins and inhibiting their function, we have uncovered an unrecognized activity of this

protein. We show that basal expression of this protein is critical in the induction of the innate immune response, and it is potentially involved in the signaling network that is constructed in response to influenza infection. These results help define the critical events mediating the host-virus interaction in infected epithelial cells. Future research for new antiviral strategies can exploit these novel pathways to enhance host responses and limit viral replication efficiency.

TABLE OF CONTENTS

LIST OF FIGURES

CHAPTER 1

INTRODUCTION

Influenza infection remains a public health concern despite active surveillance programs and advances in vaccination strategy and antiviral development. A pandemic on scale with the 1918 Spanish Flu outbreak would lead to global instability and countless losses in the economic, service, and manufacturing sectors. It is therefore imperative to develop and research innovative strategies for anti-influenza therapeutic options and to uncover the events that occur in cells that lead to an influenza infection. Current influenza defense strategies are based heavily in viral surveillance, vaccine production and development of antiviral molecules that inhibit viral enzymes. Despite worldwide serosurveys and sentinel screening, no reliable model of global transmission of newly emerged influenza strains has been produced. Because of the unpredictable nature of viral reproduction and spread, vaccines need constant reformulation as well as safety and efficacy testing for each new batch. Additionally, due to evolutionary pressure applied by currently available antivirals, drug resistant strains can emerge quickly. Novel research strategies are needed to determine the mechanisms of viral pathogenesis and host defense occurring during influenza infection, and how we might exploit those mechanisms in order to better combat the influenza threat

The events leading to a successful influenza infection are only recently becoming clear after more than 70 years of research. Influenza attaches to sialic acid residues on the surface of a cell, causing the de novo formation of clathrin

coated pits (Neumann et al., 2009). During the endosomal maturation process it is thought that innate defense proteins can sample the endosome for pathogen-associated molecular patterns (Ehrhardt et al., 2010). For the virus to successfully infect a cell, it must evade or overcome the antiviral defenses of the cell and wait for the endosome to become acidified (Lakadamyali et al., 2004). Lipid signaling regulates many features of cellular trafficking, and these pathways may serve as a potential target for altering influenza infection. Phosphatidic acid (PA), produced by phospholipase D (PLD), is a bioactive lipid that is involved in membrane formation and curvature and also acts as a second messenger in other signaling pathways (Roth, 2008). Isoform specific inhibitors of PLD have been described (Scott et al., 2009), and we have used these tools to study what role PLD is playing during influenza infection. We have found that influenza virus uses PLD to efficiently enter cells and evade detection from the innate immune proteins that guard against viral insult (Oguin et al., 2014).

Host cells have innate antiviral sensors and effector molecules that represent the first line of defense against viral invasion. Recently, a human restriction factor for influenza virus has been identified. Patients with mutations in their Interferon-induced transmembrane protein 3 (IFITM3), experienced poorer clinical outcomes when infected with the 2009 pandemic influenza virus (Everitt et al., 2012). One of the earliest influenza restriction factors discovered was Myxovirus resistance factor (Mx) 1 in mice (Chang et al., 1990; Staeheli et al., 1988) homologous to MxA in humans. Typical inbred laboratory mice do not have functional Mx1 genes and are susceptible to influenza. However, outbred or truly

wildtype mice carry the proper Mx1 gene and are resistant to lethal viral challenge. Much has been revealed considering Mx1 expression, activity, and structure but less is known regarding what Mx1 is doing at the earliest moments of infection. It is thought that Mx1 expression and activity depends on Type 1 IFN stimulation. Based on data we have collected, MxA in human cells is basally expressed and quickly activated after infection and loss of MxA leads to an attenuated transcriptional response of many interferon stimulated genes (ISGs).

The earliest immune response to invading influenza virus is the induction of the Type 1 Interferon (IFN) system. After influenza is sensed by antiviral proteins such as retinoic-acid induced gene 1 (Rig I), signal transduction leads to the phosphorylation and dimerization of interferon regulatory factors (IRF) in a mitochondrial-antiviral signaling protein (MAVS) dependent manner. Following activation, IRFs traffic to the nucleus and initiate transcription of Type 1 IFNs (IFNα and β). Type 1 IFN signaling leads to upregulation of hundreds of interferon stimulated genes (ISG) and confers an “antiviral state,” upon the cells (Garcia-Sastre, 2001). Studies of the different species of IRFs show that when cells or mice do not carry the full complement of IRFs, differential innate immune responses are initiated leading to differential outcomes for the infected subject (Morin et al., 2002). We want to determine what role specifically IRF3 is playing during influenza infection of IRF3-depleted mice. We have found that loss of IRF3 leads to survival benefits and changes in the adaptive immune response

It was the purpose of this dissertation to identify and describe host factors integral to productive influenza infection. Broadly, we have described how

influenza virus exploits phospholipase D (PLD) to enter cells and avoid detection by the innate immune system to establish a productive infection. Additionally, we find that MxA is critical in the induction of the Type 1 Interferon response, and loss of MxA leads to a reduced transcriptional response after human cells are infected with influenza. Lastly, we demonstrate how loss of IRF3 can lead to a differential immune response in mice infected with influenza, leading to increased survival in mice lacking IRF3. Taken together, we have uncovered new mechanisms in the temporospatial regulation of the innate immune response to influenza virus infection.

Literature Review

The following literature review is an overview of the current knowledge of the biology of the proteins, pathways, and concepts related to the experimental work described in chapters two, three, and four. The review is divided into three sections. The Influenza biology section will outline the relevance, epidemiology, and virology. Additionally, the concepts of lipid signaling and innate immune response caused by influenza A virus infection will be discussed. The second section is focused on interferon regulatory factor 3 (IRF3) and its activity and regulation after infection, specifically after infection has been sensed by cytoplasmic pathogen pattern recognition receptors. The last section details what is known about the activation, regulation, and antiviral action of Myxovirus resistance gene 1 (MxA).

Influenza Biology

Influenza A virus infections are an ever-present threat to global health, socioeconomics, and security. Each year millions of humans are infected with circulating influenza strains, and hundreds of thousands will die from complications due to influenza A virus infections. People most affected by influenza A virus infection are the very young, elderly, pregnant, or immunocompromised. Obesity, asthma, and diabetes have also been described as risk factors for developing influenza A infections, and as the populations of developed and developing countries accrue more chronic health conditions, more people will be at risk. World health experts project 175-300 million deaths would occur today if a pandemic such as the one seen in 1918 were to arise. Indeed, in the influenza A pandemic of 2009, it has been estimated that nearly a third of the population were infected by the novel H1N1 strain. Had the pandemic virus caused more severe pathology, the world as we know it would be a very different place today. For more than 70 years influenza A virus has been studied. Many questions remain open, and many more important questions have yet to be raised.

Influenza A virus (from now influenza virus) is in the family *Orthomyxoviridae*, a family with host diversity that spans mammals, fish, and insects with a common feature of the family being a negative-sense, segmented RNA genome. In general, the influenza virion is approximately 100 nm in size, and often presents as pleomorphic in shape, with filamentous and spherical morphology most often noted (Webster et al., 1992). The negative-sense

genome of influenza virus is carried on 8 ribonucleoprotein (RNP) segments inside the virus. The RNA from these RNPs is used to synthesize up to 13 proteins: hemagglutinin (HA), neuraminidase (NA), nucleoprotein (NP), matrix protein (M) 1 and 2, basic polymerases (PB) 1 and 2, acidic polymerase (PA), nonstructural proteins (NS) 1 and 2, PB1-F2 (from open reading frame 2 of PB1), and the less well-characterized or hypothetical proteins PB1-N40 and PA-X (Dash and Thomas, 2014). Influenza virions are surrounded by an envelope which is formed of host cell membrane during the budding process. The outer structure of influenza is made up of shell of M1 (Fig. 1, brown) that is studded with HA and NA (Fig. 1, blue and magenta, respectively). The HA and NA are also viral antigens for the humoral immune response, and current influenza nomenclature relies on serotyping of HA and NA to denote each viral strain, e.g. H1N1 or H5N1. Viral RNA is wound around NP in the inside of each virion, forming RNPs (Fig. 1, gray). The M2 protein (Fig. 1, purple) acts a proton pump to adjust pH in the virion and vesicles during entry and new viral material synthesis. The polymerase proteins, PB1, PB2 and PA, handle the business end of transcription once RNPs have entered a cell's nucleus. After a primary round of translation, PB1-F2, NS1, and NS2 function somewhat as virulence factors, influencing apoptosis and innate immune signaling.

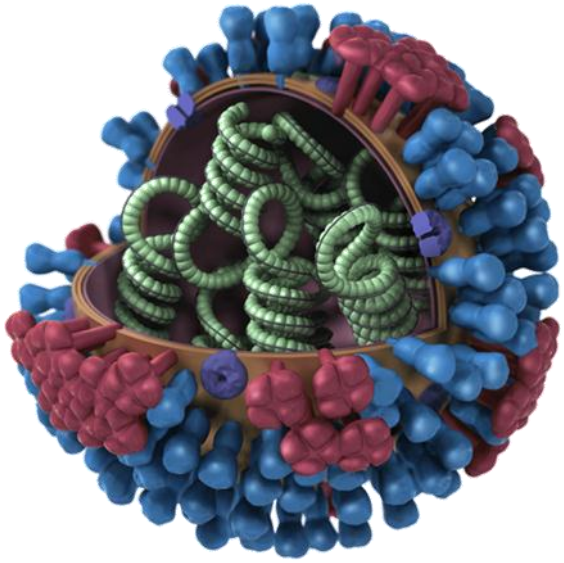

Figure 1. Schematic of an influenza virion. A spherical influenza virion, with a cutaway allowing three dimensional view of inner and outer structures. Blue stalks represent HA, magenta stalks represent NA, purple pores are M2 ion channels, and gray bundles depict RNPs. Adapted from http://www.cdc.gov/flu/images.htm

Influenza virus naturally exists in migratory waterfowl such as ducks normally causing no discernible disease. The birds shed influenza virus through feces (Medina and García-Sastre, 2011). Contact with contaminated fomites, biological and environmental particles carrying virus, can then establish infection in a susceptible host, and these unnatural infections can present as myriad disease states, from asymptomatic to catastrophic (Webster et al., 1992). Thus, in the beginning, influenza was a zoonosis originating in waterfowl and affecting species including domestic poultry, pigs, seals, horses, whales, and humans (Fig. 2). Combine the occasional zoonotic transmission alongside the global movement of people, migrations of wild birds, and industrial meat farming, and now influenza virus is endemic in not only people as a seasonal affliction but in

millions of poultry flocks and swineherds as well. The establishment of different wells of influenza strains is however not purely incidental. The ecological relationship between hosts of influenza is built upon molecular differences in viral strains and host biology.

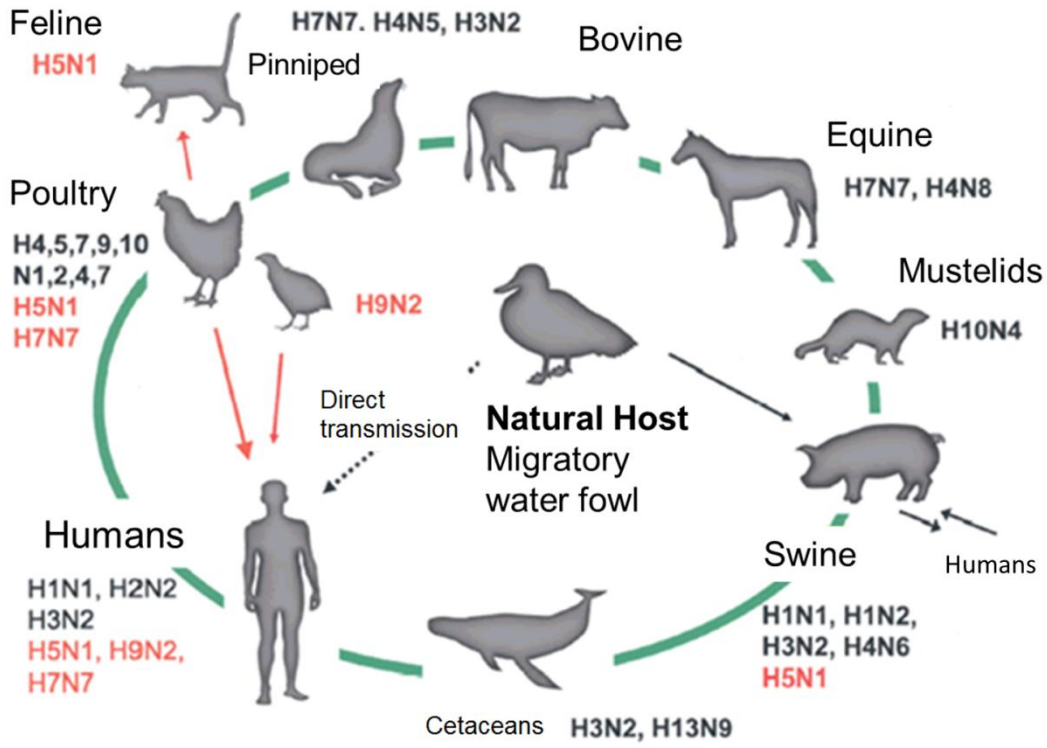

Figure 2. Transmission of influenza from waterfowl to susceptible hosts. Influenza virus exists in nature as an asymptomatic parasite of migratory waterfowl, the 'primordial' reservoir. From the natural host, influenza can be disseminated to a variety of birds and mammals. Typical influenza strains are denoted near each species. Adapted from http://www.medicalecology.org/diseases/influenza

To initiate influenza entry into a target cell, the HA first binds to sialic acid moieties on host membranes. Avian strains of influenza typically prefer α-2,3-sialic acid species, and these receptors typically line the digestive and respiratory epithelial cells of birds (Shinya et al., 2006). Influenza strains affecting humans avidly bind α-2,6,-sialic acid residues (Chandrasekaran et al., 2008). Correspondingly, the cells lining the bronchi of humans are enriched for those same glycolipids. In pigs, whose respiratory epithelial cells express both α-2,3, and α-2,6,-sialic acid residues, virologists have postulated that a human and/or avian preferring virus could reassort with endemic porcine influenza, generating the potential for the emergence of novel influenza strains with pandemic potential via drift and shift of influenza genetic material. Despite this common conclusion, numerous reverse genetics studies in which laboratory strains of influenza are created containing any combination of genes from donor isolates of influenza have not determined any particular gene constellation that can predict pathogenicity of a novel strain (Lipatov et al., 2004). The reality is much more complicated than scientists would like; there is a complex interplay of host and viral factors at loggerheads in each unique host population and virus strain to determine fitness in any system.

The greatest threat to public health posed by influenza virus is the generation of novel strains leading to pandemic. In the modern era, four major influenza pandemics have been documented. The Spanish flu of 1918 has been implicated in the deaths of 100 million people (Taubenberger et al., 2001). Over 70 thousand Americans were killed in the 1957 Asian flu pandemic, and more

than 30 thousand people in the US perished during the 1968 Hong Kong flu pandemic (Lipatov et al., 2004). In 2009, genetic shift led to the so-called swine flu pandemic. In the US, more than 60 million people were infected resulting in more than 12,000 deaths (Shrestha et al., 2011). Infections were reported in 214 countries 12 months after the virus emerged (Medina and García-Sastre, 2011). The 2009 pandemic strain was distinct from the seasonal influenza strains circulating at the time in that it was more likely to infect cells in the lower respiratory tract thanks to an HA protein that could bind both α-2,3, and α-2,6,-sialic acid residues on target cells (Maines et al., 2009). As the media fervor of the pandemic waned, much of the public expressed frustration with the response and calls for vaccination. Lay people do not understand that a pandemic does not necessarily equate to calamitous deaths. In less than a year, the pandemic H1N1 infected more than a third of the global population and displaced the seasonal H1N1. From a viral fitness standpoint, the pandemic strain performed exceptionally, by not killing the host the virus ensures efficient replication and wide transmission. As of 2015, the pandemic strain is the dominant H1N1 circulating seasonally.

The primary interest of our research is to understand the events occurring in the first few cells infected by influenza in hopes of finding a pathway or protein target that can disrupt or prevent productive infection with little or no harm to the host. Once an influenza virus encounters cells it can infect, the virion must gain entry to the cell. The pathway most often used by influenza virus for entry occurs in a clathrin-mediated endocytosis manner, (Rust et al., 2004). It should be

stated that influenza viruses have also been shown to enter cells using alternative routes, but these modes of entry are highly specific to influenza strain and cell culture model (Fujioka et al., 2011; Sieczkarski and Whittaker, 2002; de Vries et al., 2011). Regardless of the method used to gain entry, once in the cell influenza virus must be trafficked through the endosomal maturation process until the late endosome phase (Lakadamyali et al., 2004). Influenza HA protein attaches to sialic acid residues on the cell surface, triggering formation of a clathrin coated pit and dynamin-dependent pinching off of an endosome containing the virus (Roy et al., 2000). These endosomes are then trafficked through the cell in a microtubule-dependent manner (Lakadamyali et al., 2003). Endosome sorting markers Ras-related protein (Rab) 5 and Rab7 are needed for proper maturation of the vesicles in to early (Rab5) and late (Rab7) endosomes (Sieczkarski and Whittaker, 2003). As the endosome matures, the interior is acidified, and when a pH of ~5 is reached, a conformational shift of the viral HA creates a fusion pore between the viral and endosomal membranes (Yoshimura and Ohnishi, 1984). The pH of fusion is different depending on the identity of the HA (Mair et al., 2014). Once the pore is formed, influenza RNPs are ejected into the cytoplasm (Skehel and Wiley, 2000). After gaining admittance to the cytoplasm, the RNPs diffuse into the host cell nucleus, and the presence of multiple nuclear localization signals on the NP are thought to be a driver of nuclear import of influenza RNPs (Martin and Helenius, 1991). The entry process used by influenza remains controversial however. It appears that there are lab, cell, and viral-strain specific mechanisms that obfuscate any clear, unifying

theory of influenza invasion, and it may very well be the case that, being an opportunistic parasite, influenza virus takes advantage of many pieces of the puzzle to gain entry by any means necessary.

Once the viral RNPs gain entry to the nucleus, the negative sense viral RNA segments are used to transcribe messenger RNA (mRNA) and complementary RNA (cRNA). The mRNA is used to begin viral protein production, and the cRNA is used as a template to replicate the viral genome. The viral RNA-dependent polymerase add a poly(A) tail the viral mRNA, and PB1 and PB2 acquire a 5' cap from the host in a process called cap snatching (Amorim and Digard, 2006; Zheng et al., 1999). These modifications of the viral mRNA allow it to be exported from the nucleus and translated by the host cell machinery (Bouvier and Palese, 2008). The viral proteins are synthesized in the cytoplasm and sent to the Golgi apparatus where protein folding and posttranslational modifications occur similar to how host proteins are processed (Josset et al., 2008). New viral proteins and genome begin to congregate via packaging signals encoded in the viral RNAs (Fujii et al., 2003). Viral components are incorporated into vesicles and trafficked to the host cell membrane (Bruce et al., 2012). The proper assembly and sorting(Amorim and Digard, 2006) of new viral components is dependent on the viral M2 protein (Rossman et al., 2010) and host cell Rab11 (Bruce et al., 2010). The viral HA aggregates to host cell sialic acid residue, and at the membrane, the viral NA begins cleaving host sialic acid residues and the budding virion is released from the host cell, taking with it a piece of the host membrane that forms the viral

envelope (Bouvier and Palese, 2008). The newly released virions are then able to infect other cells. A simplified model of influenza virus protein function, entry, replication, and budding can be viewed in Fig. 3. It is important to note that, little to no proofreading occurs during RNA virus replication, and all of this newly synthesized genetic material is prone to mutation, referred to as genetic drift (Liu et al., 2009). Occasionally, two distinct influenza viruses may infect a single cell. Gene segments can be exchanged, resulting in the emergence of a novel influenza strain, a process called genetic shift. Both genetic shit and drift afford influenza virus the opportunity create progeny never encountered by the host. If the host has no preexisting or cross-reactive immunity to these new viruses, then uncontrolled replication and transmission may occur, potentially creating a pandemic.

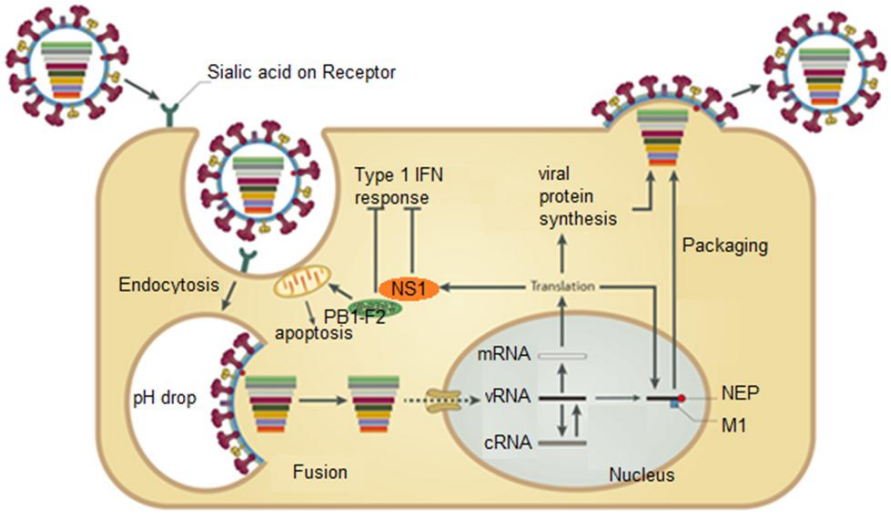

Figure 3. Influenza replication. The influenza viral proteins have missions during infection. The HA binds to the cell membrane and creates a fusion pore to release RNPs. PB1-F2 and NS1 antagonize intracellular defense mechanisms. The polymerases ensure new protein and genome replication, and NA induces scission of the budding virus from the membrane. Adapted from (Medina and García-Sastre, 2011).

The role of lipid biology and signaling during influenza infection has been understudied. Lipids are intimately linked in myriad signaling pathways, and would most likely have some function in the context of influenza invasion. Lipid rafts in the host cell membrane are used by influenza virus in both entry (Takeda et al., 2003) and egress (Carrasco et al., 2004; Ohkura et al., 2014). In fact, disruption of the lipid raft-influenza virus relationship has been a target of antiviral compound research (Agarwal et al., 2013). Sphingolipid metabolism is affected by influenza virus infection and may contribute to changes in host immune regulation and viral entry (Vijayan and Hahm, 2014). Another important node in lipid signaling networks is the phosphatidylinositol-3-kinase (PI3K). This molecule was shown to have dual roles in influenza infection, entry and innate immune signaling (Ehrhardt et al., 2006). Later, PI3K was determined to be a requirement for clathrin-independent entry of influenza virus (Fujioka et al., 2011). The adaptor protein Epsin 1 specifically tags clathrin coated pits containing influenza virus (Chen and Zhuang, 2008). The 25-hydroxycholesterol lipid species can contribute to an increase in immunopathology after influenza infection (Gold et al., 2014). Related, the statin family of drugs that mediate cholesterol biosynthesis are thought to be therapeutic in the context of influenza infection due to disturbing viral trafficking and as an inflammation mediator (Mehrbod et al., 2014). Recent work by our lab has identified another lipid metabolism enzyme playing an important role during influenza infection.

Phospholipase D (PLD) is a membrane bound phosphodiesterase responsible for hydrolyzing phosphatidylcholine into phosphatidic acid (PA) and

choline. The most well documented function of PLD is its contribution of PA in the Kennedy pathway of lipid turnover. PLD makes PA which is used by PA phosphatase to generate diacylglycerol (DAG), and both PA and DAG have multiple roles, including lipid signaling molecules and components of cell membranes. Two isoforms of PLD (PLD1 and PLD2) exist in humans, and there is evidence of a less characterized, third form of PLD that is mitochondrial (MitoPLD) (Gao and Frohman, 2012). While PLD1 and PLD2 share many similarities including 50% homology, requirement of the cofactor phosphatidylinositol 4,5-bisphophate ($PI(4,5)_2$), and stimulation by ADP-ribosylation factor (ARF), the isoforms differ in regulation, localization, and activation (Brown et al., 1993). Found mainly in the Golgi apparatus, PLD1 in not constitutively active needing direct stimulation by Rho GTPases and protein kinase C (PKC) α and β (Singer et al., 1996). Isoform PLD2 is found in plasma membrane, is constituitively active, regulated by various forms of PKC, and not affected by Rho proteins (Hammond et al., 1997). In cells that professionally exocytose material, such as neurons, PLD1 was implicated as a regulator of exocytosis (Humeau et al., 2001). In stromal or epithelial cells, PLD2 was required for proper endocytosis and sorting of incoming ligands (Padrón et al., 2006; Shen et al., 2001). A general link between pathways regulated by PLD, endocytosis, and influenza virus infection has been established (Sieczkarski et al., 2003). Using isoform-specific small molecule inhibitors of PLD (Scott et al., 2009), we investigated the interplay between PLD, viral trafficking, and the innate immune system. We found that PLD2 activity is enhanced by influenza virus

infection and this increase in activity allows for an efficient entry coupled with an escape from early detection by the antiviral defense network (Oguin et al., 2014). Our work demonstrated that there are underappreciated temporospatial regulatory networks that can be exploited to defend against viral insult. Further investigations are aimed at characterizing new PLD inhibitors to further dissect the timing of the PLD/innate immune system interplay, and using our data to develop new antiviral strategies.

The innate immune response is first line of defense against viral infection, and the type 1 IFN family of cytokines are critical members of the innate response (Sadler and Williams, 2008). In fact, some IFNs are currently being used therapeutically in some cancers, multiple sclerosis, and hepatitis C virus infection (Borden et al., 2007). The innate immune response to influenza virus infection functions to establish a local antiviral state at the site of infection while also priming the adaptive immune response for an antigen specific attack on infected cells (García-Sastre, 2011). To date detection of incoming influenza virus has been thought to rely on sensing viral genomic material, either directly from invading pathogens or from byproducts of the replication process.

Membrane-bound molecules such as Toll-like receptor (TLR) 3 initiates antiviral signaling when double-stranded RNA is encountered, and the ligand of TLR7 is single-stranded RNA (Blasius and Beutler, 2010). Ligand – receptor interactions in the case of TLRs leads to recruitment of adaptor molecules such as TRIF or MyD88, activation of IRF family members, and subsequent induction of type 1 IFNs. Influenza genomic material in the cytoplasm is detected by RigI

(Yoneyama et al., 2004). Then RigI and MAVS will complex at the mitochondrion to recruit and activate IRF3, to beginning expression of IFNβ. Following detection, of influenza virus the first wave of IFNβ binds to the IFN α/β receptor on surrounding cells, and signaling through the JAK/STAT pathway leads to expression of hundreds of IFN-stimulated genes and the establishment of an antiviral state (García-Sastre, 2011). It is not yet known if other influenza material, such as proteins or viral envelope can be detected by the innate immune system. Interestingly, the influenza non-structural protein (NS) 1, has been implicated in antagonizing the type 1 IFN response (Hale et al., 2008), demonstrating that influenza is continuing to evolve defense strategies of its own. The innate immune response to influenza virus infection will be discussed more specifically in IRF3 and MxA sections of this review.

Interferon Regulatory Factor 3

For more than 20 years, the interferon regulatory factor (IRF) gene family has been known to potently activate the production of Type I interferons (IFN) and subsequent interferon-stimulated genes (ISGs) in cells in response to myriad stimuli and stressors. Recently, IRFs have been gaining attention from being recognized as the final piece in signaling scaffolds during some viral infections, in particular those viruses that are sensed by retinoic acid inducible gene 1 (RigI)-like receptors, and Toll-Like Receptors (TLR) 3 and 9. In the context of “the first cell infected,” viruses are sensed by membrane-bound or soluble receptors and signaling cascades are induced, leading to IRF3 and IRF7 activation, driving the cell to enter an antiviral mode in which antiviral molecules are expressed

alongside extracellular molecules that can warn nearby cells and prime the tissue for induction of an adaptive immune response.

The goal of type 1 IFN response is to warn surrounding cells of incoming pathogens and to mobilize defense proteins to arm against infection. The importance of the type 1 IFN response to pathologies cannot be more succinctly demonstrated in mice lacking functional IFNα/β receptors (IFNAR). These mice are susceptible to myriad infectious challenges (Haller et al., 2006). Using the mouse model, several restriction factors for viral infection have been identified. For example, Myxovirus resistance gene 1 (Mx1) (analogous to MxA in humans) has been well described. Adding functional Mx1 back to the mouse makes it resistant to influenza virus challenge (Arnheiter et al., 1990). In the case of West Nile virus infection, 2'-5'-oligoadenylate synthetase (OAS1b), conferred immunity to mice in the laboratory (Mashimo et al., 2002). In humans, mutations in type 1 IFN genes can lead to decreases in immune fitness (Dupuis et al., 2003) as well as development of autoimmune disorders including systemic lupus eythematosus (Theofilopoulos et al., 2005) and insulin-dependent diabetes (Baccala et al., 2007). Genetic changes in interferon regulatory factor 3 (IRF3) have also influenced the outcome of bone marrow transplantation in patients with acute myeloid leukemia (Martín-Antonio et al., 2013). Recently, human populations with mutations of the ISG interferon-induced transmembrane protein 3 (IFITM3) were more likely to respond poorly to the 2009 influenza pandemic (Everitt et al., 2012).

With the proliferation of knockout and knock-in mouse lines, individual genes can be studied in whole-animal models to assess their importance or contribution to antiviral immune responses. This methodology also comes with one imperative, but oft overlooked, caveat: many inbred mice available today already carry mutations in innate defense genes due to founder effects during the establishment of colonies. It is up to the researcher to take the initiative to investigate all possible effects these mutations could have on their research goals. It must also be said that pathogens are not without their own sets of tools. Many viruses have evolved strategies to hide from or directly antagonize components of the type 1 IFN response. As interesting as their survival strategies are, however, it is the point of this review to focus on the host. Due to the complexity and subtlety of pathogens' own defense strategies, more focused review on that subject is covered in (Garcia-Sastre and Biron, 2006; Haller et al., 2006; Iwasaki and Nozima, 1977)

Depending on the identity of the stimulus, the type 1 IFN response can be initiated in several manners. To be most efficient in regards to this dissertation, the TLRs, nod-like receptors (NLR), and nuclear factor kappa-light-chain-enhancer of activated B cells (NFκB) models of the type 1 IFN response will not be discussed in depth. The IRF members of the pathway do not exist in a vacuum, and many studies have identified crosstalk of TLR, NLR, and NFκB leading to downstream activation of IRFs. More information concerning the type 1 IFN response due to signaling from TLRs or NLRs has been reviewed (Honda and Taniguchi, 2006). This work will be more concerned with the IRF family of

transcription factors, in particular the differential response to infection that occurs when an IRF is lost. It is the focus of this dissertation to look at the 'classical pathway' (Haller et al., 2006) of type 1 IFN induction during the very early events that occur after infection, specifically the RigI to mitochondrial antiviral-signaling protein (MAVS) to IRF3 pathway. The so-called classical pathway of type 1 IFN gene expression is summarized in Fig. 4.

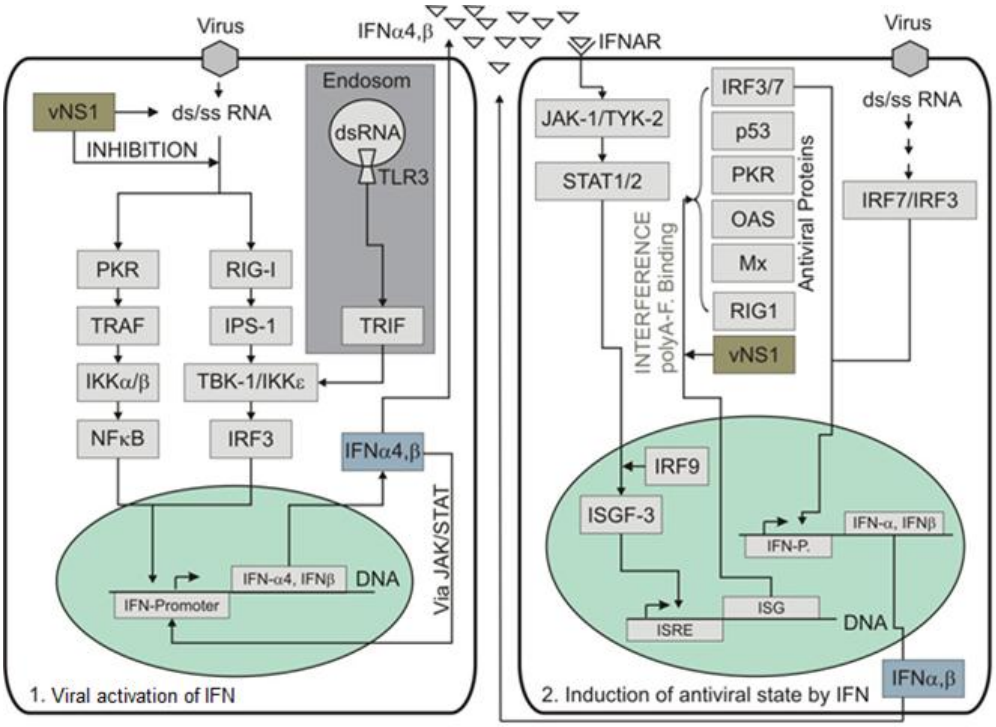

Figure 4. The classic model of type 1 IFN response. Viruses or viral-components are sensed by receptors in (RigI or MDA5) or on (TLRs) a cell. Intracellular type 1 IFN signaling molecules are then recruited and activated resulting in the induction of IFNβ production. Adjacent cells stimulated by IFNβ then induce the production of interferon stimulated genes. Adapted from (Haller et al., 2006).

There are nine known mammalian IRF family members, and each contains an approximately 120 amino acid, N-terminal helix-turn-helix motif that functions as a DNA binding domain targeting the IFN stimulated response element (ISRE) present on many type 1 IFN inducible genes (Honda and Taniguchi, 2006). In particular to the IFNβ ISRE, IRF3 assembles with other scaffolding proteins to form an enhancesome responsible for altering chromatin structure to allow IFNβ transcription (Seth et al., 2006). Gene targeting studies have found that IRF3 is constitutively expressed in all tissues and can directly target genes such as IFNβ, chemokine (C-X-C motif) ligand 9 (CXCL9), and CXCL10 demonstrating an important role in not only innate defense but in priming the adaptive response as well (Honda and Taniguchi). Similar studies have also determined that while IRF7 expression is constitutive, expression is enhanced by type 1 IFN signaling and will then lead to expression of IFNβ and IFNα (Honda and Taniguchi, 2006). Additionally, IRF7 function has been investigated more in dendritic cells than epithelial cells. The focus of this work is to discuss early innate immune signaling in epithelial cells, so accordingly IRF7 and dendritic cells will not be discussed thoroughly.

Incoming insults are sensed by cytoplasmic or membrane-bound receptors. RigI senses 5'-triphosphorlyated RNA (Kato et al., 2005). Melanoma differentiating-associated protein 5 (MDA5) recognizes double stranded RNA (Kato et al., 2006). These two surveillance molecules are present at basal levels in nearly every tissue and are stimulated by the type 1 IFN response, making RigI and MDA5 a good way to amplify antiviral signaling in an efficient manner. It

is important to note at this step, differing pattern recognition receptor substrate availability alongside subtleties in temporal-spatial signaling responses lead to differential innate immune responses (Génin et al., 2009). If one of these pattern recognition receptors encounters its target, then dimerization and ubiquitinylation (Yoneyama et al., 2015) lead to a conformational shift, exposing a caspase activation and recruitment domain (CARD). The CARD of the pattern recognition receptor then interacts with a CARD on MAVS (Kumar et al., 2006; Sun et al., 2006). At the mitochondrion, MAVS aggregates into fiber-like structures (Hou et al., 2011) to begin recruiting a signaling scaffold including TANK-binding kinase-1 (TBK1) (Fitzgerald et al., 2003) and inhibitor of nuclear factor kappa-b kinase subunit epsilon (IKKε). The terminal, downstream action of this signaling complex is to facilitate the dimerization and phosphorylation of IRF3 (activated form called p-IRF3). After IRF3 is phosphorylated by TBK1 and/or IKKε, p-IRF3 homodimerizes and coactivators of transcription p300 and CREB-binding protein (CBP) are recruited by p-IRF3 to initiate IFNβ expression and beginning the first round of antiviral gene expression (Haller et al., 2006). Lipid signaling though phosphatidylinositol-3-kinase (PI3K) and inositol pyrophosphate 1-IP7 have also shown to be necessary for complete IRF3 activation (Hrincius et al., 2011; Pulloor et al., 2014), respectively. It is thought that IRF3 is kept in a latent, nonactive form in the cytoplasm of uninfected cells through interactions between the IRF association domain of IRF3 and the IRF3 binding domain of CBP (Lin et al., 2000). This autoinhibition in unstimulated cells also keeps IRF7 in a latent state as well (Yang et al., 2003).

Outside of the cell, secreted IFNβ binds to the type 1 IFN receptor in a paracrine/autocrine manner, prompting another signaling complex that includes Janus kinase 1 (JAK1) and signal transducers and activators of transcription (STAT 1 and 2). Post-interferon β signaling leads to activation of IRF3 and IRF7, causing expression of more IFNβ, IFNα and ISGs including MxA, OAS, and protein kinase R (PKR), establishing in the cells a more potent antiviral state in the affected tissue.

Other researchers have gone on to propose a biphasic model of type1 IFN activation detailed in Fig. 5, where IRF3 induces IFNβ expression (early wave) and subsequent signaling in surrounding cells leads to IRF7 activation of IFNα and many ISGs (later phase). More emphasis is placed on the 'later' phase of signaling where pattern recognition receptors are responding to pathogens in the presences of type 1 IFN. While delineating these pathways is very important to understand immune signaling, it would seem very important to understand the events that occur in the first cell infected. If the events that lead to a successful infection in the first cell are uncovered, then targets/signaling complexes could perhaps become prophylactic drug targets aiming to prevent people from becoming infected during a pandemic situation. The technical aspects of studying the very early immune response are daunting, but as advances in technology continue to assist investigators, the entire infection and immune response can be detailed.

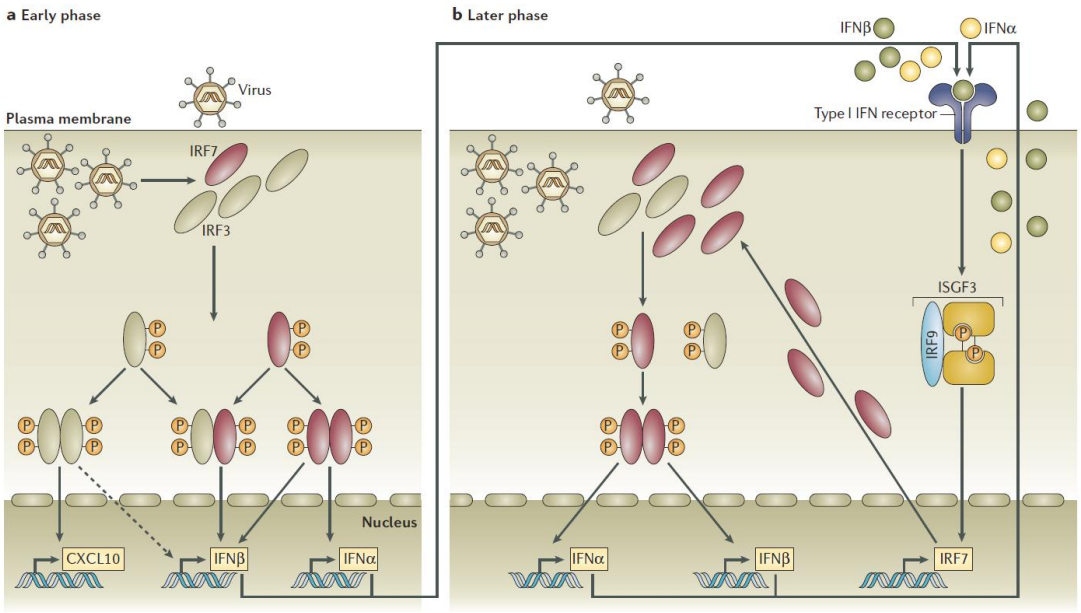

Figure 5. The biphasic model of the type 1 IFN response. The early phase of activation is comprised of danger signal sensing followed by IRF3 and IRF7 activation leading to a release of type 1 IFNs and chemokines. The later phase of the type 1 IFN response includes the sensing of danger in the presence of type 1 IFNs. This leads to the formation of the ISGF3 complex, further stimulating ISGs. Adopted from (Honda and Taniguchi, 2006).

Current evidence points to a more detailed biphasic response; the type 1 IFN response appears to begin with an initial wave of IRF3 activation, leading to IFNβ production. Downstream of IFNβ in surrounding cells, IRF7 activates and initiates transcription of the IFNα genes and subsequently, many of the ISGs. After the first step of IRF3 to IFNβ activation, IRF7 then potentiates the antiviral state by going on to induce more genes in the type 1 IFN response. It must be noted that many genetic studies have used inbred mice engineered to lose certain genes. Many of these mice are already deficient in several important innate defense genes (such as Mx1 or OAS1b). Using knockout mice on these

backgrounds confounds research because of the introduction of more variables than are unaccounted for or even mentioned by authors of these studies. In addition to the poor study design when planning to use these mice in research, many experiments use mouse embryonic fibroblasts (MEFs) or other easily sampled cell sources. While this approach is efficient for increasing sample size and limiting confounding factors introduced by using whole animal models, special attention is required to model correctly the infectious agent and host tissue in a physiologically relevant paradigm. For example, influenza studies should be ideally conducted in cells that are representative of respiratory epithelium instead of cells from a human embryonic kidney.

In an initial study using multiple gene deletions and additions, MEFs with deletions in IRF3, 7 and/or 9 as well as IFNα receptor 1 (IFNAR1) were infected with Newcastle Disease virus. To determine activation of the type 1 IFN response, downstream proteins such as OAS, PKR, or ISG15 levels were measured by western blot. The data gathered from this study suggest that type 1 IFN response genes are segregated such that IFNβ production is accomplished with IRF3 or IRF7, but IFNα production and subsequent gene expression is dependent on IRF7 only (Nakaya et al., 2001). While thorough and convincing, this study remains puzzling due to the methodology. While it is possible to force MEFs which have been subject to retroviral transformation to undergo a response to a virus which affects high throughput poultry operations, it does not necessarily predict what signaling will occur in an animal experimentally infected with a physiologically relevant agent. Regardless of the limitations of this study,

useful data and conclusions can be reaped from the work, and interesting data regarding the actions of IRF3 on expression of other soluble factors such as CXCL10 is exciting. In mice lacking IRF3, a defect in expression of CXCL9 and CXCL10 was noted after LPS stimulation (Sakaguchi et al., 2003; Werner et al., 2005). In a more recent experiment using rotavirus infection of MEFs, the early antiviral response was dependent on IRF3 (Sen et al., 2011).

In a more relevant experimental model involving mice infected with Dengue Virus, researchers found that IFNα/β levels in infected $IRF3^{-/-}$ mice were similar to wildtype mice. However in $IRF7^{-/-}$ and $IRF3^{-/-}$ $IRF7^{-/-}$ mice were found to have low levels of IFNα/β in serum 6 - 24 hr after infection and impaired expression of IFNα/β mRNA in spleens 72 hr after infection (Chen et al., 2013). In the same study, the serum of $IRF3^{-/-}IRF7^{-/-}$ mice had higher amounts of IFNγ, IL6, CXCL10, IL8, IL12p70, and TNF in serum 24 hours after infection alongside carrying higher viral titers in spleen, lung, and kidney (Chen et al., 2013). The researchers concluded that IRF3 and IRF7 played somewhat redundant roles in IFNα/β induction, but IRF7 was relied upon more than IRF3 in the initial IFNα/β response. It is interesting that a loss of both IRF3 and IRF7 leads to higher levels of CXCL10, IFNγ, and IL6 after infection as it appears the double null mice are skewing toward a type 2 IFN and adaptive immunity response to combat the infection. Blocking IFNγ with antibodies injected into the mice ablated CXCL10 levels (Chen et al., 2013), indicating that IFNγ is critical for inducing expression of the chemokine when IRF3 and IRF7 are lost perhaps pointing to a role for T cells to play as a backup response when the innate immune system is

compromised. In a similar study in our lab, we find that IRF3$^{-/-}$ mice infected with influenza have high levels of IFNγ, CXCL9, and CXCL10 in the broncheoalveolar lavage 3 days after infection leading to higher levels of CD8 T cells in the infected tissue (unpublished data). Using IRF3 single knockout mice, herpes simples virus 1 was noted to replicate to greater levels compared to wildtype mice accompanied by increases in inflammatory cytokines in the central nervous system (Menachery et al., 2010). In the past, IRF7 has been called the master regulator of the type 1 IFN immune response (Honda et al., 2005). However, it appears that this statement is highly dependent on the experimental conditions. It could be the case that different IRFs are required for the proper induction of the immune response in different experimental conditions. In fact, outside of innate defense, activation of the type 1 IFN response can lead to dendritic cell maturation, antigen presentation, chemokine secretion, CD8 T cell response, CD4 T cell polarization, protein synthesis, antibody affinity maturation, and cell survival signaling (Lendonck et al., 2014).

In addition to the classical pathway of type 1 IFN activation through IRF3 and IRF7, recent evidence has added another adaptor protein, stimulator of interferon genes (STING), that mediates type 1 IFN activation when double stranded DNA (Ishikawa et al., 2009) or cyclic dinucleotides (Burdette et al., 2011) is detected in cytoplasm . Upon activation, STING dimerizes and recruits TBK1 (Tanaka and Chen, 2012) where it can phosphorylate IRF3 to initiate a type 1 IFN response. These events take place at the mitochondria where phosphorylated STING and MAVS attract a positively charged area of IRF3 (Liu

et al., 2015) demonstrating that the mitochondrion is fast becoming recognized as a hub for type 1 IFN signaling. In fact, translocase of outer membrane 70 (Tom70) is critical in the mechanical incorporation of MAVS into the mitochondrion, and loss of Tom70 leads to an weakened type 1 IFN response due to decreased recruitment of TBK1 and IRF3 to MAVS (Liu et al., 2010). Interferon β production resulting from a MAVS to IRF3-dependent pathway is sufficient to control human metapneumovirus in neonatal mice (Spann et al., 2014). The recent findings regarding alternative signaling through IRF3 are another exciting piece of the innate immune response puzzle.

Function and regulation of Myxovirus resistance gene 1

Myxovirus resistance gene (Mx) 1 was first described in mice as restriction factor required to defend against lethal influenza challenge over 50 years ago (Lindenmann, 1962). Since that time, the details of expression induction (Holzinger et al., 2007), various viral targets (Haller et al., 2007a), and structure and function (Verhelst et al., 2013) of Mx proteins have been described. In humans the Mx1 protein is denoted as MxA. Lately, MxA is gaining attention as clinically relevant molecule to study because of its involvement in various pathologies. For example, in certain Chinese populations, polymorphisms in the MxA gene can be a predictor of susceptibility to enterovirus 71 (Zhang et al., 2014). Men who carry the rs2071430 genotype (GG) in the promoter of MxA are more at risk of developing prostate cancer than men with a GT genotype (Glymph et al., 2013). Additionally, MxA expression has been used as a biomarker for type 1 IFN responses or therapeutic changes in several disease

states such as Multiple Sclerosis (Bertolotto et al.), vitiligo (Bertolotti et al., 2014), Sjögren's syndrome (Maria et al., 2014), hepatitis (Bolen et al., 2012), and AIDS (Furuya et al., 2014). The Mx proteins are therefore very attractive targets of further research.

To date, we know that Mx genes are conserved evolutionarily down to jawless fish, and all studied Mx proteins exhibit antiviral properties of various efficacy. In Fig. 6, the evolution and conservation of Mx proteins can be appreciated. A summary of different Mx proteins and their antiviral activity is illustrated in Fig. 7. Previous reports suggest that MxA has antiviral activity against diverse RNA virus families including *orthomyxovirus*, *paramyxovirus*, *bunyavirus*, *picornavirus*, *rhabodyvirus*, and *togavirus*, as well as several DNA viruses such as *hepadnavirus*, *orthopoxvirus*, and *Asfarvirus* (Mitchell et al., 2013). This impressive list of potential targets of Mx proteins demonstrates the critical nature of innate immunity in the defense against various pathogens.

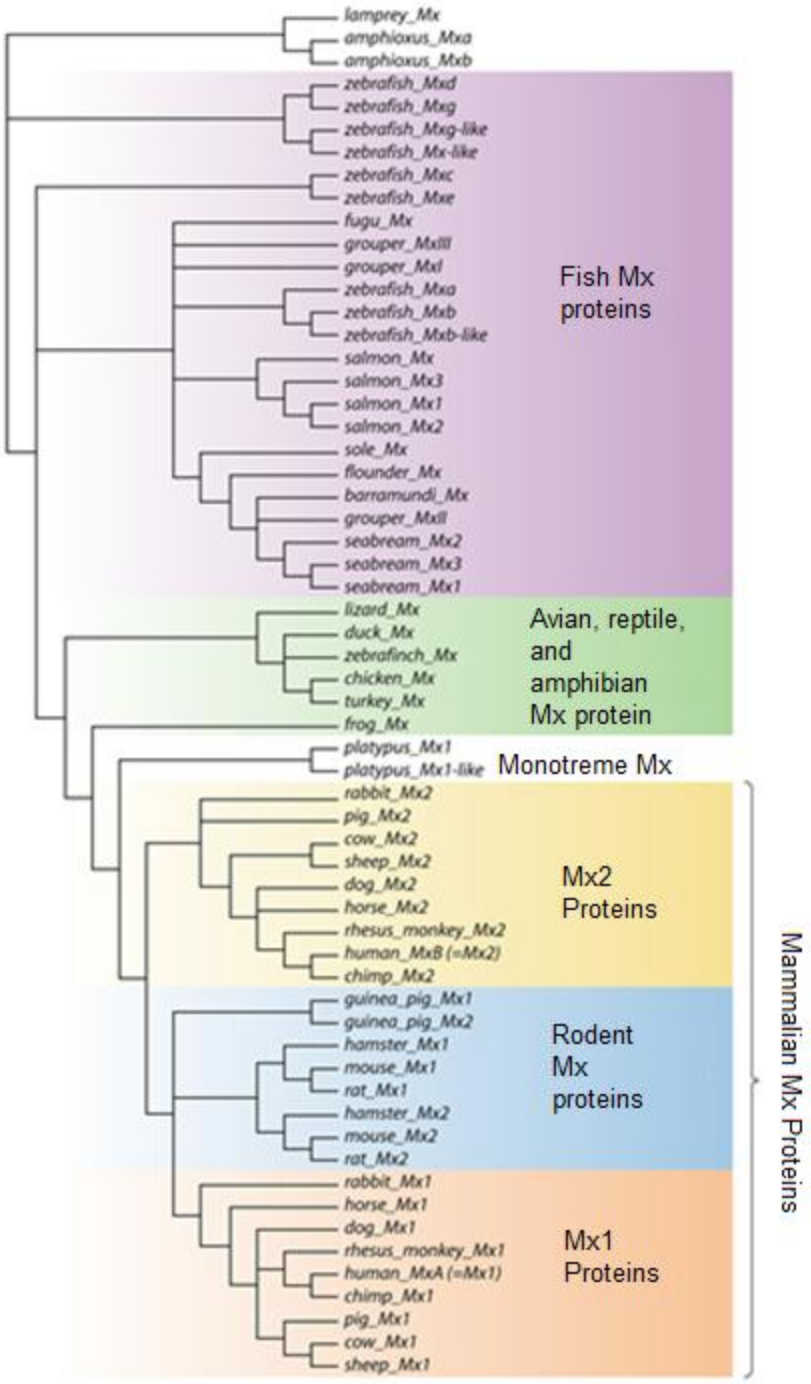

Figure 6. Phylogeny of Mx proteins in vertebrates. From fish to humans, Mx proteins have diverged in to different subsets. Adapted from (Verhelst et al., 2013).(Haller et al., 2015)

Mx protein(s)	Localization	Antiviral activity
Mouse Mx1	Nucleus	Influenza virus
		THOV
		DHOV
		BKNV
Mouse Mx2	Cytoplasm	VSV
		HTNV
Human MxA	Cytoplasm	Influenza virus
		THOV
		VSV
		Rabies virus
		HTNV
		LACV
		CCHFV
		RVFV
		PUUV
		TULV
		Measles virus
		SFV
		CSFV
		IBDV
		Reovirus
		HBV
		ASFV
Human MxB	Nucleus	None
Rat Mx1	Nucleus	Influenza virus
		THOV
		VSV
Rat Mx2	Cytoplasm	VSV
		LACV
		RVFV
Rat Mx3	Cytoplasm	None
Chicken Mx	Cytoplasm	None
		Influenza virus
		VSV
		NDV
Duck Mx	Nucleus and cytoplasm	None
Cow Mx1	Cytoplasm	VSV
		Rabies virus
Cow Mx2	Cytoplasm	VSV
Pig Mx1	Cytoplasm	Influenza virus
		VSV
Dog Mx1, Mx2	Cytoplasm	VSV
Atlantic salmon Mx1-Mx3	Cytoplasm	ISAV
		IPNV
Japanese flounder Mx	Cytoplasm	HIRRV
		VHSV
Grouper Mx1-Mx3	Cytoplasm	YGNNV
Senegalese sole Mx		Aquabirnavirus
Barramundi Mx	Cytoplasm	NNV
		IPNV-SP
Seabream Mx1-Mx3		IPNV
Rare minnow Mx		GCRV
Rainbow trout Mx1	Cytoplasm	IPNV
		SAV

Figure 7. Summary of Mx proteins throughout evolution. Antiviral activity of Mx proteins against viral challenges in different vertebrates. Adapted from (Verhelst et al., 2013).

The structure of MxA is made up of three domains, the N-terminal GTPase domain, a middle domain often referred to as the bundle-signaling element (BSE), and a C-terminal GTPase effector domain (GED) (Haller and Kochs, 2011). Fig. 8 contains an illustration of the MxA monomer, a cartoon schematic of MxA protein, and the proposed oligomerized structure (Gao et al., 2011).

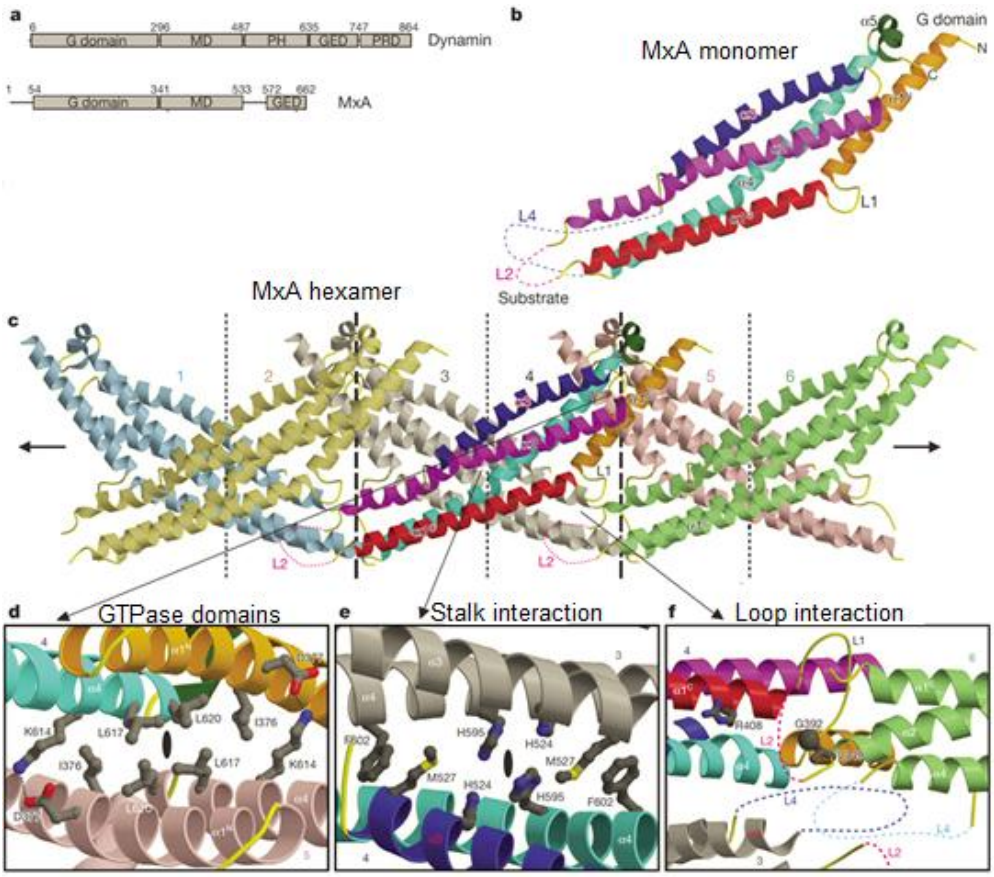

Figure 8. Mx protein structures. (A) MxA, a dynamin like protein, compared to dynamin. (B) A monomer of Mx. (C) Oligomerization of 6 Mx molecules. (D-F) Increased resolution of the Mx oligomer detailing: (D) GTPase domain orientation, (E) stalk interactions, and (F) orientation of loop regions. Adapted from (Gao et al., 2010).

The middle domain and the GED domain of MxA interact to form a stalk region around which other stalk regions oligomerize with GTPase domains hydrolyzing GTP on the outside of the ring-like oligomer (Gao et al., 2010). Similar to dynamin, the GTPase activity of MxA is described as a low-affinity for GTP with high rates of GTP hydrolysis (Mitchell et al., 2013). The oligomerization of MxA differs from its relative dynamin in that MxA monomers will self-assemble around lipid structures in a GTP hydrolysis independent manner (Malsburg et al., 2011).

MxA will assemble into oligomers, appearing as rings around liposomes and will mechanically induce tubulation of those vesicles (Haller and Kochs, 2011). Despite the lack of a pleckstrin homology (PH) domain, MxA can interact with lipids, and it is thought that the Loop (L) 4 region of the molecule mediates these interactions (Malsburg et al., 2011). This lipid binding ability may aid MxA in binding to intracellular membranes (Accola et al., 2002). Many viruses enter cells via lipid interactions, and the membrane binding of MxA may help localize it to intercept a pathogen. This L4 region of Mx proteins is highly conserved across species (Mitchell et al., 2012) and sensitive to mutation. By mutating amino acid residues at positions 561 and 526, MxA lost antiviral activity against orthomyxoviruses only, but mutations around position 577 resulted in a complete loss of antiviral activity (Patzina et al., 2014). The antiviral activity of Mx proteins is that of a mechano-chemical “intracellular wrench” (Rennie et al., 2014). Incoming viral ribonucleoproteins (RNPs) become decorated with Mx molecules, and in the case of influenza, the sequence of those RNPs determine sensitivity to

Mx (Zimmermann et al., 2011). Oligomerization of Mx proteins around viral RNPs is hypothesized to either block or otherwise interfere with viral reproduction (Verhelst et al., 2012). MxA has also been shown to block the late endosomal to nuclear transport or viral RNA in a IFN dependent manner, requiring the additional activity of the IFN-induced protein IFITM3 (Xiao et al., 2013) These findings are very interesting; implicating that previously described restriction factors need to work together to function appropriately. Of course, each vertebrate's Mx protein will have evolved to defend against that organism's pathogens, and more studies will have to be done to elucidate if Mx proteins have a singular antiviral action or if each Mx has evolved differing defense strategies. Indeed, several other methods of viral inhibition are being uncovered (Verhelst et al., 2013).

Current dogma related to Mx expression maintains that this potent antiviral effector molecule is induced by type 1 or 3 IFNs and no other soluble factor or virus (Haller et al., 2007a, 2007b, 2015; Mitchell et al., 2013). Fig. 9, taken from (Haller and Kochs, 2011), demonstrates the current hypothesis that MxA is only inducible after Type 1 or 3 IFN stimulation.

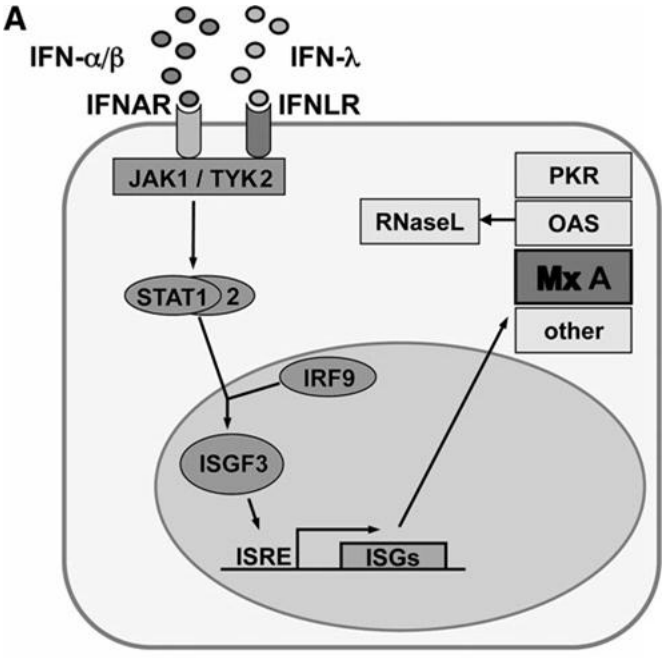

Figure 9. Current model of MxA expression. MxA is only expressed after type 1 or 3 IFNs have stimulated a target cell. Adopted from (Haller and Kochs, 2011).

Despite decades of research and data to support this hypothesis, it is puzzling that (in mice at least) the single protein responsible for defense from a lethal virus would be expressed only after IFN induction. In other words, past groups maintain that the most capable defense waits to be used until after cells are initially infected. Why would Mx not be constitutively expressed to be part of the first line defense?

Much of the evidence against constitutive Mx expression argues that basal Mx expression can cause cell death. In one such study in 293T cells (cells with an ablated IFN response), MxA was overexpressed and these human embryonic kidney cells were infected with a very high dose (10 MOI) of highly pathogenic, mouse-specific influenza virus (A/Puerto Rico/8/1934 (H1N1)), and the

researchers concluded that overexpressed MxA could inhibit cellular protein synthesis and promote apoptosis (Mibayashi et al., 2002). Despite the questionable experimental setup, the conclusion of MxA's antiviral action has later been described to be that of a "molecular wrench" which binds to viral RNPs to prevent influenza reproduction (Verhelst et al., 2012). The Mibayahsi group could overexpress MxA in 293T cells and kill the cells after a 10 MOI infection does but this is not what necessarily *will* happen in a relevant model, and after a few more years of study, their hypothesis of MxA's antiviral activity was unsupported. Another widely used source to tout the danger of constitutive MxA expression again overexpressed MxA in various cells types already engineered to be models of Faconi Anemia (Li and Youssoufian, 1997), and concluded that in these cells, IFN signaling leads to MxA expression and cell death. As stated, the overexpression model is a great system to understand what *can* happen, but it often gives little usable data regarding what *does* happen in nature.

Several of the same researchers published in 1999 that constitutively expressing MxA in IFNAR$^{-/-}$ mice are resistant to a variety of viral challenges (Hefti et al., 1999), demonstrating that MxA can fully function without type 1 IFN stimulation. If Mx expression depends on IFN stimulation, then STAT1 would be required to be part of the Jak/STAT pathway of upregulation through the IFNAR receptor. However, in mice lacking STAT1, Mx upregulation was at similar levels after a Crimean-Congo hemorrhagic fever virus challenge (Bowick et al., 2012). Admittedly, it would be more conclusive if these same experiments were conducted in mice that cannot respond to type 3 IFN as well as type 1, but much

of the available data can be used to conclude that Mx activity is not totally dependent on IFN stimulation. Many of these recent findings do not support the hypothesis that Mx proteins are only expressed after type 1 IFN signaling, and the established dogma needs revision to include the possibility that Mx proteins are basally expressed and can be stimulated by infectious challenge in addition to the actions of Mx post-IFN stimulation.

Additionally, in mice experiments where mouse or human Mx proteins are engineered to be constitutively expressed, no mention of baseline pathology has been noted (Hefti et al., 1999a; Kolb et al., 1992; Pavlovic et al., 1995). Notably, these are some of the same mouse lines generated by the same researchers who claim basal Mx expression is toxic. In China, transgenic pigs have been engineered to overexpress porcine Mx1, and these animals are more resistant to classical swine fever virus without overt or noted basal pathology due to Mx1 overexpression (Yan et al., 2014) It is the conclusion of our lab that MxA is present in basal levels in human lung cells, and MxA activity is stimulated by influenza infection very early after infection (before type 1/3 IFNs can be synthesized), and these findings have been verified by qPCR, western blot, and confocal microscopy analysis (data in MxA chapter). We would hypothesize that evolutionarily speaking; organisms would be more likely to keep a potent weapon ready for use against invasion at all times, as opposed to waiting for the invasion to gain a foothold before deployment.

CHAPTER 2

PHOSPHOLIPASE D FACILITATES EFFICIENT ENTRY OF INFLUENZA VIRUS ALLOWING ESCAPE FROM INNATE IMMUNE INHIBITION

Introduction

Lipid species play integral roles in cellular signaling and intracellular trafficking. Influenza viruses exploit these fundamental processes within the host cell to facilitate entry and subsequently drive virus replication. The cycle begins with the viral surface protein hemagglutinin (HA) binding to an epithelial cell surface sialic acid moiety. Typically, this triggers endocytosis, allowing the virus entry inside the host cell, incorporating itself within the host membrane. As the endosome matures, acidification initiates a conformational change in the HA allowing it to fuse with the host endosomal membrane and release the ribonucleoprotein complexes, which are trafficked to the nucleus where RNA-dependent polymerases replicate the viral genome and make the mRNA for viral proteins. After proteins are synthesized, they accumulate at the cell membrane, complex with viral genomes, and bud off the cell surface, forming the viral envelope from the host cell membrane. Lipids are fundamentally involved both in the entry and egress of the virus (1).

In addition to playing structural roles in viral entry and budding, lipid species also serve as intra- and extra cellular signals as part of the innate immune response. 25-hydroxycholesterol is secreted by macrophages in response to the Stat1/IFN pathway and can promote resistance to multiple viruses (2). Protectin D1 was identified as promoting an anti-inflammatory state that alleviated severe disease in an H5N1 infection (3). The 12/15 lipoxygenase

pathway that generates protectin D1 was identified in another screen as being associated with mild infection in both mice and humans (4). PI3K has been demonstrated to have a role in influenza infection and host defense (5). The lipid binding protein Epsin-1 is a regulator of clathrin-mediated endocytosis of influenza virus (6). Lipid rafts also are involved in influenza virus (7) and HIV replication (8). Clearly, lipid species are influencial during viral pathogenesis and present a ripe opportunity for further research.

Despite recent findings on the participation of sterols, arachidonic acid derived species and lipid structures (such as rafts) in the regulation of influenza infection, the roles of glycerophospholipids have been ill defined. PLD enzymes play critical roles in generating lipid signaling molecules and contributing to membrane structure. The primary lipid product of PLD, phosphatidic acid (PA), is an important bioactive lipid that is involved in membrane biogenesis and curvature, in addition to being a second messenger in signaling pathways (9,10). Specifically, PA can be converted into diacylglycerol by phosphatidic acid phosphohydrolase, which subsequently activates protein kinase C (PKC) and other signaling proteins. Prior studies demonstrated that inhibiting PKC activity during influenza infection interferes with intracellular trafficking of the virus and protects cells from infection (11). Thus, PLD appears to be a potential targetable candidate as a host restriction factor of influenza virus replication.

In mammals, the two predominant isoenzymes, PLD1 and PLD2, are well characterized. The mitochondrial form of PLD is less well studied. Recently, PLD isoform-preferring inhibitors have been designed, synthesized, and

characterized (12,13). The development of these PLD inhibitors has facilitated the interrogation of the specific role of isoenzymes in various cellular processes (14). Utilizing these novel synthetic compounds and other biochemical approaches, the upregulation of PLD activity during influenza infection is demonstrated. In addition to evidence that PLD inhibition delays virus entry, allowing for a more robust innate antiviral response to be mounted in the infected host cell, leading to a significant reduction in viral titer. Consequently, PLD is a targetable host restriction factor for influenza viruses. Influenza is using PLD to facilitate rapid endosomal trafficking and innate immune escape in the host cell.

Experimental Procedures

Chemical synthesis and purification - PLD isoenzyme-preferring inhibitors were synthesized and characterized as described in detail previously (12,13).

Mass spectrometry-based lipid analysis - For analysis of cellular lipids, A549 cells were serum starved for 1 hour, infected at 1 MOI with influenza A/California/04/2009 or other indicated strains, and then maintained in 6-well plates for the indicated treatment times. Mock infected and influenza A infected cells were harvested at indicated times after infection and administration of PLD inhibitors. To extract phospholipids, ~$1x10^6$ cells were washed with ice-cold PBS, scraped into 1 ml of ice-cold PBS, and aliquots were taken for protein analysis. After centrifugation and PBS aspiration, the pellet was extracted by a modified Bligh and Dyer method using 800 µl ice-cold 0.1 N HCl: CH_3OH (1:1) and 400 µl of ice-cold $CHCl_3$ (15). Following vortexing for 1 min at 4 °C, phases were separated by centrifugation (18,000 × g for 5 min, 4 °C). The lower organic

layer was isolated, synthetic odd-carbon phospholipids (four per phospholipid class) were added as standards, and the solvent was evaporated. The resulting lipid film was dissolved in 100 µl of isopropanol (IPA):hexane:100 mM $NH_4COOH_{(aq)}$ 58:40:2 (mobile phase A) (16). Samples containing *n*-butanol were extracted similarly and 5 µl of 10 µg/ml 32:0 phosphatidylmethanol (PtdMeOH) was added as an internal standard. Mass spectrometric analysis and quantitation were performed essentially as previously described (17-19). MDS SCIEX 4000QTRAP hybrid triple quadrupole/linear ion trap mass spectrometer (Applied Biosystems, Foster City, CA) coupled to a Shimadzu HPLC system (Shimadzu Scientific Instruments, Inc., Columbia, MD) consisting of a SCL 10 APV controller, two LC 10 ADVP pumps, and a CTC HTC PAL autosampler (Leap Technologies, Carrboro, NC) was utilized for the analyses. Phospholipids were separated on a Phenomenex Luna Silica column (Phenomenex, Torrance, CA), (2 x 250 mm, 5 µm particle size) using a 20 µl sample injection. A binary gradient consisting of isopropyl alcohol:hexane:100 mM $NH_4COOH_{(aq)}$ 58:40:2 (mobile phase A) and IPA:hexane:100 mM $NH_4COOH_{(aq)}$ 50:40:10 (mobile phase B) was used for the separation. Instrumentation parameters and solvent gradient were previously described (18). Time courses were performed in at least triplicate and repeated. Statistical analysis was performed by two-way ANOVA with Bonferroni's post-test.

Spatial infection model - A spatial infection model for testing compound efficacy and influenza replication was adapted from (20). Monolayers of A549 cells were grown on chamber slides. A semisolid overlay made of agar and

growth medium was allowed to cure on top of the monolayer. A pasteur pipette was used to create a consistent reservoir in the overlay, and influenza virus was introduced through this reservoir. Cultures were then incubated at 37 °C until time of fixation and processing for microscopy.

RNA interference - A549 cells were transfected with 100nM siRNA (Ambion) specific to PLD isoforms using NeoFX (Ambion) and were subsequently infected with 1 MOI influenza A/Brisbane/59/2007 (H1N1) for 24 hours. The indicated innate immune proteins were knocked down using 100 nM siRNA and the Neon Transfection System (Life Technologies). Knockdown was confirmed with gene specific TaqMan assays and the $2^{\Delta\Delta Ct}$ method using GAPDH to normalize alongside western blot to confirm loss of protein.

Immunofluorescence and live cell imaging - Samples were fixed in 4% formaldehyde, permeabilized with 0.3% Triton X-100, and then exposed to antisera targeting proteins of interest and corresponding fluorescent secondary antibodies alongside DAPI to visualize nuclei. Spatial infections were imaged and processed using Nikon C1Si and NIS Elements software. Confocal images were captured with a Zeiss LSM 510 NLO Meta and analyzed with Zeiss Zen 2011 software and ImageJ software (NIH). To determine colocalization, the PSC colocalization plugin was used to generate Pearson's and Spearman's coefficients. Briefly, NP and PLD2 signal channels were merged. Each Z slice was projected to maximum intensity. NP positive cells were masked, and the mask was used to determine if a positive signal for each channel colocalized. Each mask was in excess of 20000 pixels to ensure a robust data set. Live cell

imaging was performed using spinning disc laser scanning confocal microscopy, carried out on a Marianas SDC imaging system (Intelligent Imaging Innovations/3i, Denver, CO) comprised of a CSU22 confocal scan head (Yokogowa Electric Corporation) and solid state lasers with wavelengths of 488 nm and 658 nm, configured on a motorized Axio Observer Z1 inverted microscope (Carl Zeiss MicroImaging) equipped with a Definite Focus system (Carl Zeiss) and spherical aberration correction optics. Time-lapsed 3-dimensional imaging was performed at 37 °C, 5% v/v CO_2 in a humidified atmosphere using an environmental control chamber (3i), and images acquired using a Plan-Apochromat 63x 1.4 NA oil objective on an Evolve 512 EMCCD (Photometrics, Tucson, AZ) using Slidebook 5.5 software (3i).

Animal infection - All animal studies were approved by the St. Jude Children's Research Hospital Animal Care and Use Committee (Protocol # 098), following the guidelines established by the Institute of Laboratory Animal Resources, approved by the Governing Board of the U.S. National Research Council. Female C57BL/6 mice (8-10 weeks old) were anesthetized and infected with indicated doses and strains of influenza A virus. Mice were weighed and monitored daily; tissues were collected at the specified times and kept at -80 °C until analysis. For drug treatment, mice were administered 13 mg/kg VU0364739 (PLD2 inhibitor) or vehicle (10% DMSO, 90% PEG) every 8 hours from day -1 to day 3 after infection or every 12 hours during the H7N9 study. All procedures were performed according to an institutionally-approved IACUC protocol, which

includes a requirement for daily observation and euthanasia on detection of severe moribundity.

Titering - Infected animal lungs were titered using a standard plaque assay. Supernatant from infected cultures were titered using traditional $TCID_{50}$, and immunofluorescence was used to enumerate the number of infected cells in cultured samples.

Host gene expression - RNA was isolated from lungs and used in a reverse transcriptase PCR. The cDNA was then used in gene specific TaqMan assays to determine host gene expression, and the differences in expression were quantified using the $2^{\Delta\Delta Ct}$ method. Equal amounts of RNA was used in each reaction and samples were run in triplicate.

Statistical analysis - Quantitative data are presented as mean ± SEM of at least three independent experiments.

Results

Influenza infection potentiates PLD catalytic activity, and that activity is attenuated by VU0364739 treatment. To determine the effect of influenza infection on PLD activity, human adenocarcinomic alveolar basal epithelial cells (A549) were infected with 1 MOI of human influenza strain A/California/04/2009 (H1N1) for 6 hours in the presence of 0.6% *n*-butanol. Instead of the typical biological nucleophile water, in the presence of a primary alcohol PLD will utilize the alcohol to produce a metabolically stable transphosphatidylation product, phosphatidylalcohol, as an alternative to hydrolysis producing PA, that can be measured by mass spectrometry. Figure 1*A* illustrates that influenza infection

markedly stimulates PLD activity as measured by the increase in phosphatidylbutanol (PtdBuOH) production compared to cells that were not exposed to influenza virus (mock infected). Treatment with a PLD2-specific inhibitor, VU0364739, is sufficient to block the influenza mediated PLD activity increase. As shown in Fig. 1*B* both PLD1 and PLD2 are active during the viral entry phase and complete ablation of catalytic activity requires knockdown of both PLD1 and 2. This result suggests independent roles for both isoenzymes in entry.

Confocal microscopy based experiments were conducted to assess changes in the accumulation and localization of PLD during an influenza infection. A549 cells were grown on chamber slides and infected with 1 MOI influenza A/California/04/2009 (H1N1). Samples were fixed at 0, 30, 90, and 360 minutes post-infection, and were probed for influenza nucleoprotein (NP) and PLD2. PLD2 begins to accumulate at the periphery of the cell as early as 30 minutes post-infection (Fig. 1*C*, *D*, and *E*). At the same time point, very low levels of NP were detected, also occurring at the outer reaches of the cell (Fig. 1*E*). PLD2 staining continued to intensify 90 and 360 minutes post-infection (Fig. 1*D*), and the observed PLD2 signal was increasing as well as moving from the cytoplasm to a perinuclear region (Fig. 1*E*). Influenza NP signal also intensified 360 minutes post-infection, and NP was moving from the cytoplasm (30 and 90 minutes post-infection) toward the nucleus (Fig. 1*D* and *E*). During the infection, PLD2 and NP were trafficking to similar subcellular locations. The extent of this colocalization was quantified. PLD2 and NP were increasingly colocalized at 30,

90, and 360 minutes post-infection (Fig. 1*C*) as measured by both Pearson's coefficient and rank correlation (Spearman). To further confirm that siRNA treatment was knocking down levels of PLD2 and that the PLD2 antibody was specific, we probed for PLD2 expression after infection of cells electroporated with control or PLD2 siRNA. We imaged more than 75 cells for each condition and found a consistent loss of 50% or more of stainable PLD2 in the siRNA treated cells (1*F*). Together, these data suggest PLD activity is stimulated by influenza infection, endogenous PLD redistributes during the infection, and the accumulation of PLD is occurring in the same subcellular location as influenza NP.

PLD is a targetable host factor that facilitates efficient influenza infection- To determine the role of PLD-mediated PA production in influenza infection, we employed a spatial infection model in the presence of 0.6% *n*-butanol with *tert*-butanol used as a negative control. This assay utilizes the use of primary alcohols as preferred nucleophiles in a PLD transphosphatidylation reaction as an assessment of exclusively PLD- produced PA.

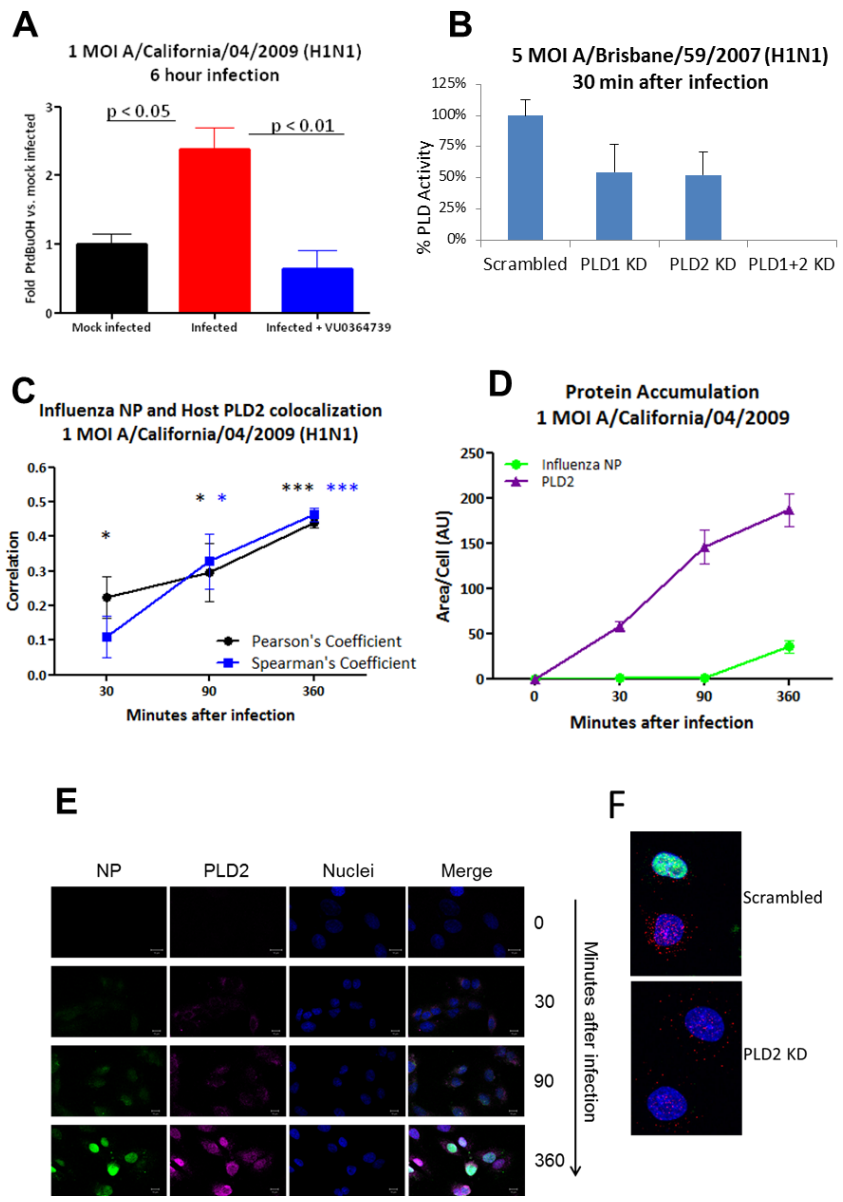

Figure 1. Influenza infection stimulates PLD activity. ***A*.** A549 cells treated for one hour with or without 10 µM PLD inhibitor VU0364739 were then infected for one hour with 1 MOI influenza A/California/04/2009 (or mock infected), after which the inoculum was removed. The cells were cultured for 6 hours in the presence of 0.6% *n*-butanol. PLD activity as a measure of phosphatidylbutanol (PtdBuOH) was determined in cell lysates by mass spectrometrometric analysis. ***B***. RNAi of PLD1, PLD2 or PLD1&2. A549 cells were transfected with isoform specific siRNA 1 day before a 5 MOI infection of influenza A/Brisbane/59/2007 (H1N1). 30 minutes after infection, PLD catalytic activity measured in the same manner as (***A***). ***C*, *D*** and ***E*.** A549 cells were infected with 1 MOI influenza A/California/04/2009 (H1N1), and samples were fixed and probed for influenza nucleoprotein (NP) and PLD2 at 0, 30, 90, and 360 minutes after infection. Z-

stacks of the infected cultures were collected using confocal microscopy, and ImageJ was used to determine PLD and influenza NP colocalization (***C***) during infection as well as protein accumulation (***D***). Quantification of the degree of correlation between NP and PLD shows that they significantly colocalize as early as 30 minutes post-infection, and the colocalization has the highest correlation coefficient 360 minutes post-infection. PLD2 signal begins to intensify 30 minutes after infection and continues to increase in both size and intensity throughout the duration of the infection. NP signal lags behind that of PLD2, but begins to intensify 90 and 360 minutes post-infection. ***E.*** Representative images from a 1 MOI influenza A/California/04/2009 (H1N1) infection taken 0, 30, 90, and 360 minutes post-infection. The green signal is influenza (NP), the magenta signal is PLD2, and the blue signal is DAPI staining, bar = 10 µm. As the infection progresses, PLD2 staining begins to accumulate at the cell periphery, then intensifies, and finally moves to a perinuclear region. NP staining first appears at the cell periphery and then intensifies in the nucleus. ***F.*** Representative images from PLD2 monoclonal antibody validation. A549 cells were electroporated with 100 nM scrambled control or PLD2 siRNA and left to rest for 24 hours. Cells were fixed 8 hours after a 1 MOI A/Brisbane/59/2007 (H1N1), green signal is influenza NP, red signal is PLD2, and blue signal is nuclei. All data are mean ± SEM.

Twenty-four hours post-infection infected cells were counted by anti-influenza NP staining (Fig. 2*A*). Infection with influenza strains A/Brisbane/59/2007 (H1N1), A/California/04/2009 (H1N1), or A/Brisbane/10/2007 (H3N2) resulted in fewer infected cells in the presence of *n*-butanol, indicating that blocking PLD production of PA substantially reduces the rate of cell to cell transmission of infection. Notably, averting the production of PLD-generated PA to PLD-generated PtdBuOH by use of primary alcohol, did not entirely prevent influenza infection but did significantly decrease the rate of infectious spread within the cultures.

In order to determine if PLD1 or PLD2 was preferentially required for efficient influenza infection, RNAi was employed to selectively knock down individual PLD isoforms. A549 cells were transiently transfected with siRNA that

targeted PLD1 or PLD2, twenty-four hours prior to a 5 MOI influenza infection of A/Brisbane/59/2007 (H1N1). Twenty-four hours post-infection, a $TCID_{50}$ was used to measure influenza virus titers in culture supernatants (Fig. 2*B*). RNAi of either PLD1 or PLD2 inhibited influenza replication. However, the magnitude of the effect was greater with PLD2 knockdown. While each isoform appears to contribute to efficient influenza replication, the stronger inhibitory effects seen after PLD2 knockdown led us to focus on PLD2 inhibition and its effect on the host and viral replication for subsequent studies.

The development and optimization of the PLD inhibitors has been described (12), with the PLD2-preferring inhibitor, VU0364739 having a 75-fold selectivity for PLD2 over PLD1 (13). Based on previous studies, VU0364739 was used at 10 μM in all cell-based assays unless otherwise indicated (21). To demonstrate the importance of PLD2 during influenza replication another RNAi experiment was conducted while treating the PLD2-deficient cells with PLD2 inhibitor VU0364739. Viral titer was measured by $TCID_{50}$ after a 24 hour, 5 MOI influenza A/Brisbane/59/2007 (H1N1) infection. Pretreatment with VU0364739 for 1 hour caused a dramatic decrease in viral replication (Fig. 2*C*). Similar reductions in titer were also observed when PLD2 was knocked down by RNAi in vehicle treated samples. Finally, the specificity of this compound was confirmed by combining the apparent marginal, non-statistically significant additive nature of RNAi with VU0364739 treatment.

These observations were extended to establish the importance of PLD2 as a host factor required for infection by other clinically relevant strains of influenza. Pretreating cells for 1 hour with VU0364739 resulted in a significant decrease in the number of infected cells measured in the spatial infection assay with multiple viral strains at both 6- and 24- hours post-infection (Fig. 2*D*). Representative images of the spatial infection model assay (Fig. 2*E*) illustrate the reduction in influenza spread observed after VU0364739 treatment. PLD2 inhibition by VU0364739 effectively protected A549 cells from cell to cell spread of influenza, further demonstrating that PLD2 is required for efficient influenza infection and spread. A time-of-addition study was conducted where inhibitor was added over a time course spanning 2 hours before infection to 4 hours post-infection. Protection from infection was observed at all times of PLD inhibitor addition.

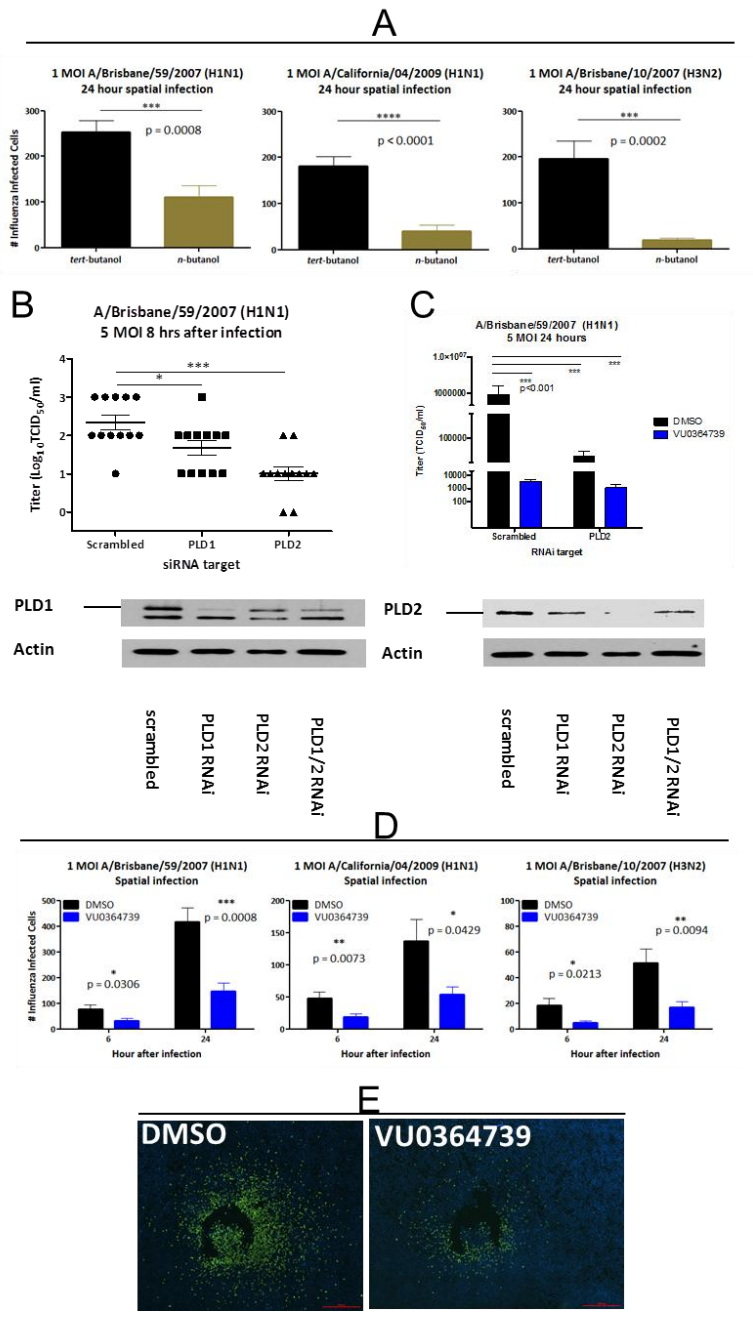

Figure 2. PLD2 is required for efficient influenza infection and inhibition of PLD-generated PA by primary alcohol, RNAi or small molecule VU0364739 dramatically hinders cell to cell spread of influenza. ***A***. Number of influenza infected cells in cultures of A549 cells treated with 0.6% *tert*- or *n*-butanol for 1 hour prior to spatial infection by 1 MOI of the indicated influenza virus strain for 24 hours. Differences were assessed by t-test. ***B***. (upper) RNAi of PLD isoforms. A549 cells were transfected with siRNA targeting PLD1 or PLD2 24 hours prior to infection with 5 MOI influenza A/Brisbane/59/2007 (H1N1); 8 hours post-infection, influenza replication was measured by $TCID_{50}$. (lower) Immunoblot of human PLD1 and PLD2 from A549 cells following RNAi treatment. Lysates were

separated on 10% polyacrylamide gel, transferred to nitrocellulose overnight, and incubated with primary antibodies for PC-PLD1 (Santa Cruz sc-25512) or PLD2 (Abgent AT3337a). Immunoblots were developed with ECL western blotting substrate (Pierce cat# 32106). ***C*.** A549 cells were transiently transfected with PLD2 specific siRNA or scrambled control siRNA 24 hours before infection. An hour before infection, the cells were treated with DMSO or VU0364739 (10 µM). The cells were infected with 5 MOI A/Brisbane/59/2007 (H1N1) and influenza replication was measured by $TCID_{50}$ 24 hours after infection. Differences between amounts of infected cells as well as influenza replication were compared using a one-way ANOVA and Dunnett's post-test. ***D*.** Influenza spatial infection (following 1-hour 10 µM PLD2-preferring inhibitor VU0364739 pretreatment) with clinically relevant strains of influenza at 1 MOI. At both 6- and 24-hours post-infection, significantly fewer numbers of influenza-infected cells were counted in VU0364739 pretreated samples. Data was analyzed by t-test. ***E***. Representative fluorescent photomicrograph mosaics following a 24-hour spatial infection of A549 cells with influenza A/Brisbane/59/2007 (H1N1). Green signal is influenza infected cells and blue signal is DAPI staining, bar = 10 µm. All data are mean ± SEM.

Inhibition of PLD activity dramatically reduces influenza replication - The spatial infection model assay data was validated using the more traditional $TCID_{50}$ assay to assess viral reproduction *in vitro*. A549 cells were treated with 10 µM VU0364739 for 1 hour before infection, and the cells were then infected with the indicated doses and strains of influenza. At indicated time points, infectious supernatant was removed from the A549 cells and titrated on MDCK cells to measure viral reproduction. Using either a low MOI (Fig. 3*A*) or a high MOI (Fig. 3*B*) of influenza A/Brisbane/10/2007 (H3N2), a lower viral reproduction was observed when PLD2 was inhibited. In the case of the low MOI infection, viral titers were first noted to be lower at 16 hours post-infection and the effect was sustained 24 hours post-infection. Using the high MOI model, when A549

cells were treated with VU0364739, a significant reduction in viral reproduction was noted 12 hours post-infection and lasted through at least 24 hours.

The H3N2 strain used in our previous experiments is considered a low pathogenicity strain of influenza. To determine if host PLD is required for high pathogenicity and quickly replicating strains of influenza, VU0364739-treated A549 cells were infected with 0.01 MOI influenza rg-A/Vietnam/1203/2004 (H5N1) and viral reproduction was assessed during a more severe infection. Twenty-four hours post-infection, a massive decrease in viral titer was observed when PLD2 was inhibited during H5N1 infection (Fig. 3*C*). Subsequent investigation whether host PLD2 activity is required for infection using a recently emergent virus with pandemic potential, influenza strain A/Anhui/01/2013 (H7N9), was conducted. After 1 hour of 10 μM VU0364739 pretreatment, viral reproduction was effectively blocked 24 hours post-infection (Fig. 3*D*). Viral titer was near the limit of detection when PLD catalytic activity was inhibited; consistent with PLD2 being a host factor required for low and high pathogenicity influenza infections.

Using the same model, *in vitro* dose response experiments were perfomed using VU0364739 to determine the efficacy of the PLD2 inhibitor during H5N1 and H7N9 infection. A549 cells were treated for 1 hour with varying concentrations of VU0364739 before a 0.01 MOI infection of either influenza rg-A/Vietnam/1204/2004 or A/Anhui/1/2013. Supernatant was then used to measure viral reproduction in a $TCID_{50}$ assay 24 hours post-infection. In the case of the H5N1 infection, the IC_{50} of VU0364739 was calculated by non-linear regression

analysis to be 2.1 μM (Fig. 3*E*). Similarly, the IC_{50} of VU0364739 was found to be 3.4 μM when cells were infected with an H7N9 influenza strain (Fig. 3*F*). These IC_{50} values are consistent with *in vitro* dose response experiments using influenza A/Brisbane/59/2007 (H1N1), A/Brisbane/10/2007 (H3N2), and A/California/04/2009 (H1N1) as well (data not shown). Based on these results, it was determined that inhibition of PLD2 can significantly lower influenza reproduction *in vitro*, and the decrease in viral titer occurs in a dose-dependent fashion.

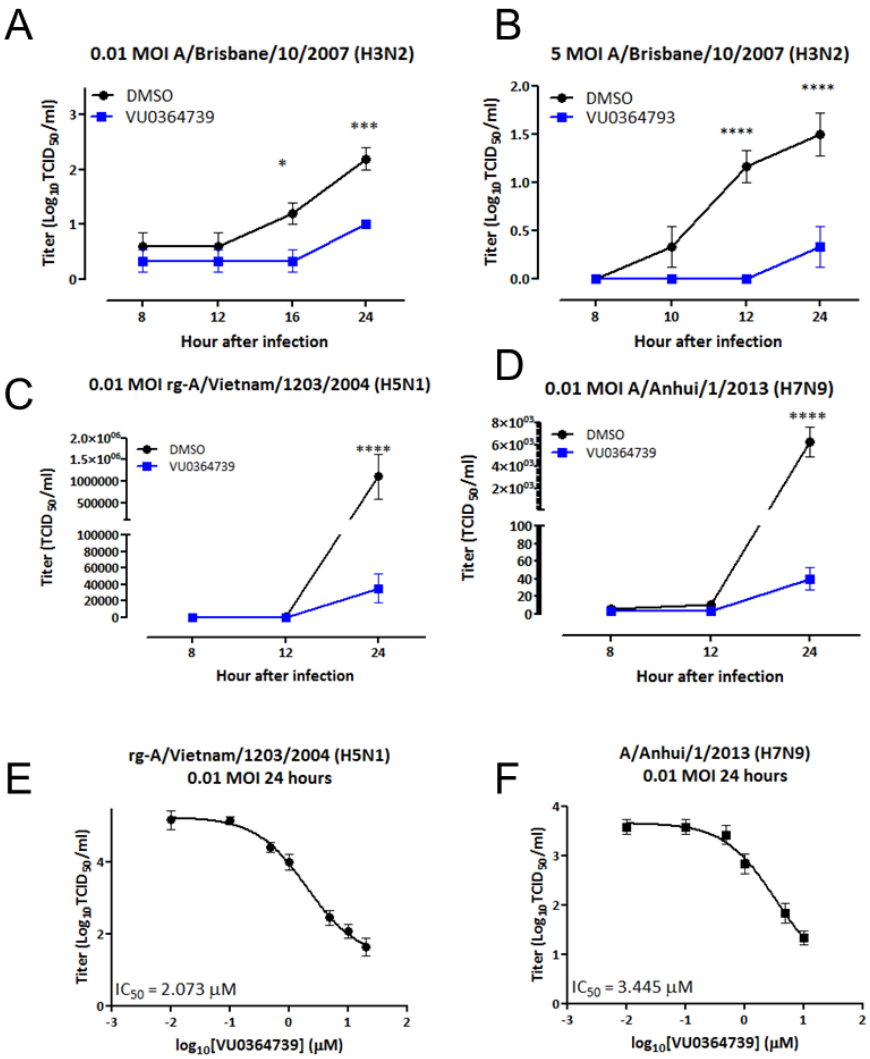

Figure 3. Influenza replication is severely reduced when PLD2 is inhibited by VU034739. A549 cells were pretreated with 10 µM VU0364739 or DMSO for 1 hour, then infected with either: ***A***. Low 0.01 MOI H3N2 influenza, ***B***. High 5.0 MOI H3N2 influenza, ***C***. 0.01 MOI H5N1 influenza, or ***D***. 0.01 MOI H7N9 influenza for an hour at 4 °C, and then the infectious supernatant containing the virus was removed and titrated on MDCK cells to assess viral production at indicated times post-infection. Under PLD2 inhibitor treatment, poor viral replication in all influenza strains tested by 24 hours post-infection was observed, and the viral output defect was noted as early as 12 hours post-infection in the case of H3N2 and H7N9. Differences were assessed using a two-way ANOVA and Bonferroni's post-test, where * $p < 0.05$, ** $p < 0.01$, *** $p < 0.001$, **** $p < 0.0001$. ***E***. and ***F***. Dose response curves to determine the IC_{50} of VU0364739 on influenza titer after a 24 hour infection with (***E***) rg-A/Vietnam/1204/2004 (H5N1) or (***F***) A/Anhui/1/2013 (H7N9). A549 cells were treated with the indicated concentration of VU0364739 for one hour before infection, $TCID_{50}$ was used to measure viral load. All data are mean ± SEM.

PLD2-preferring inhibitor VU0364739 reduced viral titer in mouse lungs and delayed mortality during lethal H7N9influenza infection- Having shown that abrogation of PLD2 activity leads to a decrease in viral spread and reproduction *in vitro*, we wanted to determine if the loss of PLD2 could reduce viral titer *in vivo*. Female C57BL/6 (B6) mice were treated intraperitoneally (IP) with dilutions of PLD2-preferring inhibitor VU0364739 every 8 hours from day -1 to 8 hours after infection with 1 LD_{50} (4000 EID_{50}) influenza A/Puerto Rico/8/1934 (H1N1) (PR8), administered intranasally on day 0. Due to solubility issues and observed acute vehicle toxicity, a long-term survival study with optimal dosing to achieve the therapeutic *in vivo* concentration continuously was not feasible at this time and viral titer was used as a readout to determine the role of PLD2 in a mouse model of influenza infection. Viral titer in lungs decreased significantly with PLD2 inhibitor VU0364739 treatment (Fig. 4*A*) and these protective effects were dose dependent. Additionally, to determine whether PLD2 inhibition could lead to lower viral titers in a more chronic situation, mice were given 13 mg/kg VU0364739 every 8 hours IP from day -1 to day 3 after infection. Animals treated with VU0364739 had significantly less viral replication in their lungs (Fig. 4*B*) on day 3. Concomitant with the decrease in viral titers, 8 hours after PR8 influenza infection significant upregulation of the innate immune proteins Mx1, OAS-L, and IFITM3 was observed when PLD2 was inhibited (Fig. 4*C*), indicating that the early immune response may be an important part of the mechanism of protection when mice are treated with VU0364739. IFITM3 has recently been described as a human restriction factor for influenza infection (22).

In order to identify survival benefits conferred by the observed reduction in viral titers, a study was conducted dosing mice with 13 mg/kg VU0364739 every 12 hours from day -1 to day 3 of a lethal influenza A/Anhui/1/2013 (H7N9) infection (Fig. 4*D*). Relative concentrations of the PLD inhibitor in various tissues of interest over time are presented in Fig. 4*E.* Administration of the PLD2-preferring inhibitor resulted in a modest, yet significant increase in survival and, in addition, delayed mortality (Fig. 4*D*). Although 80% of the mice administered VU0364739 eventually succumb, death occurs considerably later after infection (compared to influenza infected mice administered vehicle), clearly providing an extended window for further supportive therapy in a clinical setting. This demonstrates that by inhibiting PLD activity in the mouse, viral replication is decreased, and antiviral responses are upregulated leading to some protective benefits during a lethal influenza infection. No significant toxicity or neurological impairment was noted in rats receiving identical treatment (Tables 1 and 2). This inhibitor is a preclinical compound that has not been optimized for pharmacokinetic nor pharmacodynamic properties, and yet it demonstrates robust effects on viral spread and reproduction.

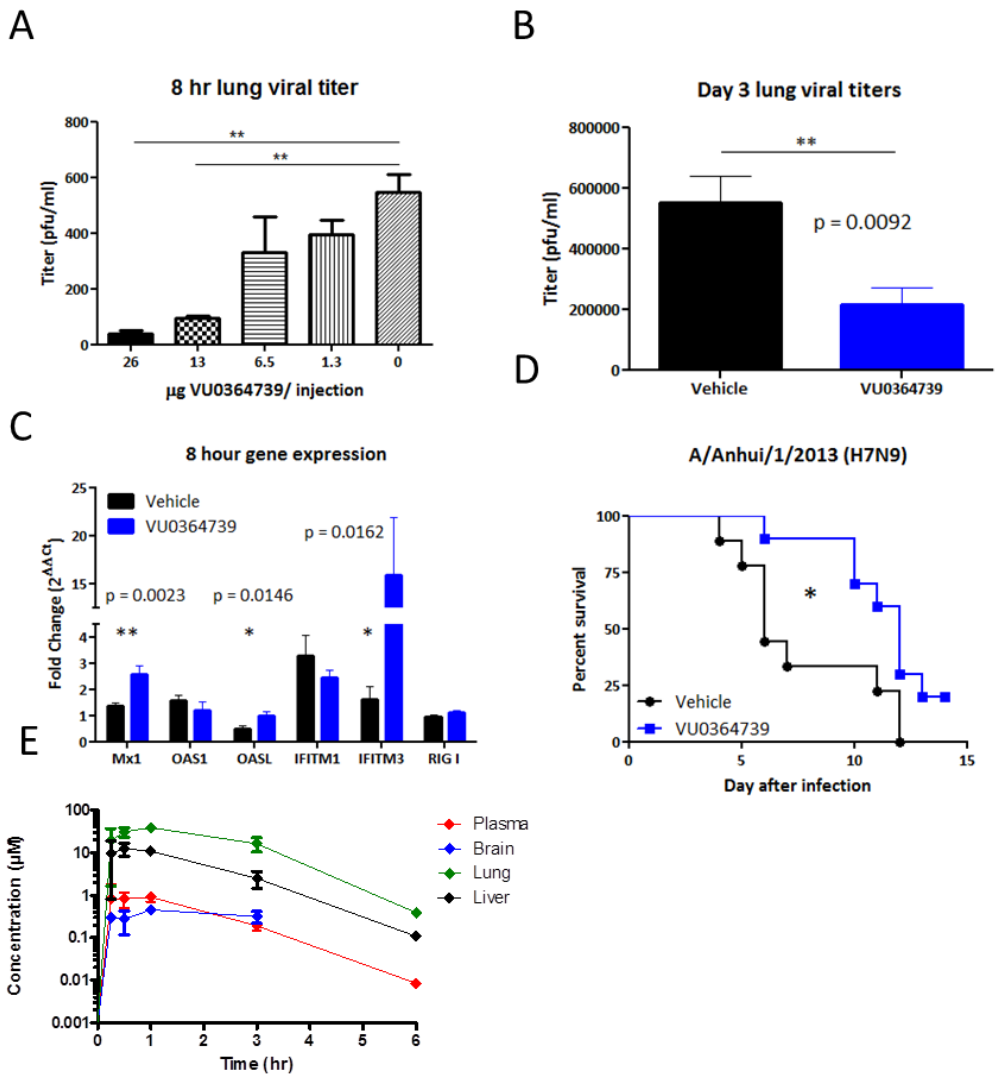

Figure 4. PLD2 inhibitor decreased early viral titer in a dose dependent manner and delayed mortality in a lethal H7N9 model. ***A***. Mice treated with VU0364739 displayed lung viral titers that were drastically reduced 8 hours after 4000 EID_{50} PR8 influenza infection, and the reduction occurred in a dose-dependent manner. Data were compared by ANOVA and Bonferroni's post-test, with N≥5 mice used for each dose, ** $p < 0.01$. ***B***. Viral replication was similarly inhibited 3 days after 4000 EID_{50} PR8 influenza infection in mice treated with 13 mg/kg VU0364739 three times a day from day -1 to day 3 post influenza infection. Data were analyzed by t-test, ** $p < 0.01$. ***C***. RNA from PR8 influenza-infected lungs was isolated and gene expression was measured using TaqMan based qPCR 8 hours after infection. Innate immune proteins Mx1, OASL, and IFITM3 were significantly upregulated as early as 8 hours after infection, as measured by t-test, * $p < 0.05$, ** $p < 0.01$. ***D***. Mice receiving 13 mg/kg VU0364739 twice/day from day -1 to day 5 post-infection were inoculated with $10^{3.5}$ $TCID_{50}$ (1 LD_{50}) influenza A/Anhui/1/2013 (H7N9). The PLD2 inhibitor conferred a substantial

delay in mortality and a 20% survival advantage, a significant benefit as measured by either Log-Rank test ($p = 0.0194$) or Gehan-Breslow-Wilcoxon test ($p = 0.0165$), * $p < 0.05$. ***E.*** Plasma, brain, lung and liver exposures following a single 10 mg/kg intraperitoneal dose of the PLD inhibitor VU0364739 in mouse. Samples were stored at -80 °C until extraction and LC-MS/MS analysis. (N = 2 samples per time point).

Table 1. Rat liver toxicity panel shows little effect of PLD inhibitor VU0364739. Only globulin and total protein showed higher levels with inhibitor treatment (N = 5 - 6 rats per treatment, $p < 0.05$ by Mann-Whitney test) and each were within normal clinical ranges for both the vehicle control and PLD inhibitor treatment groups. Principal components analysis of the z-score standardized values across the screening panel displayed no clustering of the multivariate results by treatment, and none of the principal components differed significantly either ($p > 0.05$ by t-test).

	Means ± sems		Units	P-value
	Vehicle	*VU0364739*		
Albumin	3.6±0.1	3.6±0.0	g/dL	0.5368
Alkaline phosphatase	212±11	207±13	U/L	0.7922
Alanine aminotransferase	102±8	113±5	U/L	0.5368
Amylase	1118±59	1142±41	U/L	0.6623
Blood urea nitrogen	12.0±2.0	15.6±1.5	mg/dL	0.0823
Calcium	10.8±0.2	11.0±0.2	mg/dL	0.3290
Creatinine	0.33±0.01	0.42±0.04	mg/dL	0.1255
Globulin	2.3±0.1	2.6±0.1	g/dL	0.0303
Glucose	143±7	141±5	mg/dL	0.7922
Potassium	5.72±0.42	5.72±0.15	mmol/L	0.6623
Sodium	139±2	142±1	mmol/L	0.3290
Phosphorus	8.8±0.2	9.0±0.2	mg/dL	0.5368
Total bilirubin	0.22±0.07	0.16±0.01	mg/dL	0.7922
Total protein	5.9±0.1	6.3±0.1	g/dL	0.0303

Table 2. PLD inhibitor VU0364739 is without effect in a Modified Irwin Neurological Battery in rats. Changes in the Modified Irwin Neurological Battery were evaluated using a rating scale from 0 to 2: 0, no effect; 1, modest effects; 2, robust effect. Male Harlan Sprague Dawley rats (N = 6, approximately 250 grams) were pretreated with vehicle alone or a 13 mg/kg IP dose of VU0364739 and then tested in the Irwin battery at 30 minutes after treatment and subsequently monitored for 8 hours.

Modified Irwin Neurological Battery with VU0364739

Autonomic Nervous System					
Time	30min	1hr	2hr	4hr	8hr
Ptosis	0	0	0	0	0
Exophtalmus	0	0	0	0	0
Miosis	0	0	0	0	0
Mydriasis	0	0	0	0	0
Corneal reflex loss	0	0	0	0	0
Pinna reflex loss	0	0	0	0	0
Piloerection	0	0	0	0	0
Respiratory rate	0	0	0	0	0
Writhing	0	0	0	0	0
Tail erection	0	0	0	0	0
Lacrimation	0	0	0	0	0
Salivation	0	0	0	0	0
Vasodilatation	0	0	0	0	0
Skin color	0	0	0	0	0
Irritability	0	0	0	0	0
Loose Stool	0	0.25	0.5	0.4	0
Rectal temp. (°C)	37	37.3	37.4	37.2	37
Somatomotor systems					
Motor activity	0	0	0	0	0
Convulsions	0	0	0	0	0
Arch/roll	0	0	0	0	0
Tremors	0	0	0	0	0
Leg weakness	0	0	0	0	0
Rigid stance	0	0	0	0	0
Spraddle	0	0	0	0	0
Placing loss	0	0	0	0	0
Grasping loss	0	0	0	0	0
Righting loss	0	0	0	0	0
Catalepsy	0	0	0	0	0
Tail pinch	0	0	0	0	0
Escape loss	0	0	0	0	0

PLD2 inhibition alters endocytosis kinetics and aggregation of endocytic proteins- Inhibition of PLD function has been shown to decrease uptake of ligands in various systems (9,23,24). Given that perturbation of influenza virus trafficking during the early infection process can lead to degradation of the entering virus (11), it was hypothesized that PLD inhibition during influenza infection led to alterations of entry events which occur in the first minutes of infection. To support this hypothesis, the effect of PLD2 inhibition on normal endocytosis rates was assessed using the established transferrin uptake model, a classic demonstration of a clathrin-dependent trafficking process.

A549 cells pretreated with VU0364739 were labeled with fluorescent transferrin at 4 °C for 1 hour then placed into a heated microscope for live cell imaging. Images were recorded for one hour, and the frame and time of the transferrin fluorescence disappearance was noted (Fig. 5*A* and *B*). Cells treated with vehicle control were able to take up, traffic, and degrade transferrin by the 14^{th} frame, corresponding to an average time of 26 minutes after warming. In contrast, cells treated with VU0364739 took approximately 56 minutes to process the fluorescent ligand. These data indicate that inhibiting PLD2 activity with VU0364739 alters trafficking kinetics by extending the endocytosis process, rather than acting as a strict blockade.

Influenza entry is not entirely dependent on clathrin-mediated endocytosis, but it is widely accepted that the majority of incoming viruses enter via clathrin-dependent events, primarily by the *de novo* formation of clathrin coated pits on the cell surface after exposure to influenza virus (25). After entry, influenza virus

needs to be properly trafficked from the membrane to the nucleus. Along the way, the endosome is acidified (26), and the hemagglutinin protein undergoes a conformational change that creates a fusion pore between the viral and vesicle membranes through which viral ribonucleoproteins gain access to the cytoplasm, eventually entering the nucleus to initiate new virus production. The accumulation of trafficking associated proteins was visualized by confocal microscopy in A549 cells during a 0.05 MOI influenza A/California/04/2009 (H1N1) infection. Signal intensity and particle size were gated to determine protein accumulation. As proteins accumulate, the brightness and size of the fluorescence increases on a per cell basis. Clathrin recruitment was inhibited 50 minutes post-infection, and remained significantly lower (up to 80 minutes post-infection) with VU0364739 administration (Fig. 5*C*). During the first phase of viral entry, Rab5 accumulates on the early endosomes; however, in the presence of VU0364739 much less Rab5 accumulates 10 minutes post-infection (Fig. 5*D*). Similarly, VU0364739 treatment led to a significant reduction in recruitment of the late endosome marker CD63 90 minutes post-infection (Fig. 5*E*). Vesicular trafficking is also important for key elements of the late stages of viral replication and defects in Rab11 accumulation associated with viral protein trafficking to the membrane were consistently observed (data not shown). These data indicate that when PLD2 is inhibited during an infection, the normal cascade of protein accumulation required for proper endosomal maturation is disrupted, leading to inefficient trafficking of incoming virus particles, indicating that PLD2 is a host factor required for the efficient trafficking of influenza virus once within the cell.

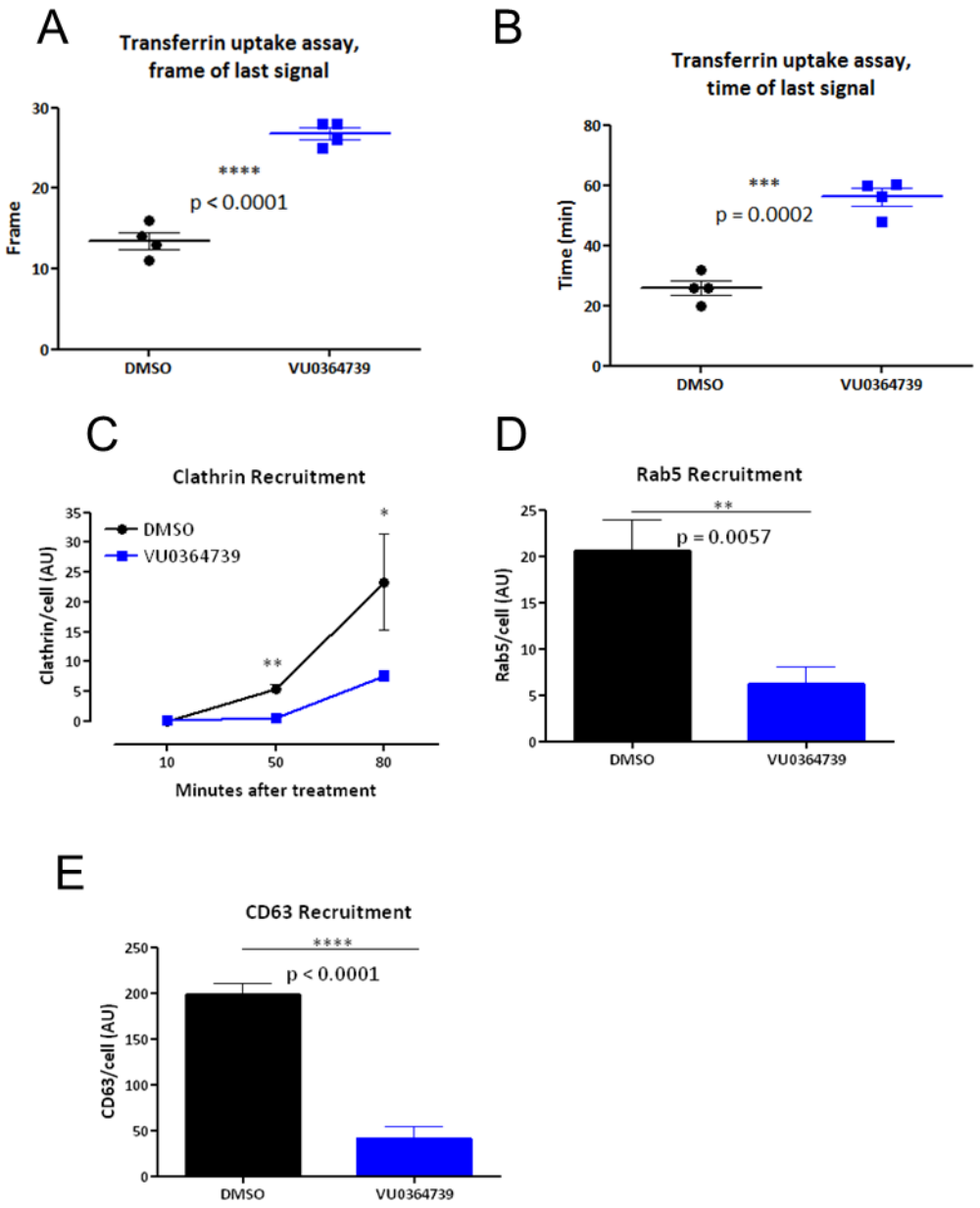

Figure 5. PLD inhibition alters ligand trafficking kinetics and accumulation of endocytosis regulatory proteins. ***A & B***. A549 cells were treated for 1 hour with DMSO or VU0364739 (10 µM) prior to being labeled for 1 hour at 4 °C with 100 nM AlexaFluor 647 – Transferrin. Live cell imaging (representative movies in supplemental) was used to assess the kinetics of transferrin uptake. To quantify this assay, both the frame (*A*) and the time (*B*) were used to determine when the fluorescent signal disappeared, signaling recycling of transferrin. Live cell imaging was performed using Slidebook imaging software and frame time measurements were compared using t-tests, data are mean ± SEM. ***C*** - ***E***. A549 cells were treated for 1 hour with DMSO or VU0364739 (10 µM) then infected with 0.05 MOI influenza A/California/04/2009 (H1N1). Cells were stained and

examined by confocal microscopy for the accumulation of: ***C-*** Clathrin; ***D***- Rab5 (early endosome); ***E-*** CD63 (late endosome). Less clathrin is recruited at 50 and 80 min post-infection under inhibitor treatment, and less Rab5 (***D***) and CD63 (***E***) accumulate after 10 and 90 min post-infection, respectively. In these experiments protein accumulation is defined by gating signal intensity as well as size such that higher y-axis values represent bigger and brighter foci of signal. A two-way ANOVA with Bonferroni's post-test was used to examine data from (***C***), * $p < 0.05$, ** $p < 0.01$, **** $p < 0.0001$; t-tests were used to analyze data from (***D***) and (***E***) with p-values indicated. Data are mean ± SEM.

Protection by PLD2 inhibition requires intact innate antiviral signaling- To assess whether the innate antiviral response was required for protection when cells are treated with the PLD2 inhibitor, an RNAi screen of essential innate immunity proteins *in vitro* was conducted. A549 cells were electroporated with 100 nM gene specific siRNA and infected with 5 MOI influenza A/Brisbane/10/2007 (H3N2) for 24 hours; decrease in protein expression was confirmed by Western blot analysis (data not shown). Viral titer was then measured using a traditional $TCID_{50}$ assay. A549 cells treated with control siRNA were protected by VU0364739 administration (Fig. 6*A*), showing a decrease in titer of 1.5 log units. However, VU0364739 treatment was not sufficient to protect cells transfected with siRNA targeting IRF3, Rig-I, or MxA. These three proteins are known to be vital to the innate defense against influenza. Interestingly, cells transfected with siRNA targeting the transcription factor IRF7 were still protected by VU0364739 treatment, but to a lower degree compared to cells transfected with control siRNA (0.9 log unit decrease in viral titer). These experiments demonstrate that altering trafficking kinetics with a

PLD2 inhibitor alone was insufficient for complete protection from influenza infection. Cells need an intact antiviral response to attack and neutralize the invading virus, suggesting that PLD2 plays a critical role in the temporal-spatial regulation of endocytosis and innate antiviral sensing/defense during influenza infection. Disruption of PLD2 regulation of these events affords the host cell more time to detect the virus and mount an immune response.

One potential benefit of the delayed trafficking kinetics is the greater window allowed for innate immune interference during influenza infection. A key component of the innate response in the respiratory epithelium is MxA, a cytoplasmic dynamin-like GTPase, which is transcriptionally induced to high levels as part of the Type I IFN response, but is also found at basal levels in resting cells. MxA can interfere with early virus replication events by binding to viral NP (27). MxA recruitment was measured in A549 cells post-infection by the same manner employed to measure the endosomal markers. When PLD2 is inhibited during infection, MxA is observed to accumulate in foci at significant levels as early as 30 minutes post-infection (Fig. 6*B* and *C*). These data support a model whereby the slower rate of endocytosis following PLD2 inhibition allows cells more time to detect and respond to incoming influenza virus. Afforded this additional time, PLD inhibitor treated host cells are able to mount an immune response of greater magnitude and efficacy to neutralize the incoming virus, thus promoting survival of the cell and protection from degradation of the invading virus.

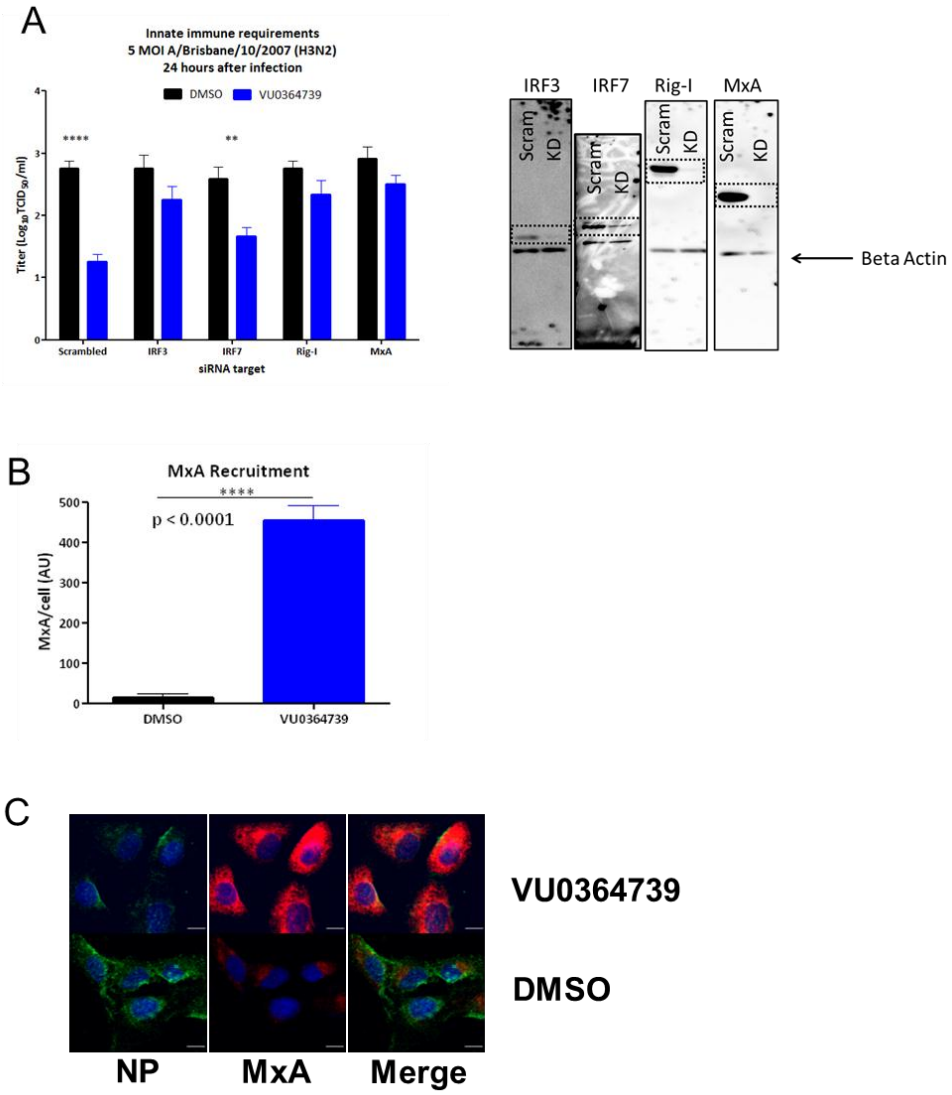

Figure 6. Innate immune factors are required for PLD2 inhibitor mediated protection from influenza. ***A***. A549 cells were transfected with siRNA targeting effectors or transcription factors involved in the Type I IFN pathway, then subsequently infected with 5 MOI influenza A/Brisbane/10/2007 (H3N2) for 24 hours, and supernatant was titered on MDCK cells to measure viral reproduction. As a control viral replication was significantly reduced in cells transfected with scrambled siRNA and treated with PLD2 inhibitor. When cells lack IRF3, Rig-I or MxA, treatment with VU0364739 cannot protect against influenza infection. The innate requirements are restricted to IRF3 mediated signaling, as protection was afforded to cells with IRF7 knocked down. Representative Western blots are presented to confirm loss of protein expression after RNAi. ***B***. To demonstrate the robust innate antiviral response to influenza infection after PLD2 inhibition, A549 cells were infected with 1 MOI influenza A/California/04/2009 (H1N1) and levels of MxA were assessed by confocal microscopy 30 minutes post-infection. ***C***. MxA accumulates much more rapidly and to a much greater magnitude when

PLD2 is inhibited. The dramatic MxA activity is visualized in representative images where green signal marks influenza NP, red signal is MxA, and blue signal is DAPI, bar = 10 μm. A two-way ANOVA with Bonferroni's post-test was used to examine data from (***A***), ** $p < 0.01$, **** $p < 0.0001$; a t-test was used to analyze data from (***B***). Data are mean ± SEM.

Discussion

PLD has been identified as a host restriction factor for influenza virus replication, and PLD catalytic activity is stimulated by influenza infection that colocalizes with NP positive staining structures over time. In addition, PLD2 functions to facilitate rapid endosomal trafficking, allowing the virus to escape an otherwise effective innate antiviral response. This response depends on RIG-I, IRF3, and the well-known antiviral protein MxA, but is largely independent of the antiviral targets of IRF7. Importantly, this work identifies a host cell process exploited by the virus to maximize its reproductive capacity and accelerate life cycle kinetics, allowing the pathogen to escape innate immune detection and neutralization.

The roles of PLD in endosomal trafficking are well documented (9,10). One advantage of targeting the PLD isoenzymes of host cells as an experimental antiviral strategy is that minimal evolution pressure would be exerted on the virus, which would otherwise encourage mutation and variant viral escape. Importantly, these enzymes have been shown to be nonessential to animal survival when either the PLD1 or PLD2 genes are knocked out (28,29). While the amount of PA generated by PLD2 alone may not be a significant fraction of the total cellular PA pool, discrete processes are likely to be linked to individual

sources of PA-PLD2. For example, Yang et al. (30) reported that PLD2 was involved in opioid receptor endocytosis via a PA-p38 MAPK pathway. This may explain the negligible levels of toxicity observed using VU0364739 *in vivo*.

PA serves a multitude of roles in membrane biogenesis and curvature as well as cellular signaling, and has the potential to facilitate viral entry, replication, and egress. A detailed lipidomic analysis demonstrated that cytomegalovirus infection elicited a robust generation of PA in human fibroblasts (16). It is also interesting to note that PKC is a direct regulator of PLD activity and the role of PKC in influenza virion transport (11) through the late endosome may include some as yet unelucidated role for PLD. A more recently described PLD isoform known as PLD3 or HuK4 is related by sequence homology to p37, an essential protein in vaccinia virus. Although this PLD isoenzyme is not as well characterized, genetic variants in PLD3 were recently found to be of predictive value for risk in Alzheimer's disease (31). Overexpression of PLD3 leads to a significant decrease in intracellular amyloid-β-precursor protein and extracellular Aβ42 and Aβ40. Although human PLD3 cannot complement a p37 deficient vaccinia virus (32) primary alcohols similarly inhibit its function and its localization in the endoplasmic reticulum, suggesting some conservation of function. These recent discoveries provide further evidence that lipid signaling is a central process in many disease states. The identification of a role for PLD in influenza entry and innate immune escape expands our understanding that host cell signaling lipases have diverse and essential roles in viral infection and potentially offer a new series of therapeutic targets for pharmacological intervention.

Influenza virus, and potentially other enveloped viruses, are hijacking the endosomal compartments of infected host cells to hide from detection and to safely mature to a state that is favorable for efficient viral infection. Inhibition of PLD2 appears to alter the temporal spatial kinetics of this process. Despite the mode of entry, there is consensus that influenza virus must gain access to an endosome and be sorted to late endosomes with lower pH environments to undergo viral membrane-host membrane fusion. Our data suggest that when PLD2 is inhibited, endosomal sorting occurs more slowly than normal. We chose to stain clathrin, Rab5 and CD63 to elucidate well known markers of intracellular trafficking. Taken together the results suggest that PLD2 inhibition perturbs multiple pathways of influenza entry. The findings suggest that these proteins are accumulating more slowly when PLD2 is inhibited. Interestingly, PLD has been noted to be involved in various trafficking paradigms including clathrin, caveolin, and macropinocytosis (33,34,35). By shifting the kinetics of influenza trafficking much less viral spread was observed using the spatial infection model method and reduced viral replication using the traditional $TCID_{50}$ and plaque assays. Concomitant with the shift in influenza trafficking, accumulation of antiviral sensors and effectors was observed. The protective mechanism is dependent on the innate immune system, indicating that the invading virus can be detected and the immune response mounted before it can begin an efficient infection. The inhibition of PLD effectively alters the host factor required by influenza to allow the infected cell to defend itself. Using the transferrin uptake model, the precise kinetics of ligand trafficking were defined and it was

demonstrated that without PLD function, these events take approximately twice as long.

Recent development of isoform-preferring PLD inhibitors (12) presented an opportunity to disrupt the formation of PA by PLD and interrogate each isoenzyme's contribution during influenza infection. Based on the results using small molecule inhibitors and RNAi, PLD2 is proposed as a host factor that is used for efficient influenza infection. Importantly, our data suggest that PLD1 also plays a role in influenza infection. PLD1 RNAi can inhibit influenza replication. The focus on PLD2 over PLD1 in this study stems from interests in viral entry and host factors that are exploited by influenza to gain entry. Because of their subcellular location, PLD1 associates with the Golgi complex while PLD2 is distributed in the cell membrane. Hence, PLD2 regulation would be more relevant during entry whereas PLD1 would have a role in viral egress, assembly, and budding (9) The role of PLD1 and its relationship to the signaling pathways in which PLD2 are also involved is an important area for future studies.

The PLD2 pathway is a potentially attractive target for development of therapeutic agents, as minimal toxicity was observed from the administration of VU0364739 alone (any toxicity *in vivo* was associated with the vehicle and no *in vitro* toxicity was observed), and knocking out PLD2 in a mouse model is not obviously deleterious. Additional research is necessary to decode how host factors are co-opted by viruses to aid their pathogenesis, and the intervention necessary to prevent or minimize efficient viral infection. Since no current therapeutic alone is capable of completely protecting against influenza infection,

future studies are required to evaluate the intriguing possibility that combinations of antiviral agents which work via distinct mechanisms could afford protection.

References

1. Rossman, J.S., Jing, X., Leser, G.P., and Lamb, R.A. (2010) Influenza virus M2 protein mediates ESCRT-independent membrane scission. *Cell* **142**, 902–913.
2. Blanc, M., Hsieh, W.Y., Robertson, K.A., Kropp, K.A., Forster, T., Shui, G., Lacaze, P., Watterson, S., Griffiths, S.J., Spann, N.J., et al. (2013) The transcription factor STAT-1 couples macrophage synthesis of 25-hydroxycholesterol to the interferon antiviral response. *Immunity* **38**, 106–118.
3. Morita, M., Kuba, K., Ichikawa, A., Nakayama, M., Katahira, J., Iwamoto, R., Watanebe, T., Sakabe, S., Daidoji, T., Nakamura, S., et al. (2013) The lipid mediator protectin D1 inhibits influenza virus replication and improves severe influenza. *Cell* **153**, 112–125.
4. Tam, V.C., Quehenberger, O., Oshansky, C.M., Suen, R., Armando, A.M., Treuting, P.M., Thomas, P.G., Dennis, E.A., and Aderem, A. (2013) Lipidomic profiling of influenza infection identifies mediators that induce and resolve inflammation. *Cell* **154**, 213–227.
5. Ehrhardt, C., Marjuki, H., Wolff, T., Nürnberg, B., Planz, O., Pleschka, S., and Ludwig, S. (2006) Bivalent role of the phosphatidylinositol-3-kinase (PI3K) during influenza virus infection and host cell defence*. Cell Microbiol* **8**, 1336-1348
6. Chen, C. and Zhuang, X. (2008) Epsin 1 is a cargo-specific adaptor for the clathrin-mediated endocytosis of the influenza virus. *PNAS* **105**, 11790-11495
7. Carrasco, M., Amorim, M.J., and Digard, P. (2004) Lipid raft-dependent targeting of the influenza A virus nucleoprotein to the apical plasma membrane. *Traffic* **12**, 979-992.
8. Campbell, S.M., Crowe, S.M., and Mak, J. (2001) Lipid rafts and HIV-1: from viral entry to assembly of progeny virions. *J Clin Virol* **22**, 217-227
9. Roth, M.G. (2008) Molecular mechanisms of PLD function in membrane traffic. *Traffic* **9**, 1233–1239.
10. Selvy, P.E., Lavieri, R.R., Lindsley, C.W., and Brown, H.A. (2011) Phospholipase D: enzymology, functionality, and chemical modulation. *Chem. Rev.* **111**, 6064–6119.
11. Sieczkarski, S.B., Brown, H.A., and Whittaker, G.R. (2003) Role of protein kinase C {beta}II in influenza virus entry via late endosomes. *J. Virol.* **77**, 460–469.
12. Scott, S.A., Selvy, P.E., Buck, J.R., Cho, H.P., Criswell, T.L., Thomas, A.L., Armstrong, M.D., Arteaga, C.L., Lindsley, C.W., and Brown, H.A. (2009) Design of isoform-selective phospholipase D inhibitors that modulate cancer cell invasiveness. *Nat. Chem. Biol.* **5**, 108–117.

13. Lavieri, R.R., Scott, S.A., Selvy, P.E., Kim, K., Jadhav, S., Morrison, R.D., Daniels, J.S., Brown, H.A., and Lindsley, C.W. (2010) Design, synthesis, and biological evaluation of halogenated N-(2-(4-Oxo-1-phenyl-1,3,8-triazaspiro[4.5]decan-8-yl)ethyl)benzamides: Discovery of an isoform-selective small molecule phospholipase D2 inhibitor. *J. Med. Chem.* **53**, 6706–6719.
14. Scott, S.A., Mathews, T.P., Ivanova, P.T., Lindsley, C.W., Brown, H.A. (2014) Chemical modulation of glycerolipid signaling and metabolic pathways. *Biochim. Biophys. Acta – Mol. Cell Biol. Lipids* **1841,** 1060-1084.
15. Bligh, E.G., and Dyer, W.J. (1959) A rapid method of total lipid extraction and purification. *Can. J. Biochem. Physiol.* **37**, 911–917.
16. Liu, S.T.H., Sharon-Friling, R., Ivanova, P., Milne, S.B., Myers, D.S., Rabinowitz, J.D., Brown, H.A., and Shenk, T. (2011) Synaptic vesicle-like lipidome of human cytomegalovirus virions reveals a role for SNARE machinery in virion egress. *Proc. Natl. Acad. Sci. U. S. A.* **108**, 12869–12874.
17. Brown, H.A., Henage, L.G., Preininger, A.M., Xiang, Y., and Exton, J.H. (2007) Biochemical analysis of phospholipase D. *Methods Enzymol.* **434**, 49–87.
18. Ivanova, P.T., Milne, S.B., Byrne, M.O., Xiang, Y., and Brown, H.A. (2007) Glycerophospholipid identification and quantitation by electrospray ionization mass spectrometry. *Methods Enzymol.* **432**, 21–57.
19. Myers, D.S., Ivanova, P.T., Milne, S.B., and Brown, H.A. (2011) Quantitative analysis of glycerophospholipids by LC-MS: acquisition, data handling, and interpretation. *Biochim. Biophys. Acta- Mol. Biol. Lipids* **1811**, 748–757.
20. Lam, V., Duca, K.A., and Yin, J. (2005) Arrested spread of vesicular stomatitis virus infections in vitro depends on interferon-mediated antiviral activity. *Biotechnol. Bioeng.* **90**, 793–804.
21. Scott, S.A., Xiang, Y., Mathews, T.P., Cho, H.P., Myers, D.S., Armstrong, M.D., Tallman, K.A., O'Reilly, M.C., Lindsley, C.W., and Brown, H.A. (2013) Regulation of phospholipase D activity and phosphatidic acid production after purinergic (P2Y6) receptor stimulation. *J. Biol. Chem.* **288**, 20477–20487.
22. Everitt, A.R., Clare, S., Pertel, T., John, S.P., Wash, R.S., Smith, S.E., Chin, C.R., Feeley, E.M., Sims, J.S., Adams, D.J., et al. (2012) IFITM3 restricts the morbidity and mortality associated with influenza. *Nature* **484**, 519–523.
23. Antonescu, C.N., Danuser, G., and Schmid, S.L. (2010) Phosphatidic acid plays a regulatory role in clathrin-mediated endocytosis. *Mol. Biol. Cell* **21**, 2944-2952.
24. Corrotte, M., Chasserot-Golaz, S., Huang, P., Du, G., Ktistakis, N.T., Frohman, M.A., Vitale, N., Bader, M.-F., and Grant, N.J. (2006) Dynamics and function of phospholipase D and phosphatidic acid during phagocytosis. *Traffic* **7**, 365–377.

25. Lakadamyali, M., Rust, M.J., and Zhuang, X. (2004) Endocytosis of influenza viruses. *Microbes Infect.* **6**, 929–936.
26. Skehel, J.J., Cross, K., Steinhauer, D., and Wiley, D.C. (2001) Influenza fusion peptides. *Biochem. Soc. Trans.* **29**, 623–626.
27. Verhelst, J., Parthoens, E., Schepens, B., Fiers, W., and Saelens, X. (2012) Interferon-inducible Mx1 protein inhibits influenza virus by interfering with functional viral ribonucleoprotein complex assembly. *J. Virol.* **86**, 13445-13455.
28. Elvers, M., Stegner, D., Hagedorn, I., Kleinschnitz, C., Braun, A., Kuijpers, M.E.J., Boesl, M., Chen, Q., Heemskerk, J.W.M., Stoll, G., et al. (2010) Impaired {alpha}IIb{beta}3 integrin activation and shear-dependent thrombus formation in mice lacking phospholipase D1. *Sci. Signal.* **3**, ra1.
29. Oliveira, T.G., Chan, R.B., Tian, H., Laredo, M., Shui, G., Staniszewski, A., Zhang, H., Wang, L., Kim, T.-W., Duff, K.E., et al. (2010) Phospholipase D2 ablation ameliorates Alzheimer's disease-linked synaptic dysfunction and cognitive deficits. *J. Neurosci.* **30**, 16419 – 16428.
30. Yang, L., Seifert, A., Wu, D., Wang, X., Rankovic, V., Schröder, H., Brandenburg, L.O., Höllt, V., and Koch, T. (2010) Role of phospholipase D2/phosphatidic acid signal transduction in micro- and delta-opioid receptor endocytosis. *Mol. Pharmacol.* **78**, 105–113.
31. Cruchaga, C., Karch, C.M., Jin, S.C., Benitez, B.A., Cai, Y., Guerreiro, R., Harari, O., Norton, J., Budde, J., Bertelsen, S., et al. (2013) Rare coding variants in the phospholipase D3 gene confer risk for Alzheimer's disease. *Nature* **505**, 550-554.
33. Munck, A., Böhm, C., Seibel, N.M., Hashemol Hosseini, Z., and Hampe, W. (2005) Hu-K4 is a ubiquitously expressed type 2 transmembrane protein associated with the endoplasmic reticulum. *FEBS J.* **272**, 1718–1726.
34. Padron, D., Tall, R.D., and Roth, M.G. (2006) Phospholipase D2 is required for efficient endocytic recycling of transferrin receptors. *Mol Biol Cell* **17**, 598-606
35. Czarny, M., Fiucci, G., Lavie, G., Banno, Y., Nozawa, Y., and Liscovitch, M. (2000) Phospholipase D2: functional interaction with caveolin in low-density membrane microdomains. *FEBS Letters* **467**, 326-332.
36. Manhankali, M., Peng, H.J., Cox, D., and Gomex-Cambronero, J. (2011) The mechanism of cell membrane ruffling relies on a phospholipase D2 (PLD2), Grb2 and Rac2 association. *Cell Signal* **23**, 1291-1298.

CHAPTER 3

IRF3-DEPENDENT DIFFERENTIAL IMMUNE RESPONSE TO INFLUENZA INFECTION

Introduction

The innate immune system constitutes the front line of defense against invading pathogens. Cells encountering threats must defend themselves and also communicate to surrounding cells that a pathogen is present. The primary defense cells possess antiviral sensors and effector molecules that recognize pathogen associated molecular patterns (PAMP) and then begin to assemble a network of proteins that relay signals to the nucleus. In the case of antiviral immunity, the ubiquitously expressed IRF3 plays a critical role in not only the first-wave of type 1 IFN signaling but also primes the adaptive immune response to prepare an antigen-specific defense (Lendonck et al., 2014).

Innate defense against influenza virus infection begins with pattern recognition receptors such as RigI, TLR3, or TLR7 depending on the state of viral invasion and replication or subcellular location of PAMP (Iwasaki and Pillai, 2014). The type 1 IFN response begins when phosphorylated and dimerized IRF3 enters the nucleus, binds to specific interferon-sensitive response elements on IFN genes as well as CXCL9, CXCL10, IFIT1, and CLIC4 (Honda and Taniguchi, 2006). In this network of transcription induction occurring after the initial wave of IFNβ, IRF7 has been noted to work in concert with IRF3, and could be considered redundant in certain circumstances (Honda and Taniguchi, 2006). Activation of IRF3 can result from downstream signaling from RigI (Yoneyama et

al., 2004), MDA5 (Kato et al., 2006), TLR3 (Wang et al., 2004), or TLR4 (Kurt-Jones et al., 2000). It could be said that IRF3 is a central terminus for the beginning of the type 1 IFN response in a variety of models.

Surprisingly, there has been very little research to uncover the role for IRF3 with respect to influenza virus infection. Our initial hypothesis was that loss of IRF3 would lead to an inability to control viral replication and an increased pathology in cells and mice, but the data we have generated suggests otherwise. In this work we demonstrate that IRF3$^{-/-}$ mice are more likely to survive an otherwise lethal influenza infection. This survival benefit is independent of viral replication. Protection from death most likely arose from an enhanced CD8 T cell response after infection that was primed by a more robust expression of IFNγ, CXCL9, and CXCL10 in IRF3$^{-/-}$ mice. Our findings demonstrate that the loss of IRF3 leads to a differential immune response to influenza virus infection resulting in an unexpected survival benefit.

Methods and materials

Cells, mice and viruses

Human lung epithelial cells (A549) were maintained in growth medium: DMEM (Gibco) supplemented with 5% fetal bovine serum (Atlanta biological), 100 U/ml penicillin (Gibco), and100 µg/ ml streptomycin (Gibco). For infection studies, cells were treated with virus diluted in serum free growth medium, supplemented with 0.3% bovine serum albumin and antibiotics.

IRF3$^{-/-}$ mice were a gift from the Alan Aderem lab. The knockout mice were backcrossed to C57Bl/6 (wild type) mice and genotyped to confirm gene

deletion as well as efficacy of the backcross. Heterozygous litter mate controls were unavailable at the time of experiments but are being generated currently. All animal studies were approved by the St. Jude Children's Research Hospital Animal Care and Use Committee (Protocol number 098) following the guidelines established by the Institute of Laboratory Animal Resources approved by the Governing Board of the United States National Research Council.

Mice were anesthetized with avertin (2,2,2-tribromoethanol) and intranasally infected with virus at the doses indicated in the text. All animal infections and viral tittering were conducted as described in (Stry et al., 2012). The right lung of infected mice were taken to measure viral titer. All viruses were grown in embryonated chicken eggs.

siRNA knockdown

A Neon transfection system (Life Technologies) was used to electroporate 200 nM of noncoding (scrambled) or IRF3 targeting siRNA into A549 cells. Cells were allowed to adhere overnight before being infected. Western blot analysis was used to confirm protein knockdown efficacy.

Flow cytometry

Spleen, mediastinal lymph node (MLN), broncheoalveolar lavage (BAL), and the left lung were harvested from infected mice and processed into single cell suspensions and stained with appropriate antibodies and influenza-specific CD8 tetramers as described previously (Rutigliano et al., 2013). All flow cytometry analysis was conducted on a Foretessa cytometer (BD biosciences). Myeloid cells were selected by gating standard lymphocyte gating using forward

and side scatter. Neutrophils were gated by selecting the MHCII low Gr1hi populations from CD11b and Gr1 double positive cells. Alveolar macrophages were MHCII+ population of CD11b+ CD11c+ cells. Inflammatory monocytes are a Gr1- subset from a CD11b+ CD11c- population.

Cytokine analysis

To measure cytokine levels in BAL, equal amounts of total protein as measured with a BCA assay (Pierce) from infected BAL were used in a 32-plex Mouse MILLIPLEX (Millipore) kit run on a Luminex instrument (Life Technologies). An ELISA was used to measure IFNβ (R&D systems). All cytokine concentrations were normalized to total amount of protein in each sample.

Data analysis

Flow cytometry data were prepared using FlowJo v10 (FlowJo). GraphPad Prism 5 was used to graph and statistically analyze data from flow cytometry, cytokine analysis, and *in vitro* and *in vivo* experiments.

Results

Influenza virus replication is not restricted by IRF3 *in vitro*

A common model of investigating host genes critical to defense against influenza infection is the siRNA screen. Human lung epithelial cells (A549) were transfected with either noncoding (scrambled) or IRF3 specific siRNA and infected with influenza virus. No differences in viral output as measured by $TCID_{50}$ were observed in either a long-term, low dose challenge of 0.1 MOI (Fig. 1A) or a short-term, high dose challenge of 5 MOI (Fig. 1B) using

A/Brisbane/59/2007 (H1N1). The efficacy of IRF3 knockdown was measured by western blot (Fig. 1C), and we did not achieve total loss of protein, as analysis of our western blot shows and approximately 75% reduction in protein This could be due to the fact that IRF3 is constitutively expressed to high levels and/or that IRF3 expression is massively upregulated by type 1 IFN.

Loss of IRF3 confers a survival advantage after lethal influenza challenge in mice

To determine any role IRF3 is playing during influenza infection of mice, wildtype (WT) and IRF3$^{-/-}$ mice were intranasally infected with one lethal-dose$_{50}$ of mouse-adapted A/California/04/2009 (H1N1). Weight loss was monitored as an indicator of general well-being, and between days 4-6 after infection, IRF3$^{-/-}$ mice retained significantly more of their body weight (Fig. 1D). All WT mice eventually succumbed to infection, but 20% of the IRF3$^{-/-}$ mice survived the infection (Fig. 1E). The survival benefit was significant (p = 0.0032) when analyzed using the Log-Rank test. To measure viral reproduction in the lungs of infected animals, the right lungs were used in a plaque assay. Viral titer was not different on either days one, three, or seven after a lethal infection of A/Puerto Rico/8/1934 (H1N1) (PR8-rg) (Fig. 1F). Weight loss and survival benefits observed in IRF3$^{-/-}$ mice were independent of viral reproduction.

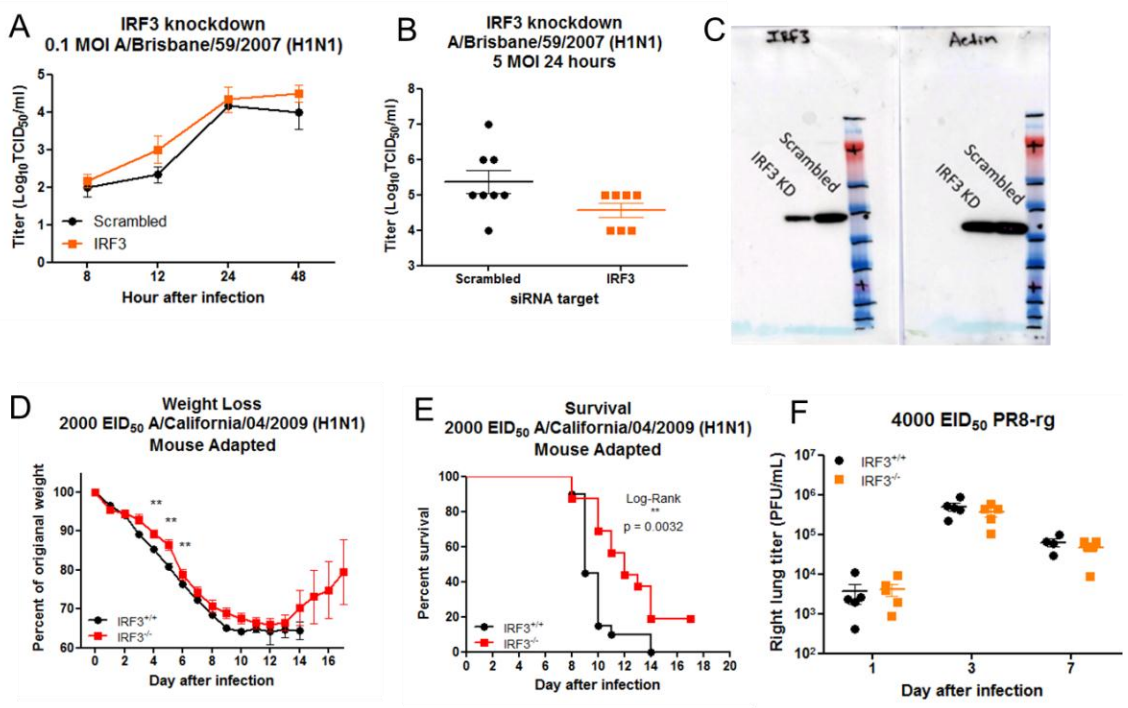

Figure 1. Analysis of IRF3 mediated changes during influenza infection. Lung epithelial cells were transfected with either control (scrambled) or IRF3 targeting siRNA. (A) A549 cells were infected with 1 MOI A/Brisbane/59/2007 (H1N1) and supernatant was taken for titer determination by $TCID_{50}$ at the indicated time after infection. (B) Using the same knockdown protocol, A549 cell were infected with 5 MOI of the same virus in (A), and 24 hours after infection, supernatant was collected for $TCID_{50}$. No difference in titer was noted between scrambled and IRF3 knockdown cell. A western blot was used to determine the amount of IRF3 in A549 after knockdown (C). Wild type and $IRF3^{-/-}$ mice were infected with 1 LD_{50} of a mouse adapted A/California/04/2009 (H1N1) and weight loss (D) and survival (E) were monitored until mice recovered. The right lung of infected mice was used to determine viral replication by plaque assay at the indicated time points after a 1 LD_{50} dose of PR8-rg. Weight loss differences were assessed using a two-way ANOVA and Bonferroni's post-test where ** $p < 0.01$. Survival data were analyzed using the Log-Rank test.

Loss of IRF3 skews cytokine response during influenza infection

Having demonstrated that IRF3$^{-/-}$ mice fare better during infection in a virus-independent manner, we next investigated the role of IRF3 in the immune response to influenza virus. Animals were infected with PR8-rg, and BAL was collected one, three, and seven days after infection. To assess the damage to the lungs after infection, total protein in the BAL was determined using a BCA assay, and BAL from IRF3$^{-/-}$ mice contained significantly less protein seven days after infection (Fig. 2A). Less protein in the BAL is indicative of a more intact barrier inside the lungs. Knowing that IRF3 is a major inducer of IFNβ expression, an ELISA was used to measure IFNβ in the BAL after infection (Fig. 2B). We observed less IFNβ in the BAL from IRF3$^{-/-}$ mice three days after infection, but the difference was not significant. However, IRF3 is not the only known transcription factor responsible for IFNβ expression, and it is possible there are compensatory mechanisms to promote IFNβ expression during influenza virus infection.

To expand our assays for soluble immune factors induced after infection, a 32-plex bead-based system was used. Of the 32 cytokines and chemokines measured, only three were statistically different between groups of mice. More IFNγ was in the BAL of IRF3$^{-/-}$ mice three and seven days after infection (Fig. 2C). Levels of CXCL9 and CXCL10, IFNγ-induced T cell chemoattractants, were significantly increased in the BAL of IRF3$^{-/-}$ mice on day 3 after infection (Figs. 2D

and 2E, respectively). During influenza infection, IRF3$^{-/-}$ mice were making more soluble T cell attractants compared to WT mice.

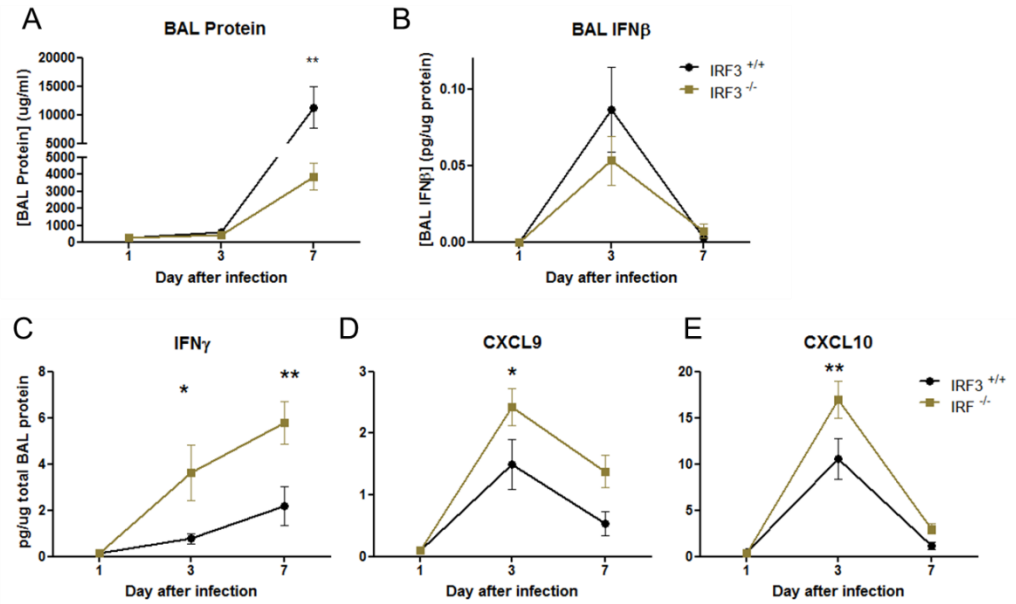

Figure 2. Changes in soluble factors during influenza infection. Mice were infected with 4000 EID_{50} PR8-rg, and the lungs were washed to obtain BAL at one, three, and seven days after infection. Total protein in the BAL was measured using a standard BCA assay (A). An ELISA was used to measure the about of IFNβ (B). A 32-plex Mouse MILLIPLEX kit was used to measure soluble factors in the BAL, and the only statistically significant levels of IFNγ (C), CXCL9 (D), and CXCL10 (E) in the BAL. Differences were measured using a two-way ANOVA and Bonferroni's post-test, where * $p < 0.05$ and ** $p < 0.01$.

Flow cytometry analysis of IRF3$^{-/-}$ mice during influenza infection

Having observed changes in the presence of cytokines and chemokines after influenza infection in IRF3$^{-/-}$ mice, we next conducted flow cytometric studies to uncover any changes in the cellular immune response. Mice were intranasally infected with PR8-rg, and BAL, lung, MLN, and spleen was harvested one, three, and seven days after infection. The tissues were processed and stained for flow cytometry. Figure 3 is an illustration of the gating strategy used to determine

specific cellular populations. Live cells were gated out of the total cells (Fig. 3A), and further characterized in to CD8 T cells (Fig. 3B), inflammatory monocytes (Fig. 3C), macrophages (Fig. 3C), or neutrophils (Fig. 3D). No striking differences were observed in populations other than CD8 T cells. Figure 4 is a representative schematic of the changes in CD8 T cells in the MLN of infected mice, where we consistently found more CD8 T cells in the IRF3 null mice.

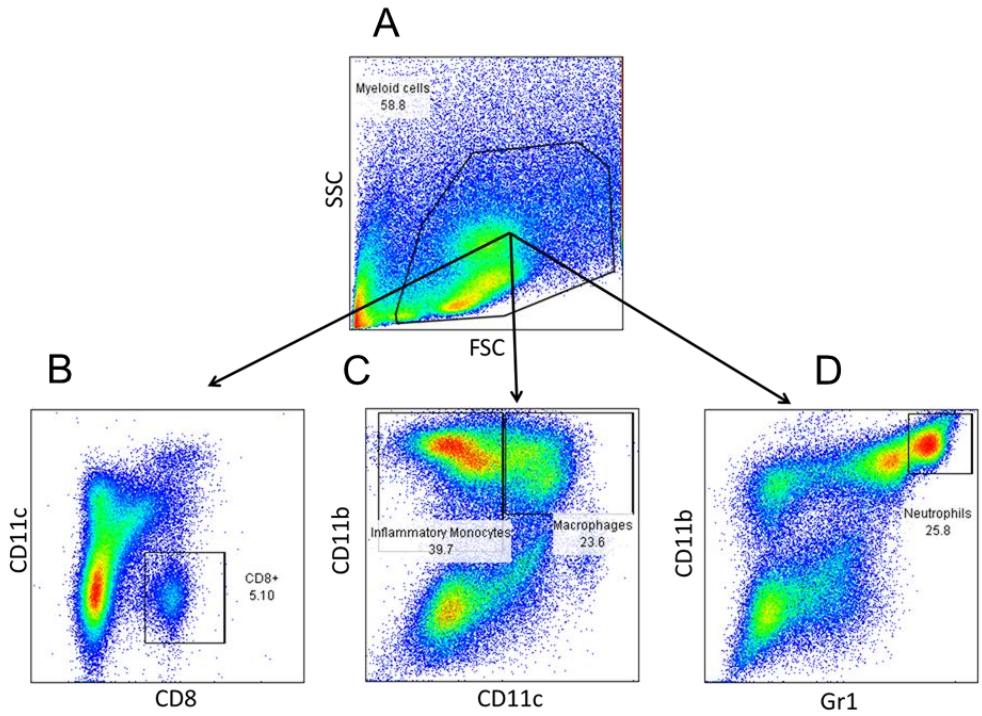

Figure 3. Gating strategy used for flow cytometry experiments. To separate different populations of myeloid cells, we first gated the live cells (A). To find CD8 T cells, we gated on the CD8 positive CD11c negative population (B). Inflammatory monocytes were CD11b positive and CD11c negative (C), and macrophats were double positive for CD11b and CD11c (C). To select neutrophils, the brightest CD11b and Gr1 cells were gated.

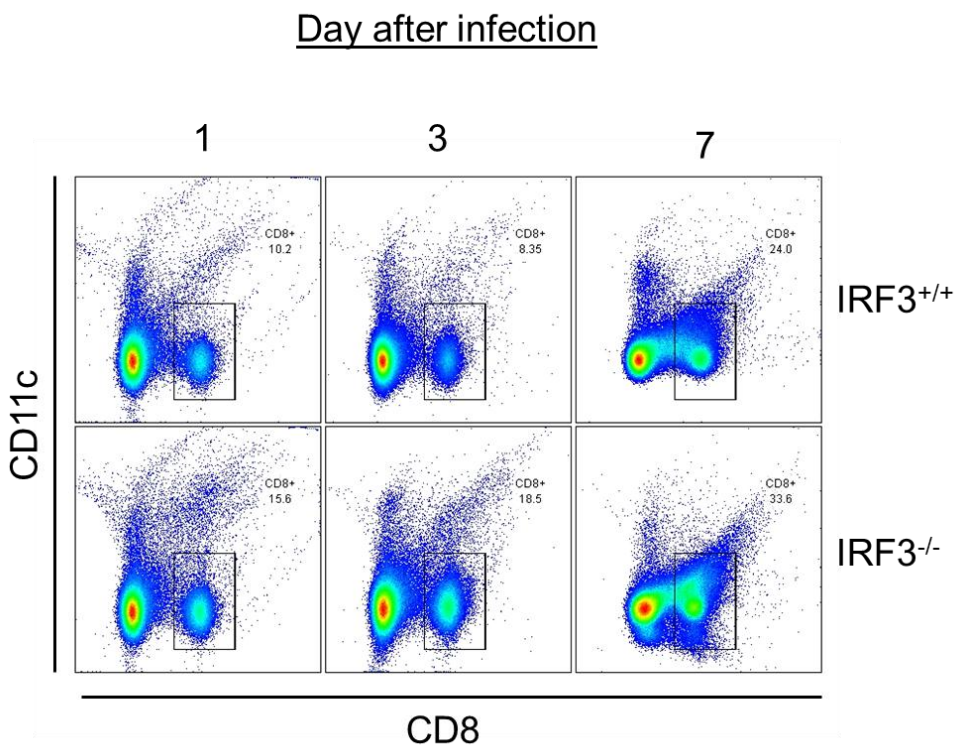

Figure 4. Changes in CD8 T cell populations in MLN of infected mice. After infection the lymphoid tissue of IRF3-/- mice consistently contained more CD8 T cells compared to WT mice. These are representative plots from the MLN of WT and IRF3-/- mice during infection. At each time assayed, IRF3-/- mice had higher percentages of CD8 T cells.

We found no changes in either proportion or number of CD8 T cells in the BAL of IRF3$^{-/-}$ mice compared to WT at all the time points we analyzed. In the MLN, IRF3$^{-/-}$ mice had significantly more CD8 T cells (Fig. 5A) on day three after infection, and CD8 T cells made up a larger proportion of total cells one and three days after infection (Fig. 5B). More CD8 T cells as measured by total number and percentage were seen within the lung parenchyma of IRF3$^{-/-}$ mice seven days after infection (Fig. 5C and 5D, respectively). Three days after infection, IRF3$^{-/-}$ mice also had more CD8 T cells in the spleen (Fig. 5E). Thus,

IRF3 deficiency seems to promote greater accumulation of T cells largely in lymphoid organs.

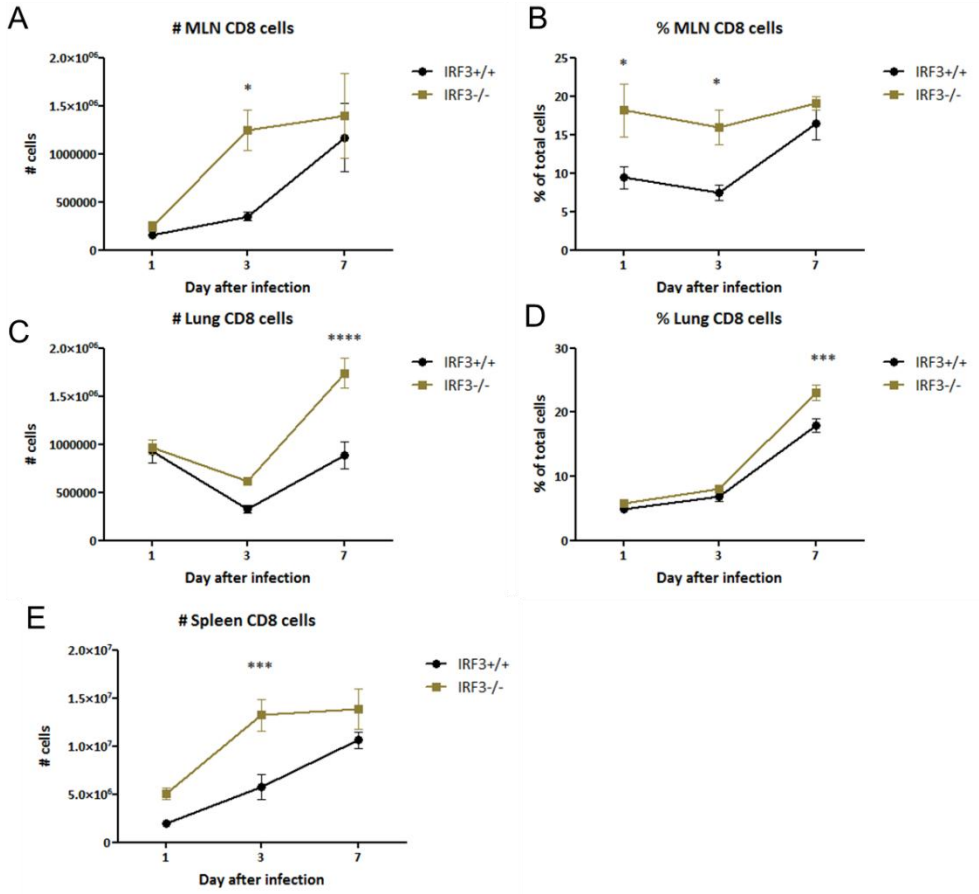

Figure 5. Changes in CD8 T cell populations after influenza infection. During influenza virus infection, BAL, lung, MLN, and spleen were harvested for flow cytometry detection of CD8 T cells. No differences were noted in the BAL (data not shown). In the MLN, IRF3⁄- mice had greater absolute numbes of CD8 T cells on three days after infection (A), and higher percentages of CD8 T cells at day day one and three (B). In the lungs IRF3⁄- mice had dramatically more amount CD8 T cells seven days after infection (C), and the percentage of CD8 T cells in IRF3⁄- mice lungs was also higher than WT at the same time point (D). In the spleen, no differences were observed in the proportion of CD8 T cells, but IRF3⁄- spleens had more total CD8 T cells three days after infection (E). To test differences in the CD8 T cell populations we used a two-way ANOVA and Bonferroni's post-test, where * $p < 0.05$, *** $p < 0.001$, **** $p < 0.0001$.

Influenza specific CD8 T cell response in IRF3$^{-/-}$ mice after influenza infection.

Having more CD8 T cells in various tissues during an influenza infection does little unless those cells are influenza-specific. To measure influenza-specific CD8 T cells, lung, MLN, and spleen were processed for flow cytometry using influenza NP specific tetramers to label specific CD8 T cells seven days after infection. Statistically significant increases of the proportion of NP positive cells were seen in the MLN of IRF3$^{-/-}$ mice (Fig. 6A). Additionally more total numbers of NP specific cells were seen in the MLN of IRF3$^{-/-}$ mice, but this difference was not significant (Fig. 6B). At day seven after infection, the adaptive immune response is just beginning to amplify, and further investigation is needed to determine if any other changes occur during the immune response to influenza virus in IRF3$^{-/-}$ mice.

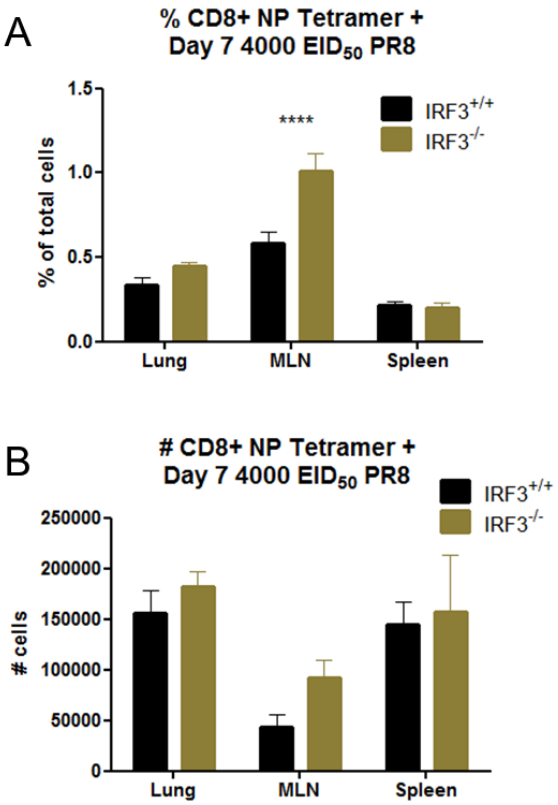

Figure 6. Influenza specific CD8 T cell response during influenza infection. To determine if the CD8 T cells responding to the influenza infection were influenza antigen specific, seven days after infection we labeld the CD8 T cells with NP specific tetramers that bind to T cell receptors specific for the NP antigen. No differences were seen in NP specific cells in the BAL (data not shown). In the MLN of IRF3-/- mice, the proportion of NP specific cells was dramatically increased (A). Though changes were noted in lung or spleen, they were not significant. While the total number of NP specific cells were observed to be increased in the MLN and lung (B), the differences were not significant between WT and IRF3-/- mice. A two way ANOVA was used to test for significant changes in NP positive populations, **** $p < 0.0001$.

Discussion

Initiation of the type 1 IFN antiviral response can occur via several mechanisms, but the first wave of IFNβ expression is thought to rely heavily on IRF3. Our findings that viral titer *in vitro* was unaffected by siRNA mediated IRF3 knockdown came as a surprise. We expected to observe uncontrolled influenza replication after IRF3 knockdown, but instead measured the same amount of viral progeny produced during infection of A549 cells. It is known that IRF7 can also induce IFNβ expression (Honda et al., 2005). However, IRF7 has been studied more vigorously in IFNα expression induction, in populations of dendritic cells, and in the positive feedback of type 1 IFN responses (Sato et al., 2000). It is possible the IRF7 mediated expression of IFNβ is compensating for establishing an antiviral state in our model. Another explanation could be the release of pre-formed IFNβ granules that could be release as soon as the infected cells sense danger. In future experiments, we plan on analyzing the supernatant of A549 cells to determine if any inflammatory molecules are present. Additionally, our knockdown of IRF3 was not perfect. We could recreate these studies in A549 cells engineered to have a permanent deletion of IRF3 to definitively determine if loss of IRF3 has an effect on viral replication.

The loss of IRF3 in the mouse model of influenza infection leads to a survival benefit that is independent of viral replication. Our findings disagree with previous reports suggesting only deletions of several IRF family members lead to loss of viral control (Chen et al., 2013). We believe that controversy surrounding the importance of each IRF family member is rooted in the different mice and model systems used around the world. It could be true that one IRF is more

central to defense than others in a certain disease state, but the research needed to clear up these discrepancies will take a long time to generate. We also believe that the current practice of humane euthanasia of mice based on weight loss is fundamentally flawed. Many institutions hamstring their researchers by requiring them to sacrifice mice once they lose a predetermined amount of body weight. These rules are established for the animals' welfare, but in reality, they are forcing animal research to be a race to their human cutoff. Our ethical guidelines are somewhat more generous than many other institutions, but we consistently observe recovery of mice that have lost greater that 25% of their original weight. A unified model of survival will be an important tool for further research.

The induction of the adaptive immune response requires signals from the innate immune system. In the case of an antigen-specific CD8 T cell response, IFNγ signaling is central to the development of an efficacious defense. Additionally, the IFNγ-induced chemokines CXCL9 and CXCL10 function to attract CD8 T cells to sites of infection and the drain lymph nodes for selection and amplification of antigen specific CD8 T cell populations. The BAL from $IRF3^{-/-}$ mice contained less total protein than WT BAL, indicating that the airways of the WT mice were more permeable and thus more damaged during the infection. More IFNγ, CXCL9, and CXCL10 was produced by $IRF3^{-/-}$ mice during the infection, suggesting that this cytokine cascade was driving the differences in CD8 T cell levels we observed. It is known that IRF3 can directly bind to and induce the expression of both CXCL9 and CXCL10 (Honda and Taniguchi, 2006), but our data indicate that a loss of IRF3 leads to greater expression during

influenza infection. The discrepancies could be due to different models and mice, and only further investigation could rectify the different data.

The role of IRF3 in the generation of an adaptive immune response is controversial (Lendonck et al., 2014). In our model, loss of IRF3 leads to the generation of a more robust antigen-specific CD8 T cell response. However, we need to resolve our data farther with further phenotypic analysis of the cellular response and additional functional characterization of the cells at different times during the infection. Generation of bone marrow chimera mice would allow us to investigate if any differences are due to myeloid cells only, or if the stroma is playing a role as well. We plan on further dissecting the contribution of IRF3 to the immune response during influenza infection with more focused experiments in the future.

CHAPTER 4

MxA IS PRESENT AT BASAL LEVELS AND A KEY PLAYER OF ANTIVIRAL SIGNALING

Introduction

The Myxovirus resistance gene 1 (Mx1 in mice, MxA in man) was discovered more than 50 years ago (Lindenmann, 1962) and is known as a viral restriction factor in a variety of experimental settings (Haller et al., 2007a). Since that time, the Mx proteins have been thoroughly researched for their role in the types 1 and 3 interferon (IFN)-stimulated antiviral response; however very few studies aknowledge the fact most laboratory strains have no Mx gene due to truncation or deletion as a result of inbreeding. Initial reports of the antiviral properties of Mx proteins were modeled using common lab strain mice, transgenically engineered to express mouse Mx1 or human MxA, and then infected with Orthomyxoviridae family members of influenza or Thogoto virus (Frese et al., 1995; Haller et al., 1995). Mice expressing a wildtype Mx gene were more resistant to infection. Subsequently it has been discovered that Mx proteins can inhibit a wide variety of viruses including paramyxovirus, bunyavirus, pircornavirus, hepadnavirs, and even HIV in studies tracking the MxB isoform (Kane et al., 2013; Verhelst et al., 2013). In humans, mutations in MxA can predict sensitivity to enterovirus 71 infection outcome (Zhang et al., 2014) and predisposure to prostate cancer (Glymph et al., 2013). Expression patterns of MxA are also being used to monitor the state of type 1 IFN response in patients with multiple sclerosis (Bertolotto et al.), vitiligo (Bertolotti et al., 2014), and

hepatitis (Bolen et al., 2012). In addition to the innate antiviral role of Mx proteins, there appear to be intimate but unresolved responsibilities of Mx proteins in the type 1 IFN response.

Previous research has consistently described the expression of Mx proteins as being IFN-induced. That is, Mx proteins are only translated after a cell is stimulated with IFN (Haller and Kochs, 2011). However, in mice engineered to express MxA but lacking the type 1 IFN receptor (IFNAR), MxA activity was unperturbed and was sufficient to defend against several viral challenges (Hefti et al., 1999). In the Hefti group, the transcription of the MxA transgene was under the control of the 3-hydroxy-3-methyl- glutaryl coenzyme A reductase gene promoter. In a similar study, mice expressing Mx1 but lacking signal transducer and activator of transcription 1 (STAT1), the animals were able to defend against Crimean-Congo hemorrhagic fever virus by upregulating Mx1 (Bowick et al., 2012). These data suggest that basal MxA expression can defend against the earliest insults to target cells. This idea has even led to the production of transgenic pigs overexpressing porcine Mx to defend industrial swineherds against influenza A and classical swine fever virus (Yan et al., 2014).

The purpose of this work is to discover any early expression or activity of MxA in human lung cells (A549) in the context of influenza virus challenge. Additionally, we want to uncover any role MxA may play during the early phases of infection and the innate immune response. We use siRNA to knockdown MxA in A549 cells and then monitor the expression levels of various antiviral genes involved in the sensing, signaling, and defending pathways of the antiviral

response. Confocal microscopy is also employed to track the activation of MxA after infection and to monitor any defect in signaling molecules when MxA is knocked down. During the course of our work we have basal expression of MxA is capable of responding to incoming virus, loss of MxA causes a distinct loss of expression in many type 1 IFN genes, and this change in expression is most likely caused by a defect in IRF3 activation. We find that during infection, MxA immunoprecipitates with at least four of the influenza virus proteins as well as several important signal scaffolding molecules. Together, we propose that MxA is playing an intimate role in viral sensing/signaling upstream of the induction of the type 1 IFN response. These findings add an important early defense and detection function to the already impressive list of antiviral actions ascribed to Mx proteins.

Methods and Materials

Cells and viruses

Human lung cell line (A549) was maintained in growth medium (high glucose DMEM (Gibco) supplemented with 10% fetal bovine serum (Atlanta Biologics), 100 U/ml penicillin (Gibco), and 100 µg/ml streptomycin (Gibco)). Before infections, cells were washed three times with PBS. Virus was diluted in infection medium (high glucose DMEM supplemented with 0.3% bovine serum albumin (Sigma) and 100 U/ml penicillin (Gibco), and 100 µg/ml streptomycin (Gibco)). All influenza viruses were grown in embryonated chicken eggs and aliquots of high titer virus were stored in allantoic fluid at -80°C. Viral titers were measured using the $TCID_{50}$ method as described in (Oguin et al., 2014).

Gene Knockdown

To knockdown gene expression in A549 cells, 100-200 nM of MxA specific siRNA (Ambion) or noncoding (Scrambled) control siRNA was electroporated using the Neon Transfection System (Life Technologies) according to manufacturer's recommendations. Cells were allowed to adhere overnight after transfection.

Gene Expression

To conduct gene expression assays, A549 cells were seeded into 6 well plates and incubated at 36°C overnight. Cells were washed 3 times in Dulbecco's phosphate buffere saline (DPBS) (Gibco) and then infected with virus diluted in infection medium. Virus was incubated on the cells for 1 hour at 4°C. The virus was aspirated from the cells and fresh, 35°C infection medium was added to the cells, and this moment is regarded as time = 0. The RNA was collected using an RNeasy kit (Qiagen), reverse transcription PCR was performed as directed in the iScript cDNA Synthesis Kit (Bio-Rad), and qPCR was performed using TaqMan Gene Expression Assays (Life Technologies) as directed in a 7900HT (Applied Biosystems). To determine gene expression levels, the $2^{-\Delta\Delta Ct}$ method was used (Livak and Schmittgen, 2001), with GAPDH expression used as the housekeeping gene and normalized to uninfected sample expression level. These experiments have been repeated and were conducted with at least 3 biological replicates and 2 technical replicates for each repeat.

Western Blot

To detect protein levels in cells, A549 were lysed using lysis buffer (Pierce) prepared with one tablet of protease inhibitor cocktail (Roche). Protein was quantified with a BCA assay (Pierce), and equal amounts of protein was loaded into pre-made 4-12% Bis-Tris SDS-PAGE (Life Technologies) and separated by electrophoresis. Protein was transferred to nitrocellulose membranes using the iBlot System (Life Technologies), and the membranes were blocked with 5% milk in 1X TBS with Tween 20 (Life Technologies). Probing was conducted with antibodies diluted in the blocking buffer, and the primary antibodies were detected with appropriately horseradish peroxidase labeled secondary antibodies. Protein was detected using the SuperSignal chemiluminescent kit (Pierce) and an Amersham Imager 600 (General Electric).

Confocal microscopy studies

Cells were seeded on chamber slides (Nunc) and allowed to adhere overnight. Cells were washed 3 times in DPBS and then infected with virus diluted in infection medium. Virus was incubated on the cells for 1 hour at 4°C. The virus was aspirated from the cells and fresh, 37°C infection medium was added to the cells, and this moment is regarded as time = 0. Cells were fixed in 4% paraformaldehyde for 20 minutes, permeabilized in 0.3% Tween-20 in DPBS for 15 minutes, and blocked using 10% FBS in DPBS for at least 1 hour. Probing was accomplished using antibodies diluted in blocking buffer, and the antibodies were left on the cells for 1 hour at room temperature on a plate rocker. Primary antibodies were detected with appropriate fluorescently labeled secondary

antibodies (all from Molecular Probes), and DNA was stained with DAPI. After staining, coverslips were mounted using ProLong Gold (Molecular Probes). Data were collected and analyzed as described in (Oguin et al., 2014).

Co-immunoprecipation assay

A549 cells were infected with 1 MOI A/California/04/2009 (H1N1) for 18 hours. Using an antibody cross-linking co-immunoprecipitation kit (Pierce), a monoclonal MxA antibody was bound to beads and used to pull down any protein complexes formed by MxA during influenza infection. Eluted product was subjected to mass spectrometry (MS) analysis in the St. Jude Children's Research Hospital Proteomics Core. The proteins in the gel bands were reduced with DTT to break disulfide bonds, and the Cys residues were alkylated by iodoacetamide to allow the recovery of Cys-containing peptides. The gel bands were then washed, dried in a speed vacuum, and rehydrated with a buffer containing trypsin, for overnight proteolysis. The next day digested samples were acidified, and the peptides were extracted multiple times. The extracts were pooled, dried, and reconstituted. The peptide sample were loaded on a nanoscale capillary reverse phase C18 column by a HPLC system (Thermo EASY-nLC 1000), and eluted by a gradient (~45 min). The eluted peptides were ionized by electrospray ionization, and detected by an inline mass spectrometer (Thermo Orbitrap Elite). The MS spectra were collected first, and the top 10 abundant ions were sequentially isolated for MS/MS analysis. This process was repeated for product throughout the entire liquid chromatography gradient. Database searches were performed using Sequest search engine in an in-house

SPIDERS software package. All matched MS/MS spectra were filtered by mass accuracy and matching scores to reduce protein false discovery rate to less than 1%. In addition, the total number of spectra (i.e. spectra count) matching to individual proteins may reflect the abundance after the protein size is normalized. False discovery rate was set at 1%.

Data analysis

Data were analyzed in GraphPad Prism 5, and the statistical tests used are listed in each experiment.

Results

MxA is present at basal levels and activated early after viral infection.

As stated previously, current dogma surrounding the expression and activation of Mx proteins maintains that Mx proteins are induced after an IFN signal has triggered expression in a target cell. This means that IFN would have to be released from a source and then activate surrounding cells to begin the type 1 IFN response, a process that would take quite some time. Not only would the IFN release and subsequent Jak/STAT signaling have to occur, but the transcription and translation of Mx proteins and other ISGs, such as IRF3, that promote the feed-forward type 1 IFN pathway would also have to occur. To test if MxA is present at basal levels in human lung cells, we infected A549 cells with 1 MOI A/Brisbane/10/1997 (H3N2) and harvested protein from the cells for western blot detection of MxA. Cells harvested at time 0 were positive for MxA by western blot (Fig. 1A), indicating that A549 cells express basal levels of. Additionally, we detected the activation of MxA protein during infection. The MxA

bands increased in size and intensity at 0.5, 1 and 8 hours after infection compared to time 0 (Fig. 1A). From these data, we conclude that not only is MxA expressed in uninfected cells, but that MxA can also be activated by influenza virus infection before a type 1 IFN response is able to stimulate expression of new MxA.

Using a similar model, we wanted to track MxA activation during infection by confocal microscopy. We uncovered a kinetic relationship of MxA activation during influenza infection of A549 cells where MxA accumulation increased as early as 30 minutes after infection, peaking at 90 minutes after infection, and beginning to wane at least360 minutes after infection just as influenza NP was beginning to be synthesized (Fig. 1B). During 6 hours of a 1 MOI A/California/04/2009 (H1N1), we observed MxA forming puncta of increasing size and intensity occurring in cells that were also positive for influenza NP (Fig. 1C). The accumulation of MxA that begins as early as 30 minutes after infection leads us to conclude that latent MxA in A549 cells is able to respond to viral infection very early during influenza infection to our knowledge. This is the first report that details basal expression of MxA and its ability to respond to virus during the earliest events of infection.

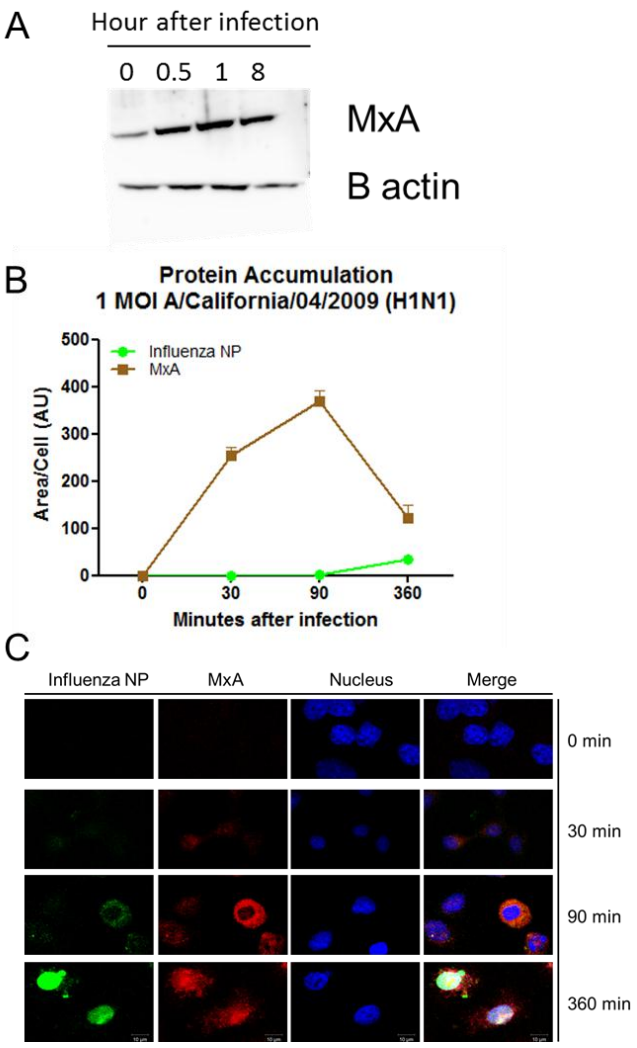

Figure 1. Accumulation of MxA during the early phases of influenza infection. Human lung epithelial cells were infected with 1 MOI A/Brisbane/10/2007 (H3N2), and protein was extracted at indicated time points for western blot detection of MxA (**A**). Protein concentration was standardized, and 10 µg of total protein was loaded in each well of a 4-12% Bis, Tris polyacrylamide gel. The proteins were transferred to a nitrocellulose membrane. Polyclonal antibodies were used to probe for MxA and β-actin (loading control), and monoclonal horseradish peroxidase linked antibodies were used to detect the primary antibodies. MxA staining intensity and size were detected by confocal microscopy (**B** and **C**). A549 cells were grown in chamber-slides and infected with 1 MOI A/California/04/2009 (H1N1). At indicated times after infection, cells were fixed and processed for microscopic analysis. The same antibody used in (**A**) was used to detect MxA in (**B** and **C**), and a monoclonal anti-influenza NP antibody was used to detect viral protein.

MxA restricts viral reproduction and is a critical player in the stimulation of Type 1 IFN signaling.

Long described as a viral restriction factor, we used siRNA to knockdown the expression of MxA in A549 cells to determine if MxA could restrict influenza viral reproduction in our model. To knockdown MxA expression, we transfected siRNA into A549 cells and allowed the cells to adhere overnight. Viral output was near the limit of detection for our assay in control cells, demonstrating the protective effects of MxA expression. After MxA expression has been obliterated, we find that viral reproduction is enhanced by nearly 2.5 fold, 8 hours after a 5 MOI A/Brisbane/10/2007 (H3N2) infection (Fig. 2A). We chose this method to measure viral reproduction because we are relying on detecting *de novo* virions produced from infected cells, and the earliest we could detect these virions is 8 hours after infection. Therefore, loss of MxA in influenza infected A549 cells leads to more viral replication.

By demonstrating that MxA was active very early during influenza infection and that loss of this activity allows more viruses to be made, we hypothesized that MxA may be involved in establishing an antiviral state in cells. We knocked down expression of MxA in A549 cells, and infected the cells with 1 MOI A/California/04/2009 (H1N1). During the infection, RNA was isolated from cells, and we determined changes in expression of several genes involved in the type 1 IFN response using real-time PCR and the $2^{-\Delta\Delta Ct}$ method to determine relative expression. When MxA expression is knocked down, we observed a marked decrease in expression levels of IFITM1, IFITM3, IFNα, IFNβ, IRF3, IRF7, MAVS,

and OAS1 compared to A549 cells transfected with noncoding (Scrambled) siRNA (Fig. 2B). In scrambled siRNA treated cells upregulation of all genes assayed was noted, but in the MxA knockdown model we observed very mild expression increases in IFITM1, IRF7, and OAS1 alongside no measurable induction of IFITM3, IFNα4, IFNβ, IRF3, or MAVS. Efficacy of siRNA knockdown of MxA was determined by western blot (Fig. 2C).

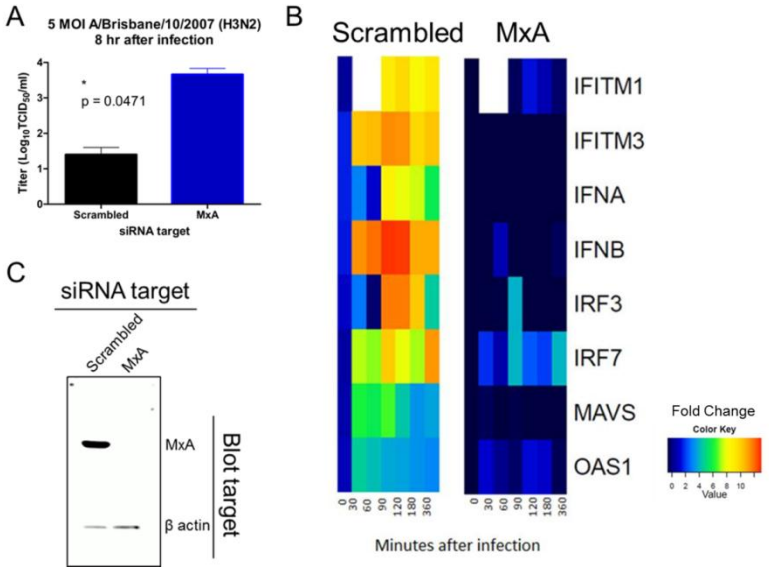

Figure 2. Expression of MxA protects A549 cells from influenza and plays a critical role in the induction of an antiviral state. (**A**) Viral replication of cells treated with scrambled siRNA is near the limit of detection using the $TCID_{50}$ method, but when MxA expression is knocked down, viral reproduction is unrestricted (p = 0.041 unpaired t-test). Loss of MxA leads to a dramatic loss of expression of several innate immune proteins (**B**). Real-time PCR was used to determine the relative expression of the listed genes during the first 6 hours of 1 MOI A/California/04/2009 (H1N1) infection. Relative gene expression was calculated using the $2^{-\Delta\Delta Ct}$ method and GAPDH was used as a reference gene, increases in fold expression are indicated by warmer colors on the heat map. (**C**) Validation of gene knockdown using western blot. Protein from A549 cells transfected with scrambled or MxA siRNA were probed for the presence of MxA and β actin

Translocation of p-IRF3 to the nucleus is impaired when MxA is knocked down.

A hallmark of type 1 IFN pathway induction is the phosphorylation and subsequent nuclear translocation of IRF3 into the nucleus. Having observed a marked decrease in antiviral gene expression when MxA is knocked down, we measured p-IRF3 accumulation in the nuclei of A549 cells infected with either 1 MOI A/Brisbane/59/2007 (H1N1) or A/California/04/2009 (H1N1) 180 minutes after infection. We transfected A549 cells with siRNA targeting MxA, infected the cells, and used confocal microscopy to track the movement of p-IRF3 into the nucleus. In cells infected with A/Brisbane/59/2007 (H1N1), we observed much less (p = 0.0484) p-IRF3 in nuclei 180 minutes after infection when MxA is knocked down compared to cells transfected with the noncoding control (Fig. 3A). We also observed less p-IRF3 in the MxA knockdown model after an A/California/04/2009 (H1N1) infection (Fig. 3B), but the difference was not statically significant (p = 0.0714). Representative images of the translocation of p-IRF3 to the nucleus during infection can be viewed in Fig. 3C, where the red signal is p-IRF3 and the blue signal is the nuclei of A549 cells. We suspect loss of MxA is somehow disrupting upstream antiviral sensing and signaling pathways leading to a loss of type 1 IFN induction via activation of p-IRF3. Importantly, we also observed a differential response that is virus dependent. The A/Brisbane/59/2007 (H1N1) isolate induces more p-IRF3 translocation of ~6 AU compared to the pandemic A/California/04/2009 (H1N1) which causes a ~2.5 AU p-IRF3 accumulation in A549.

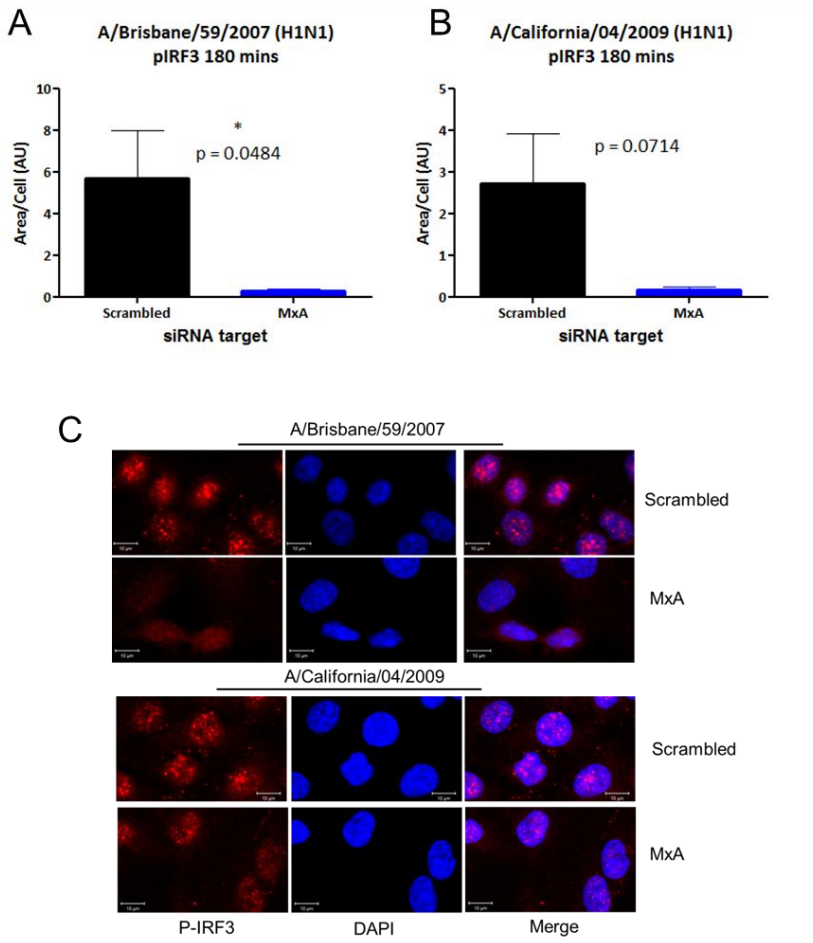

Figure 3. Loss of p-IRF3 nuclear translocation during infection after MxA knockdown. A549 cells were treated with either noncoding (scrambled) or MxA specific siRNA and plated on chamber slides. The cells were infected with 1 MOI of the indicated influenza virus strains, and 180 minutes after infection, the samples were processed for confocal microscopic detection of p-IRF3. Accumulation of nuclear p-IRF3 was measured by size and intentisty (**A** and **B**), and compared using a t-test in GraphPad Prism. Representative images (**C**) were prepared using ImageJ. Red signal represents p-IRF3 staining, and blue signals are the cell nuclei.

MxA interacts with signaling scaffolding molecules and viral proteins during influenza infection.

After noting the defects in antiviral signaling when MxA is lost, we wanted to determine if MxA is interacting with proteins that are involved in the antiviral sensing and signaling network. Using a co-immunoprecipitation kit (Pierce), we pulled down MxA from A549 cells 18 hours after a 1 MOI A/California/04/2009 (H1N1) infection. Eluate from the assay was submitted for protein identification by mass spectrometry conducted by the Proteomics Core facility at St. Jude Children's Research Hospital. Over 500 proteins were identified from the MxA pulldown, and a stringent analysis was conducted to narrow our pulldown results to a list of 20 proteins (Table 1). Only proteins with a spectral count greater than 30, and total peptide identification greater than 5 were included in our initial results. The most abundant protein identified was our target, MxA. We also pulled down several mitochondrial metabolic proteins. Interestingly, a scaffolding molecule involved in mitochondrial signaling and structure Prohibitin 2 (PHB2) (Artal-Sanz and Tavernarakis, 2009), was pulled down with MxA, and this interaction was confirmed with a post-immunoprecipitation western blot (Fig. 4). These data indicate that MxA is located near mitochondria after infection. Recently, mitochondria have been described as a key organelle involved in innate immunity as a nexus of scaffolding molecules (Khan et al.).

In our analysis, we also observed MxA interacting with influenza virus proteins. Using somewhat less stringent parameters, spectral count greater than 5, and total peptide count greater than 2, we identified (in decreasing order of

abundance) influenza non-structural protein 1 (NS1), nucleoprotein (NP), hemagglutinin (HA), and an RNA-directed RNA polymerase catalytic subunit (Table 2). The NS1 gene of influenza virus has been implicated in antagonizing the type 1 IFN response (Krug, 2015), but has not been reported to bind with MxA. Additionally, MxA has been thought to bind viral RNPs (Haller and Kochs, 2011), but no direct evidence of this interaction has been demonstrated during influenza infection.

Table 1. Proteins interacting with MxA during influenza infection. A549 cells were infected for 18 hours with 1 MOI A/California/04/2009 (H1N1). An MxA antibody was used to perform a co-immunoprecipitation. Eluted proteins were sequenced using mass spectrometry. Limiting spectral count to 30 or more and total peptide counts to greater than five, we have listed the top 20 non-contaminant proteins that pulled down with MxA after infection.

Accession#	Protein Annotation	Spectral Count	Total Peptides	MW (KD)	Abundance
sp|P20591|MX1_HUMAN	Interferon-induced GTP-binding protein Mx1	143	18	75	94.73
sp|O60701|UGDH_HUMAN	UDP-glucose 6-dehydrogenase	87	15	55	79.1
sp|P06733|ENOA_HUMAN	Alpha-enolase	65	11	47	68.94
sp|P08238|HS90B_HUMAN	Heat shock protein HSP 90-beta	108	17	83	64.89
sp|P10809|CH60_HUMAN	60 kDa heat shock protein, mitochondrial	74	17	61	60.64
sp|Q99623|PHB2_HUMAN	Prohibitin-2	40	9	33	60.1
sp|P06576|ATPB_HUMAN	ATP synthase subunit beta, mitochondrial	65	13	57	57.5
sp|Q13011|ECH1_HUMAN	Delta(3,5)-Delta(2,4)-dienoyl-CoA isomerase, mitochondrial	38	9	36	53.08
sp|P25705|ATPA_HUMAN	ATP synthase subunit alpha, mitochondrial	63	14	60	52.75
sp|P38646|GRP75_HUMAN	Stress-70 protein, mitochondrial	73	15	74	49.57
sp|P53396|ACLY_HUMAN	ATP-citrate synthase	103	20	121	42.65
sp|P11413-2|G6PD_HUMAN	Isoform Long of Glucose-6-phosphate 1-dehydrogenase	51	14	64	39.98
sp|P20592|MX2_HUMAN	Interferon-induced GTP-binding protein Mx2	51	9	82	31.08
sp|P06744|G6PI_HUMAN	Glucose-6-phosphate isomerase	38	7	63	30.11
sp|P49327|FAS_HUMAN	Fatty acid synthase	122	35	273	22.32
sp|Q13200|PSMD2_HUMAN	26S proteasome non-ATPase regulatory subunit 2	44	11	100	21.97
sp|P55072|TERA_HUMAN	Transitional endoplasmic reticulum ATPase	31	8	89	17.36
sp|Q14974|IMB1_HUMAN	Importin subunit beta-1	33	8	97	16.99
sp|P46940|IQGA1_HUMAN	Ras GTPase-activating-like protein IQGAP1	63	23	189	16.65
sp|Q14204|DYHC1_HUMAN	Cytoplasmic dynein 1 heavy chain 1	90	41	532	8.46

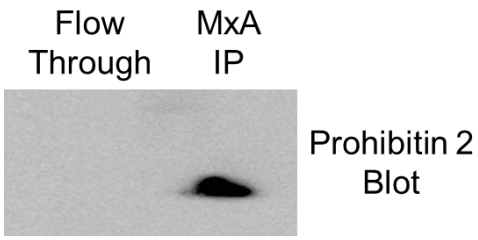

Figure 4. Confirmation of MxA-PHB2 interaction. After co-immunoprecipitation of protein from A549 cells infected for 18 hours with 1 MOI A/California/04/2009 (H1N1), lysate flow through and eluate (MxA IP) were subjected to western blot detection of PHB2.

Table 2. Influenza proteins interacting with MxA. Using the same conditions for co-immunoprecipiation as Table 1, influenza proteins were identified as interacting with MxA during infection. Inclusion parameters were such that spectral count was greater than five, and total peptide count was greater than two.

Accession#	Protein Annotation	Spectral Count	Total Peptides	MW (KD)	Abundance
sp|A8C8K0|NS1_I07A0	Non-structural protein 1	46	5	26	89.15
sp|Q07FI1|NCAP_I96A3	Nucleoprotein	56	5	56	50.05
sp|A3DRP0|HEMA_I96A2	Hemagglutinin	18	2	63	14.19
sp|P16512|RDRP_I77AD	RNA-directed RNA polymerase catalytic subunit	10	2	86	5.79

Discussion

We have demonstrated that of MxA was present in uninfected human lung epithelial cells, activated by viral infection, was a key piece to the antiviral signaling network, and interacts with various host and viral proteins. We present these findings not in contradiction to the current view of MxA activity (Haller and Kochs, 2011; Haller et al., 2007) but in addition to the past work conducted on this important antiviral molecule. Many groups have added to the idea that Mx

proteins are primarily induced by type 1 IFN signaling in similar experimental settings, but our model is unique in that we are investigating the earliest events of antiviral signaling using different technologies to accomplish our goals. The Mx proteins are some of the most effective antiviral defense molecules in the innate immune arsenal, from humans down to fish (Verhelst et al., 2013). Our hypothesis was that these vitally important proteins would be better suited as first-line defenders in addition to being enhanced further by type 1 IFN stimulation. In Fig. 1A, we establish that MxA protein was present in A549 cells by western blot. Additionally, our confocal microscopy model allowed us to track the activation of MxA (Fig. 1 B&C) very early during influenza virus infection. By choosing early time points, we were able to take a look at MxA activity before type 1 IFN signaling could induce *de novo* MxA fabrication. The virus infection induced, first-line activation of MxA is a new finding that could aid in the research for new investigations to help defend people and agricultural species from viral infection.

We also found a surprising new role for MxA. By knocking down MxA with siRNA and measuring expression of type 1 IFN pathway proteins during infection, we discovered that without MxA, a proper type 1 IFN response could not be initiated (Fig. 2B). In addition, loss of MxA expression leads to unrestricted influenza viral replication (Fig. 2A), further confirming the importance of MxA in the defense against influenza virus infection. Most studies of MxA activity during infection focus on post-type 1 IFN stimulation, usually beginning 6 hours after infection. Our approach to study gene expression very early during the infection

allowed us to uncover the first events that occur after infection. In our control experiment, we see a robust increase in antiviral gene expression, but the loss of MxA nearly abolished antiviral signaling for as long as six hours after infection. With the growing interest in research focusing on upstream molecules in the type 1 IFN pathway such as MAVS (Belgnaoui et al., 2011), RigI (Ehrhardt et al., 2010), and the IFITMs (Perreira et al., 2013), our findings could help fill in gaps in the current knowledge of how viruses are sensed by cells and how the cells defend themselves from infections. Eventually, we would like to validate our findings in more relevant models such as primary cell lines and in mice that have had their Mx genes repaired.

To understand how MxA is contributing to antiviral signaling, we investigated the terminal step in the type 1 IFN response, activation of IRF3. The IRF family of genes has been identified as critical to mounting a proper type 1 IFN response and priming the adaptive immune response (Honda and Taniguchi, 2006; Nakaya et al., 2001). The constitutive expression of IRF3 further points to its importance to the immune system. To be activated, IRF3 must be phosphorylated, dimerize, and translocate to the nucleus of infected cells where it acts as a transcription factor for type 1 IFNs and genes involved in the adaptive immune response such as CXCL9 and CXCL10 (Honda and Taniguchi, 2006). This activation of IRF3 occurs proximal to the mitochondria in many models (Fitzgerald et al., 2003). Our findings that loss of MxA expression leads to deficient IRF3 activation during infection add another layer of regulation occurring during the type 1 IFN pathway. With further research, we may find that MxA is a

critical but member of the type 1 IFN signaling scaffold. It is clear now that, in our model, MxA is intimately tied to the activation of IRF3.

We have also identified novel binding partners of MxA during influenza virus infection. Our findings are lead us to hypothesize that MxA has some role to play in the antiviral signaling events occurring near the mitochondria (Table 1). Using a co-immunoprecipitation model, we identified several mitochondrial metabolic proteins that interact with MxA during infection, but we need to further validate these interactions. We found that PHB2 interacts with MxA during influenza infection. This is interesting because PHB2 has been implicated as a critical player in the maintenance of mitochondrial form and function (Osman et al., 2009) as well as in the formation of signaling scaffolds (Nijtmans et al., 2000). The mitochondria are now appreciated as a vital construction platform for signaling molecules in the induction of the type 1 IFN response to a variety of stimuli (Khan et al.; Scott, 2009). Discovering MxA interacting with mitochondrial protein PHB2 could lead to MxA being included as another key molecule regulating antiviral signaling. We would like to further resolve these interactions by pulling down MxA at very early time points during infection, but the amount of bait protein available during these events has made this approach exceptionally challenging. With the advent of multicolor, superresolution microscopy, we could attempt to image proteins colocalizing with MxA during the earliest events of infection.

We would like to suggest an alteration of the current model of MxA activity to include MxA as a first line defender that senses virus and interacts with the

type 1 IFN signaling response somewhere in proximity to the mitochondrial-mediated scaffolding network. Much work remains to be conducted to validate and complete this model and our data will add to the future of antiviral signaling research.

OVERALL CONCLUSIONS

The innate response to influenza virus infection is a critical layer of immunological defense. If the innate response can defeat an incoming pathogen before it establishes productive infection, then a better chance for survival is conferred. We have shown that lipid signaling through PLD is an imporatant mechanism during viral entry and subsequent defensive actions by the cell. By inhibiting PLD, viral entry kinetics are slowed. This alteration in viral invasion gives the affected cell more time to sense the pathogen and mobilize defense molecules, and this protection is dependent on an intact type 1 IFN response. The transcription factor IRF3 is an integral player in the type 1 IFN response. We hypothesized that loss of IRF3 would be detrimental to cells and mice during influenza infection, however loss of IRF3 does not affect viral replication in cells or mice. In addition, IRF3$^{-/-}$ mice are more likely to survive a lethal influenza infection compared to intact mice. This benefit is related to an increase in antigen-specific CD8 T cells, but more work is needed to understand the mechanism of protection. An antiviral effector protein, MxA, has long been thought to be an IFN inducible ISG. We find that while MxA is upregulated after IFN release, it is also present at basal levels in human lung cells. During infection, MxA interacts with both influenza proteins and host cell molecules

involved in building signal scaffolds, suggesting a that MxA is involved in type 1 IFN signaling. It remains to us to decipher the temporospatial regulation of MxA during influenza infection. Such a potent antiviral molecule could be an ideal target for defensive therapeutic development. Overall, the innate immune system is a fascinating interplay between pathogen and host cell. Components of the innate system are showing potential to be targets for supportive or prophylactic agents. If an influenza pandemic such as the 1918 pandemic occurs again, we would do well to investigate all possible strategies for defense.

REFERENCES

Accola, M.A., Huang, B., Masri, A.A., and McNiven, M.A. (2002). The antiviral dynamin family member, MxA, tubulates lipids and localizes to the smooth endoplasmic reticulum. J. Biol. Chem. *277*, 21829–21835.

Agarwal, S., Schroeder, C., Schlechtingen, G., Braxmeier, T., Jennings, G., and Knölker, H.-J. (2013). Evaluation of steroidal amines as lipid raft modulators and potential anti-influenza agents. Bioorg. Med. Chem. Lett. *23*, 5165–5169.

Amorim, M.J., and Digard, P. (2006). Influenza A virus and the cell nucleus. Vaccine *24*, 6651–6655.

Arnheiter, H., Skuntz, S., Noteborn, M., Chang, S., and Meier, E. (1990). Transgenic mice with intracellular immunity to influenza virus. Cell *62*, 51–61.

Artal-Sanz, M., and Tavernarakis, N. (2009). Prohibitin and mitochondrial biology. Trends Endocrinol. Metab. *20*, 394–401.

Baccala, R., Hoebe, K., Kono, D.H., Beutler, B., and Theofilopoulos, A.N. (2007). TLR-dependent and TLR-independent pathways of type I interferon induction in systemic autoimmunity. Nat. Med. *13*, 543–551.

Belgnaoui, S.M., Paz, S., and Hiscott, J. (2011). Orchestrating the interferon antiviral response through the mitochondrial antiviral signaling (MAVS) adapter. Curr. Opin. Immunol. *23*, 564–572.

Bertolotti, A., Boniface, K., Vergier, B., Mossalayi, D., Taieb, A., Ezzedine, K., and Seneschal, J. (2014). Type I interferon signature in the initiation of the immune response in vitiligo. Pigment Cell Melanoma Res. *27*, 398–407.

Bertolotto, A., Granieri, L., Marnetto, F., Valentino, P., Sala, A., Capobianco, M., Malucchi, S., Di Sapio, A., Malentacchi, M., Matta, M., and Caldano, M. (2015). Biological monitoring of IFN-β therapy in Multiple Sclerosis. Cytokine Growth Factor Rev. *26*, 241-8

Blasius, A.L., and Beutler, B. (2010). Intracellular Toll-like Receptors. Immunity *32*, 305–315.

Bolen, C.R., Robek, M.D., Brodsky, L., Schulz, V., Lim, J.K., Taylor, M.W., and Kleinstein, S.H. (2012). The blood transcriptional signature of chronic hepatitis C virus is consistent with an ongoing interferon-mediated antiviral response. J. Interferon Cytokine Res. *33*, 15–23.

Borden, E.C., Sen, G.C., Uze, G., Silverman, R.H., Ransohoff, R.M., Foster, G.R., and Stark, G.R. (2007). Interferons at age 50: past, current and future impact on biomedicine. Nat. Rev. Drug Discov. *6*, 975–990.

Bouvier, N.M., and Palese, P. (2008). The biology of influenza viruses. Vaccine *26*, D49–D53.

Bowick, G.C., Airo, A.M., and Bente, D.A. (2012). Expression of interferon-induced antiviral genes is delayed in a STAT1 knockout mouse model of Crimean-Congo hemorrhagic fever. Virol. J. *9*, 122.

Brown, H.A., Gutowski, S., Moomaw, C.R., Slaughter, C., and Sternweis, P.C. (1993). ADP-ribosylation factor, a small GTP-dependent regulatory protein, stimulates phospholipase D activity. Cell *75*, 1137–1144.

Bruce, E.A., Digard, P., and Stuart, A.D. (2010). The Rab11 pathway is required for influenza A virus budding and filament formation. J. Virol. *84*, 5848–5859.

Bruce, E.A., Stuart, A., McCaffrey, M.W., and Digard, P. (2012). Role of the Rab11 pathway in negative-strand virus assembly. Biochem. Soc. Trans. *40*, 1409–1415.

Burdette, D.L., Monroe, K.M., Sotelo-Troha, K., Iwig, J.S., Eckert, B., Hyodo, M., Hayakawa, Y., and Vance, R.E. (2011). STING is a direct innate immune sensor of cyclic di-GMP. Nature *478*, 515–518.

Carrasco, M., Amorim, M.J., and Digard, P. (2004). Lipid raft-dependent rargeting of the influenza A virus nucleoprotein to the apical plasma membrane. Traffic *5*, 979–992.

Chandrasekaran, A., Srinivasan, A., Raman, R., Viswanathan, K., Raguram, S., Tumpey, T.M., Sasisekharan, V., and Sasisekharan, R. (2008). Glycan topology determines human adaptation of avian H5N1 virus hemagglutinin. Nat. Biotechnol. *26*, 107–113.

Chang, K.-C., Goldspink, G., and Lida, J. (1990). Studies in the in vivo expression of the influenza resistance gene Mx by in-situ hybridisation. Arch. Virol. *110*, 151–164.

Chen, C., and Zhuang, X. (2008). Epsin 1 is a cargo-specific adaptor for the clathrin-mediated endocytosis of the influenza virus. Proc. Natl. Acad. Sci. *105*, 11790–11795.

Chen, H.-W., King, K., Tu, J., Sanchez, M., Luster, A.D., and Shresta, S. (2013). The roles of IRF-3 and IRF-7 in innate antiviral immunity against dengue virus. J. Immunol. Baltim. Md 1950 *191*, 4194–4201.

Dash, P., and Thomas, P.G. (2014). Host detection and the stealthy phenotype in influenza virus infection. In influenza pathogenesis and control - Volume II, M.B.A. Oldstone, and R.W. Compans, eds. (Springer International Publishing), pp. 121–147.

Dupuis, S., Jouanguy, E., Al-Hajjar, S., Fieschi, C., Al-Mohsen, I.Z., Al-Jumaah, S., Yang, K., Chapgier, A., Eidenschenk, C., Eid, P., et al. (2003). Impaired response to interferon-α/β and lethal viral disease in human STAT1 deficiency. Nat. Genet. *33*, 388–391.

Ehrhardt, C., Marjuki, H., Wolff, T., Nürnberg, B., Planz, O., Pleschka, S., and Ludwig, S. (2006). Bivalent role of the phosphatidylinositol-3-kinase (PI3K) during influenza virus infection and host cell defence. Cell. Microbiol. *8*, 1336–1348.

Ehrhardt, C., Seyer, R., Hrincius, E.R., Eierhoff, T., Wolff, T., and Ludwig, S. (2010). Interplay between influenza A virus and the innate immune signaling. Microbes Infect. *12*, 81–87.

Everitt, A.R., Clare, S., Pertel, T., John, S.P., Wash, R.S., Smith, S.E., Chin, C.R., Feeley, E.M., Sims, J.S., Adams, D.J., et al. (2012). IFITM3 restricts the morbidity and mortality associated with influenza. Nature *484*, 519–523.

Fitzgerald, K.A., McWhirter, S.M., Faia, K.L., Rowe, D.C., Latz, E., Golenbock, D.T., Coyle, A.J., Liao, S.-M., and Maniatis, T. (2003). IKKε and TBK1 are essential components of the IRF3 signaling pathway. Nat. Immunol. *4*, 491–496.

Frese, M., Kochs, G., Meier-Dieter, U., Siebler, J., and Haller, O. (1995). Human MxA protein inhibits tick-borne Thogoto virus but not Dhori virus. J. Virol. *69*, 3904–3909.

Fujii, Y., Goto, H., Watanabe, T., Yoshida, T., and Kawaoka, Y. (2003). Selective incorporation of influenza virus RNA segments into virions. Proc. Natl. Acad. Sci. *100*, 2002–2007.

Fujioka, Y., Tsuda, M., Hattori, T., Sasaki, J., Sasaki, T., Miyazaki, T., and Ohba, Y. (2011). The Ras–PI3K Signaling Pathway Is Involved in Clathrin-Independent Endocytosis and the Internalization of Influenza Viruses. PLoS ONE *6*, e16324.

Furuya, A.K.M., Sharifi, H.J., and de Noronha, C.M.C. (2014). The curious case of type I IFN and MxA: tipping the immune balance in AIDS. Microb. Immunol. *5*, 419.

Gao, Q., and Frohman, M.A. (2012). Roles for the lipid-signaling enzyme MitoPLD in mitochondrial dynamics, piRNA biogenesis, and spermatogenesis. BMB Rep. *45*, 7–13.

Gao, S., von der Malsburg, A., Paeschke, S., Behlke, J., Haller, O., Kochs, G., and Daumke, O. (2010). Structural basis of oligomerization in the stalk region of dynamin-like MxA. Nature *465*, 502–506.

Gao, S., von der Malsburg, A., Dick, A., Faelber, K., Schröder, G.F., Haller, O., Kochs, G., and Daumke, O. (2011). Structure of myxovirus resistance protein A reveals intra- and intermolecular domain interactions required for the antiviral function. Immunity *35*, 514–525.

Garcia-Sastre, A. (2001). Inhibition of interferon-mediated antiviral responses by influenza A viruses and other negative-strand RNA viruses. Virology *279*, 375–384.

García-Sastre, A. (2011). Induction and evasion of type I interferon responses by influenza viruses. Virus Res. *162*, 12–18.

Garcia-Sastre, A., and Biron, C.A. (2006). Type 1 interferons and the virus-host relationship: a lesson in detente. Science *312*, 879–882.

Génin, P., Vaccaro, A., and Civas, A. (2009). The role of differential expression of human interferon-A genes in antiviral immunity. Cytokine Growth Factor Rev. *20*, 283–295.

Glymph, S., Mandal, S., Knowell, A.E., Abebe, F., and Chaudhary, J. (2013). The myxovirus resistance A (MxA) gene −88G>T single nucleotide polymorphism is associated with prostate cancer. Infect. Genet. Evol. *16*, 186–190.

Gold, E.S., Diercks, A.H., Podolsky, I., Podyminogin, R.L., Askovich, P.S., Treuting, P.M., and Aderem, A. (2014). 25-Hydroxycholesterol acts as an amplifier of inflammatory signaling. Proc. Natl. Acad. Sci. *111*, 10666–10671.

Hale, B.G., Randall, R.E., Ortín, J., and Jackson, D. (2008). The multifunctional NS1 protein of influenza A viruses. J. Gen. Virol. *89*, 2359–2376.

Haller, O., and Kochs, G. (2011). Human MxA Protein: An Interferon-Induced Dynamin-Like GTPase with Broad Antiviral Activity. J. Interferon Cytokine Res. *31*, 79–87.

Haller, O., Frese, M., Rost, D., Nuttall, P.A., and Kochs, G. (1995). Tick-borne thogoto virus infection in mice is inhibited by the orthomyxovirus resistance gene product Mx1. J. Virol. *69*, 2596–2601.

Haller, O., Kochs, G., and Weber, F. (2006). The interferon response circuit: Induction and suppression by pathogenic viruses. Virology *344*, 119–130.

Haller, O., Staeheli, P., and Kochs, G. (2007a). Interferon-induced Mx proteins in antiviral host defense. Biochimie *89*, 812–818.

Haller, O., Kochs, G., and Weber, F. (2007b). Interferon, Mx, and viral countermeasures. Cytokine Growth Factor Rev. *18*, 425–433.

Haller, O., Staeheli, P., Schwemmle, M., and Kochs, G. (2015). Mx GTPases: dynamin-like antiviral machines of innate immunity. Trends Microbiol. *0*.

Hammond, S.M., Jenco, J.M., Nakashima, S., Cadwallader, K., Gu, Q., Cook, S., Nozawa, Y., Prestwich, G.D., Frohman, M.A., and Morris, A.J. (1997). Characterization of two alternately spliced forms of phospholipase D1. Activation of the purified enzymes by phosphatidylinositol 4,5-bisphosphate, ADP-ribosylation factor, and Rho family monomeric GTP-binding proteins and protein kinase C-alpha. J. Biol. Chem. *272*, 3860–3868.

Hefti, H.P., Frese, M., Landis, H., Paolo, C.D., Aguzzi, A., Haller, O., and Pavlovic, J. (1999). Human MxA Protein Protects Mice Lacking a Functional Alpha/Beta Interferon System against La Crosse Virus and Other Lethal Viral Infections. J. Virol. *73*, 6984–6991.

Holzinger, D., Jorns, C., Stertz, S., Boisson-Dupuis, S., Thimme, R., Weidmann, M., Casanova, J.-L., Haller, O., and Kochs, G. (2007). Induction of MxA Gene Expression by Influenza A Virus Requires Type I or Type III Interferon Signaling. J. Virol. *81*, 7776–7785.

Honda, K., and Taniguchi, T. (2006). IRFs: master regulators of signalling by Toll-like receptors and cytosolic pattern-recognition receptors. Nat. Rev. Immunol. *6*, 644–658.

Honda, K., Yanai, H., Negishi, H., Asagiri, M., Sato, M., Mizutani, T., Shimada, N., Ohba, Y., Takaoka, A., Yoshida, N., et al. (2005). IRF-7 is the master regulator of type-I interferon-dependent immune responses. Nature *434*, 772–777.

Hou, F., Sun, L., Zheng, H., Skaug, B., Jiang, Q.-X., and Chen, Z.J. (2011). MAVS forms functional prion-like aggregates to activate and propagate antiviral innate immune response. Cell *146*, 448–461.

Hrincius, E.R., Dierkes, R., Anhlan, D., Wixler, V., Ludwig, S., and Ehrhardt, C. (2011). Phosphatidylinositol-3-kinase (PI3K) is activated by influenza virus vRNA via the pathogen pattern receptor Rig-I to promote efficient type I interferon production. Cell. Microbiol. *13*, 1907–1919.

Humeau, Y., Vitale, N., Chasserot-Golaz, S., Dupont, J.L., Du, G., Frohman, M.A., Bader, M.F., and Poulain, B. (2001). A role for phospholipase D1 in neurotransmitter release. Proc. Natl. Acad. Sci. U. S. A. *98*, 15300–15305.

Ishikawa, H., Ma, Z., and Barber, G.N. (2009). STING regulates intracellular DNA-mediated, type I interferon-dependent innate immunity. Nature *461*, 788–792.

Iwasaki, A., and Pillai, P.S. (2014). Innate immunity to influenza virus infection. Nat. Rev. Immunol. *14*, 315–328.

Iwasaki, T., and Nozima, T. (1977). Defense mechanisms against primary influenza virus infection in mice. I. The roles of interferon and neutralizing antibodies and thymus dependence of interferon and antibody production. J Immunol *118*, 256–263.

Josset, L., Frobert, E., and Rosa-Calatrava, M. (2008). Influenza A replication and host nuclear compartments: Many changes and many questions. J. Clin. Virol. *43*, 381–390.

Kane, M., Yadav, S.S., Bitzegeio, J., Kutluay, S.B., Zang, T., Wilson, S.J., Schoggins, J.W., Rice, C.M., Yamashita, M., Hatziioannou, T., et al. (2013). MX2 is an interferon-induced inhibitor of HIV-1 infection. Nature *502*, 563–566.

Kato, H., Sato, S., Yoneyama, M., Yamamoto, M., Uematsu, S., Matsui, K., Tsujimura, T., Takeda, K., Fujita, T., Takeuchi, O., et al. (2005). Cell type-specific involvement of RIG-I in antiviral response. Immunity *23*, 19–28.

Kato, H., Takeuchi, O., Sato, S., Yoneyama, M., Yamamoto, M., Matsui, K., Uematsu, S., Jung, A., Kawai, T., Ishii, K.J., et al. (2006). Differential roles of MDA5 and RIG-I helicases in the recognition of RNA viruses. Nature *441*, 101–105.

Khan, M., Syed, G.H., Kim, S.-J., and Siddiqui, A. Mitochondrial dynamics and viral infections: A close nexus. Biochim. Biophys. Acta BBA - Mol. Cell Res.

Kolb, E., Laine, E., Strehler, D., and Staeheli, P. (1992). Resistance to influenza virus infection of Mx transgenic mice expressing Mx protein under the control of two constitutive promoters. J. Virol. *66*, 1709–1716.

Krug, R.M. (2015). Functions of the influenza A virus NS1 protein in antiviral defense. Curr. Opin. Virol. *12*, 1–6.

Kumar, H., Kawai, T., Kato, H., Sato, S., Takahashi, K., Coban, C., Yamamoto, M., Uematsu, S., Ishii, K.J., Takeuchi, O., et al. (2006). Essential role of IPS-1 in innate immune responses against RNA viruses. J. Exp. Med. *203*, 1795–1803.

Kurt-Jones, E.A., Popova, L., Kwinn, L., Haynes, L.M., Jones, L.P., Tripp, R.A., Walsh, E.E., Freeman, M.W., Golenbock, D.T., Anderson, L.J., et al. (2000). Pattern recognition receptors TLR4 and CD14 mediate response to respiratory syncytial virus. Nat. Immunol. *1*, 398–401.

Lakadamyali, M., Rust, M.J., Babcock, H.P., and Zhuang, X. (2003). Visualizing infection of individual influenza viruses. Proc. Natl. Acad. Sci. *100*, 9280–9285.

Lakadamyali, M., Rust, M.J., and Zhuang, X. (2004). Endocytosis of influenza viruses. Microbes Infect. *6*, 929–936.

Lendonck, L.Y. de, Martinet, V., and Goriely, S. (2014). Interferon regulatory factor 3 in adaptive immune responses. Cell. Mol. Life Sci. *71*, 3873–3883.

Li, Y., and Youssoufian, H. (1997). MxA overexpression reveals a common genetic link in four Fanconi anemia complementation groups. J. Clin. Invest. *100*, 2873–2880.

Lin, R., Génin, P., Mamane, Y., and Hiscott, J. (2000). Selective DNA binding and association with the CREB binding protein coactivator contribute to differential activation of Alpha/Beta interferon cenes by interferon regulatory factors 3 and 7. Mol. Cell. Biol. *20*, 6342–6353.

Lindenmann, J. (1962). Resistance of mice to mouse-adapted influenza A virus. Virology *16*, 203–204.

Lipatov, A.S., Govorkova, E.A., Webby, R.J., Ozaki, H., Peiris, M., Guan, Y., Poon, L., and Webster, R.G. (2004). Influenza: emergence and control. J. Virol. *78*, 8951–8959.

Liu, N., Wang, G., Lee, K.C., Guan, Y., Chen, H., and Cai, Z. (2009). Mutations in influenza virus replication and transcription: detection of amino acid substitutions in hemagglutinin of an avian influenza virus (H1N1). FASEB J. *23*, 3377–3382.

Liu, S., Cai, X., Wu, J., Cong, Q., Chen, X., Li, T., Du, F., Ren, J., Wu, Y., Grishin, N., et al. (2015). Phosphorylation of innate immune adaptor proteins MAVS, STING, and TRIF induces IRF3 activation. Science aaa2630.

Liu, X.-Y., Wei, B., Shi, H.-X., Shan, Y.-F., and Wang, C. (2010). Tom70 mediates activation of interferon regulatory factor 3 on mitochondria. Cell Res. *20*, 994–1011.

Livak, K.J., and Schmittgen, T.D. (2001). Analysis of Relative Gene Expression Data Using Real-Time Quantitative PCR and the $2^{-\Delta\Delta CT}$ Method. Methods *25*, 402–408.

Maines, T.R., Jayaraman, A., Belser, J.A., Wadford, D.A., Pappas, C., Zeng, H., Gustin, K.M., Pearce, M.B., Viswanathan, K., Shriver, Z.H., et al. (2009). Transmission and pathogenesis of swine-origin 2009 A(H1N1) influenza viruses in ferrets and mice. Science *325*, 484–487.

Mair, C.M., Meyer, T., Schneider, K., Huang, Q., Veit, M., and Herrmann, A. (2014). A histidine residue of the influenza virus hemagglutinin controls the pH dependence of the conformational change mediating membrane fusion. J. Virol. *88*, 13189–13200.

Malsburg, A. von der, Abutbul-Ionita, I., Haller, O., Kochs, G., and Danino, D. (2011). Stalk domain of the dynamin-like MxA GTPase protein mediates membrane binding and liposome tubulation via the unstructured L4 loop. J. Biol. Chem. *286*, 37858–37865.

Maria, N.I., Brkic, Z., Waris, M., Helden-Meeuwsen, C.G. van, Heezen, K., Merwe, J.P. van de, Daele, P.L. van, Dalm, V.A.S.H., Drexhage, H.A., and Versnel, M.A. (2014). MxA as a clinically applicable biomarker for identifying systemic interferon type I in primary Sjögren's syndrome. Ann. Rheum. Dis. *73*, 1052–1059.

Martin, K., and Helenius, A. (1991). Transport of incoming influenza virus nucleocapsids into the nucleus. J. Virol. *65*, 232–244.

Martín-Antonio, B., Suarez-Lledo, M., Arroyes, M., Fernández-Avilés, F., Martínez, C., Rovira, M., Espigado, I., Gallardo, D., Bosch, A., Buño, I., et al. (2013). A variant in IRF3 impacts on the clinical outcome of AML patients submitted to Allo-SCT. Bone Marrow Transplant. *48*, 1205–1211.

Mashimo, T., Lucas, M., Simon-Chazottes, D., Frenkiel, M.-P., Montagutelli, X., Ceccaldi, P.-E., Deubel, V., Guénet, J.-L., and Desprès, P. (2002). A nonsense mutation in the gene encoding 2′-5′-oligoadenylate synthetase/L1 isoform is associated with West Nile virus susceptibility in laboratory mice. Proc. Natl. Acad. Sci. *99*, 11311–11316.

Medina, R.A., and García-Sastre, A. (2011). Influenza A viruses: new research developments. Nat. Rev. Microbiol. *9*, 590–603.

Mehrbod, P., Omar, A.R., Hair-Bejo, M., Haghani, A., and Ideris, A. (2014). Mechanisms of action and efficacy of statins against influenza. BioMed Res. Int. *2014*, e872370.

Menachery, V.D., Pasieka, T.J., and Leib, D.A. (2010). Interferon regulatory factor 3-dependent pathways are critical for control of herpes simplex virus type 1 central nervous system infection. J. Virol. *84*, 9685–9694.

Mibayashi, M., Nakade, K., and Nagata, K. (2002). Promoted cell death of cells expressing human MxA by influenza virus infection. Microbiol. Immunol. *46*, 29–36.

Mitchell, P.S., Patzina, C., Emerman, M., Haller, O., Malik, H.S., and Kochs, G. (2012). Evolution-guided identification of antiviral specificity determinants in the broadly acting interferon-induced innate immunity factor MxA. Cell Host Microbe *12*, 598–604.

Mitchell, P.S., Emerman, M., and Malik, H.S. (2013). An evolutionary perspective on the broad antiviral specificity of MxA. Curr. Opin. Microbiol. *16*, 493–499.

Morin, P., Bragança, J., Bandu, M.-T., Lin, R., Hiscott, J., Doly, J., and Civas, A. (2002). Preferential binding sites for interferon regulatory factors 3 and 7 involved in interferon-A gene transcription. J. Mol. Biol. *316*, 1009–1022.

Nakaya, T., Sato, M., Hata, N., Asagiri, M., Suemori, H., Noguchi, S., Tanaka, N., and Taniguchi, T. (2001). Gene induction pathways mediated by distinct IRFs during viral infection. Biochem. Biophys. Res. Commun. *283*, 1150–1156.

Neumann, G., Noda, T., and Kawaoka, Y. (2009). Emergence and pandemic potential of swine-origin H1N1 influenza virus. Nature *459*, 931–939.

Nijtmans, L.G.J., Jong, L. de, Sanz, M.A., Coates, P.J., Berden, J.A., Back, J.W., Muijsers, A.O., Spek, H. van der, and Grivell, L.A. (2000). Prohibitins act as a membrane-bound chaperone for the stabilization of mitochondrial proteins. EMBO J. *19*, 2444–2451.

Oguin, T.H., Sharma, S., Stuart, A.D., Duan, S., Scott, S.A., Jones, C.K., Daniels, J.S., Lindsley, C.W., Thomas, P.G., and Brown, H.A. (2014). Phospholipase D facilitates efficient entry of influenza virus allowing escape from innate mmune inhibition. J. Biol. Chem. *289*, 25405-17

Ohkura, T., Momose, F., Ichikawa, R., Takeuchi, K., and Morikawa, Y. (2014). Influenza A virus hemagglutinin and neuraminidase mutually accelerate their apical targeting through clustering of lipid rafts. J. Virol. *88*, 10039–10055.

Osman, C., Merkwirth, C., and Langer, T. (2009). Prohibitins and the functional compartmentalization of mitochondrial membranes. J. Cell Sci. *122*, 3823–3830.

Padrón, D., Tall, R.D., and Roth, M.G. (2006). Phospholipase D2 Is required for efficient endocytic recycling of transferrin receptors. Mol. Biol. Cell *17*, 598–606.

Patzina, C., Haller, O., and Kochs, G. (2014). Structural requirements for the antiviral activity of the human MxA protein against Thogoto and influenza A virus. J. Biol. Chem. *289*, 6020–6027.

Pavlovic, J., Arzet, H.A., Hefti, H.P., Frese, M., Rost, D., Ernst, B., Kolb, E., Staeheli, P., and Haller, O. (1995). Enhanced virus resistance of transgenic mice expressing the human MxA protein. J. Virol. *69*, 4506–4510.

Perreira, J.M., Chin, C.R., Feeley, E.M., and Brass, A.L. (2013). IFITMs restrict the replication of multiple pathogenic viruses. J. Mol. Biol. *425*, 4937–4955.

Pulloor, N.K., Nair, S., Kostic, A.D., Bist, P., Weaver, J.D., Riley, A.M., Tyagi, R., Uchil, P.D., York, J.D., Snyder, S.H., et al. (2014). Human genome-wide RNAi screen identifies an essential role for inositol pyrophosphates in type-I interferon response. PLoS Pathog *10*, e1003981.

Rennie, M.L., McKelvie, S.A., Bulloch, E.M.M., and Kingston, R.L. (2014). Transient Dimerization of Human MxA Promotes GTP Hydrolysis, Resulting in a Mechanical Power Stroke. Structure *22*, 1433–1445.

Rossman, J.S., Jing, X., Leser, G.P., and Lamb, R.A. (2010). Influenza virus M2 protein mediates ESCRT-independent membrane scission. Cell *142*, 902–913.

Roth, M.G. (2008). Molecular mechanisms of PLD function in membrane traffic. Traffic *9*, 1233–1239.

Roy, A.M., Parker, J.S., Parrish, C.R., and Whittaker, G.R. (2000). Early stages of influenza virus entry into Mv-1 lung cells: involvement of dynamin. Virology *267*, 17–28.

Rust, M.J., Lakadamyali, M., Zhang, F., and Zhuang, X. (2004). Assembly of endocytic machinery around individual influenza viruses during viral entry. Nat. Struct. Mol. Biol. *11*, 567–573.

Rutigliano, J.A., Sharma, S., Morris, M.Y., Oguin, T.H., McClaren, J.L., Doherty, P.C., and Thomas, P.G. (2013). Highly pathologic influenza A virus infection is associated with augmented expression of PD-1 by functionally-compromised virus-specific CD8+ T cells. J. Virol. JVI.02851–13.

Sadler, A.J., and Williams, B.R.G. (2008). Interferon-inducible antiviral effectors. Nat. Rev. Immunol. *8*, 559–568.

Sakaguchi, S., Negishi, H., Asagiri, M., Nakajima, C., Mizutani, T., Takaoka, A., Honda, K., and Taniguchi, T. (2003). Essential role of IRF-3 in lipopolysaccharide-induced interferon-β gene expression and endotoxin shock. Biochem. Biophys. Res. Commun. *306*, 860–866.

Sato, M., Suemori, H., Hata, N., Asagiri, M., Ogasawara, K., Nakao, K., Nakaya, T., Katsuki, M., Noguchi, S., Tanaka, N., et al. (2000). Distinct and essential roles of transcription factors IRF-3 and IRF-7 in response to viruses for IFN-α/β gene induction. Immunity *13*, 539–548.

Scott, I. (2009). Mitochondrial factors in the regulation of innate immunity. Microbes Infect. *11*, 729–736.

Scott, S.A., Selvy, P.E., Buck, J.R., Cho, H.P., Criswell, T.L., Thomas, A.L., Armstrong, M.D., Arteaga, C.L., Lindsley, C.W., and Brown, H.A. (2009). Design of isoform-selective phospholipase D inhibitors that modulate cancer cell invasiveness. Nat. Chem. Biol. *5*, 108–117.

Sen, A., Pruijssers, A.J., Dermody, T.S., García-Sastre, A., and Greenberg, H.B. (2011). The early interferon response to rotavirus is regulated by PKR and depends on MAVS/IPS-1, RIG-I, MDA-5, and IRF3. J. Virol. *85*, 3717–3732.

Seth, R.B., Sun, L., and Chen, Z.J. (2006). Antiviral innate immunity pathways. Cell Res. *16*, 141–147.

Shen, Y., Xu, L., and Foster, D.A. (2001). Role for phospholipase D in receptor-mediated endocytosis. Mol. Cell. Biol. *21*, 595–602.

Shinya, K., Ebina, M., Yamada, S., Ono, M., Kasai, N., and Kawaoka, Y. (2006). Avian flu: Influenza virus receptors in the human airway. Nature *440*, 435–436.

Shrestha, S.S., Swerdlow, D.L., Borse, R.H., Prabhu, V.S., Finelli, L., Atkins, C.Y., Owusu-Edusei, K., Bell, B., Mead, P.S., Biggerstaff, M., et al. (2011). Estimating the burden of 2009 pandemic influenza A (H1N1) in the United States (April 2009–April 2010). Clin. Infect. Dis. *52*, S75–S82.

Sieczkarski, S.B., and Whittaker, G.R. (2002). Influenza virus can enter and infect cells in the absence of clathrin-mediated endocytosis. J. Virol. *76*, 10455–10464.

Sieczkarski, S.B., and Whittaker, G.R. (2003). Differential requirements of Rab5 and Rab7 for endocytosis of influenza and other enveloped viruses. Traffic Cph. Den. *4*, 333–343.

Sieczkarski, S.B., Brown, H.A., and Whittaker, G.R. (2003). Role of protein kinase C {beta}II in influenza virus entry via late endosomes. J Virol *77*, 460–469.

Singer, W.D., Brown, H.A., Jiang, X., and Sternweis, P.C. (1996). Regulation of phospholipase D by protein kinase C is synergistic with ADP-ribosylation factor and independent of protein kinase activity. J. Biol. Chem. *271*, 4504–4510.

Skehel, J.J., and Wiley, D.C. (2000). Receptor binding and membrane fusion in virus entry: the influenza hemagglutinin. Annu. Rev. Biochem. *69*, 531–569.

Spann, K.M., Loh, Z., Lynch, J.P., Ullah, A., Zhang, V., Baturcam, E., Werder, R.B., Khajornjiraphan, N., Rudd, P., Loo, Y.-M., et al. (2014). IRF-3, IRF-7, and IPS-1 promote host defense against acute human metapneumovirus infection in neonatal mice. Am. J. Pathol. *184*, 1795–1806.

Staeheli, P., Grob, R., Meier, E., Sutcliffe, J.G., and Haller, O. (1988). Influenza virus-susceptible mice carry Mx genes with a large deletion or a nonsense mutation. Mol. Cell. Biol. *8*, 4518–4523.

Stry, M.V., Oguin, T.H., Cheloufi, S., Vogel, P., Watanabe, M., Pillai, M.R., Dash, P., Thomas, P.G., Hannon, G.J., and Bix, M. (2012). Enhanced susceptibility of Ago1/3 double-null mice to influenza A virus infection. J. Virol. *86*, 4151–4157.

Sun, Q., Sun, L., Liu, H.-H., Chen, X., Seth, R.B., Forman, J., and Chen, Z.J. (2006). The specific and essential role of MAVS in antiviral innate immune responses. Immunity *24*, 633–642.

Takeda, M., Leser, G.P., Russell, C.J., and Lamb, R.A. (2003). Influenza virus hemagglutinin concentrates in lipid raft microdomains for efficient viral fusion. Proc. Natl. Acad. Sci. *100*, 14610–14617.

Tanaka, Y., and Chen, Z.J. (2012). STING specifies IRF3 phosphorylation by TBK1 in the cytosolic DNA signaling pathway. Sci. Signal. *5*, ra20–ra20.

Taubenberger, J.K., Reid, A.H., Janczewski, T.A., and Fanning, T.G. (2001). Integrating historical, clinical and molecular genetic data in order to explain the origin and virulence of the 1918 Spanish influenza virus. Philos. Trans. R. Soc. Lond. B. Biol. Sci. *356*, 1829–1839.

Theofilopoulos, A.N., Baccala, R., Beutler, B., and Kono, D.H. (2005). Type I interferons (α/β) in immunity and autoimmunity. Annu. Rev. Immunol. *23*, 307–335.

Verhelst, J., Parthoens, E., Schepens, B., Fiers, W., and Saelens, X. (2012). Interferon-inducible protein Mx1 inhibits influenza virus by interfering with functional viral ribonucleoprotein complex assembly. J. Virol. *86*, 13445–13455.

Verhelst, J., Hulpiau, P., and Saelens, X. (2013). Mx proteins: antiviral gatekeepers that restrain the uninvited. Microbiol. Mol. Biol. Rev. *77*, 551–566.

Vijayan, M., and Hahm, B. (2014). Influenza viral manipulation of sphingolipid metabolism and signaling to modulate host defense system. Scientifica *2014*, e793815.

De Vries, E., Tscherne, D.M., Wienholts, M.J., Cobos-Jiménez, V., Scholte, F., García-Sastre, A., Rottier, P.J.M., and de Haan, C.A.M. (2011). Dissection of the influenza A virus endocytic routes reveals macropinocytosis as an alternative entry pathway. PLoS Pathog. *7*, e1001329.

Wang, T., Town, T., Alexopoulou, L., Anderson, J.F., Fikrig, E., and Flavell, R.A. (2004). Toll-like receptor 3 mediates West Nile virus entry into the brain causing lethal encephalitis. Nat. Med. *10*, 1366–1373.

Webster, R.G., Bean, W.J., Gorman, O.T., Chambers, T.M., and Kawaoka, Y. (1992). Evolution and ecology of influenza A viruses. Microbiol. Rev. *56*, 152–179.

Werner, S.L., Barken, D., and Hoffmann, A. (2005). Stimulus specificity of gene expression programs determined by temporal control of IKK activity. Science *309*, 1857–1861.

Xiao, H., Killip, M.J., Staeheli, P., Randall, R.E., and Jackson, D. (2013). The human interferon-induced MxA protein inhibits early stages of influenza A virus infection by retaining the incoming viral genome in the cytoplasm. J. Virol. *87*, 13053–13058.

Yan, Q., Yang, H., Yang, D., Zhao, B., Ouyang, Z., Liu, Z., Fan, N., Ouyang, H., Gu, W., and Lai, L. (2014). Production of transgenic pigs over-expressing the antiviral gene Mx1. Cell Regen. *3*.

Yang, H., Lin, C.H., Ma, G., Baffi, M.O., and Wathelet, M.G. (2003). Interferon regulatory factor-7 synergizes with other transcription factors through multiple interactions with p300/CBP coactivators. J. Biol. Chem. *278*, 15495–15504.

Yoneyama, M., Kikuchi, M., Natsukawa, T., Shinobu, N., Imaizumi, T., Miyagishi, M., Taira, K., Akira, S., and Fujita, T. (2004). The RNA helicase RIG-I has an essential function in double-stranded RNA-induced innate antiviral responses. Nat. Immunol. *5*, 730–737.

Yoneyama, M., Onomoto, K., Jogi, M., Akaboshi, T., and Fujita, T. (2015). Viral RNA detection by RIG-I-like receptors. Curr. Opin. Immunol. *32*, 48–53.

Yoshimura, A., and Ohnishi, S. (1984). Uncoating of influenza virus in endosomes. J. Virol. *51*, 497–504.

Zhang, X., Xu, H., Chen, X., Li, X., Wang, X., Ding, S., Zhang, R., Liu, L., He, C., Zhuang, L., et al. (2014). Association of functional polymorphisms in the MxA gene with susceptibility to enterovirus 71 infection. Hum. Genet. *133*, 187–197.

Zheng, H., Lee, H.A., Palese, P., and García-Sastre, A. (1999). Influenza A virus RNA polymerase has the ability to stutter at the polyadenylation site of a viral RNA template during RNA replication. J. Virol. *73*, 5240–5243.

Zimmermann, P., Mänz, B., Haller, O., Schwemmle, M., and Kochs, G. (2011). The viral nucleoprotein determines Mx sensitivity of influenza A viruses. J. Virol. *85*, 8133–8140.